Analysis, Modeling, and Control of Electric Spring for a DC Microgrid with High Penetration of Renewable Energies to Improve its Stability and Power Quality

by

DANIAL MOEINI

THESIS PRESENTED TO ÉCOLE DE TECHNOLOGIE SUPÉRIEURE IN
PARTIAL FULFILLMENT FOR A MASTER'S DEGREE
WITH THESIS IN ELECTRICAL ENGINEERING
M.A.Sc.

MONTREAL, JULY 25, 2023

ÉCOLE DE TECHNOLOGIE SUPÉRIEURE
UNIVERSITÉ DU QUÉBEC

BOARD OF EXAMINERS

THIS THESIS HAS BEEN EVALUATED

BY THE FOLLOWING BOARD OF EXAMINERS

Mr. Ambrish Chandra, Thesis Supervisor
Department of Electrical Engineering, École de Technologie Supérieure

Mr. Qingsong Wang, President of the Board of Examiners
Department of Electrical Engineering, École de Technologie supérieure

Mr. Miloud Rezkallah , External Evaluator
Senior researcher, ITMI, Sept-Îles

THIS THESIS WAS PRESENTED AND DEFENDED

IN THE PRESENCE OF A BOARD OF EXAMINERS AND PUBLIC

JULY 25, 2023

AT ÉCOLE DE TECHNOLOGIE SUPÉRIEURE

ACKNOWLEDGMENT

I would like to acknowledge and express my gratitude to my supervisor Prof. Chandra for giving me the chance to work with him. His continuous support and advice through all stages of my master's degree helped me a lot in reaching the end of my journey.

I would like also to thank my parents for their support and prayers that definitively facilitate dealing with dilemmas in my personal life and during my master's degree.

Analyse, modélisation et contrôle d'un ressort électrique pour un micro-réseau à courant continu à forte pénétration d'énergies renouvelables afin d'améliorer sa stabilité et sa qualité d'alimentation

Danial Moeini

RÉSUMÉ

Ça fait plus d'un siècle que le système d'alimentation à courant alternatif (CA) a dominé le secteur de l'énergie électrique grâce à des performances supérieures par rapport aux systèmes d'alimentation à courant continu (CC). Le réseau électrique CA peut alimenter les clients en transférant la puissance générée sur une longue distance. Cependant, les systèmes électriques modernes sont supposés non seulement rentables, mais aussi durables. Le système à courant continu est fondamentalement plus fiable et robuste et pourrait être adopté localement pour la distribution d'énergie. Enfin, l'idée d'un micro-réseau CC, en tant que solution pour les futurs réseaux intelligents, a gagné en popularité en raison de ses nombreux avantages. Le micro-réseau CC peut fonctionner sur la base de l'alimentation CC et offre tous les avantages des réseaux CC ainsi que la possibilité d'opérer en mode sois connecté au réseau principal ou îloté pour l'électrification des régions éloignées.

Malgré tous les avantages liés au concept de micro-réseaux CC, il reste des défis concernant leur fonctionnement et contrôle en présence de ressources énergétiques renouvelables massivement intégrées exacerbées par leurs caractéristiques naturelles de production intermittente. Ce problème est plus important dans les micro-réseaux, en particulier dans le mode de fonctionnement îloté, qui basé principalement sur les panneau solaire (PV) et éoliennes. Pour résoudre ce problème, la mise en place de nouveaux schémas de régulation semble d'être nécessaire pour maintenir l'équilibre entre consommation et production. Plusieurs solutions sont proposées dans la littérature, par exemple, la gestion de la demande, l'équilibrage de charge, le système de gestion de l'énergie en temps réel et le stockage de l'énergie.

Dans cette thèse, notre objectif est d'utiliser une méthode très moderne proposée dans la littérature qui est l'application d'électrique à ressort pour améliorer les performances des

micro-réseaux CC. Nous proposons un schéma de partage d'énergie pour coordonner le rôle d'un électrique à ressort CC (ÉRCC) et d'un système de source d'énergie de batterie hybride (BESS hybride) pour améliorer la tension du bus CC lorsque la source principale du micro-réseau CC est un système PV. Ensuite, deux sont simulées : (1) situation nuageuse dans laquelle la production du système PV principal diminue (2) un défaut à la terre au niveau du bus CC. Les résultats de simulation effectués montrent que (ÉRCC) peut contribuer efficacement et positivement à la stabilité du bus CC, amortir les oscillations, améliorer la qualité de la puissance et de la tension fournies, et libérer le stress du BESS hybride.

Mots-clés: électrique à ressort, système d'nergie distribuée, micro-réseau, système d'alimentation à courant continu, panneau solaire (PV), contrôle de tension, source d'énergie de batterie, charge critique, charge non-critique, schéma de partage d'énergie

Analysis, Modeling, and Control of Electric Spring for a DC Microgrid with High Penetration of Renewable Energies to Improve its Stability and Power Quality

Danial Moeini

ABSTRACT

It has been more than a century since the AC-based power system dominated the electric power business upon superior performance against DC-based power systems. The AC power system can supply the clients by transferring the generated power over a long distance. However, modern power systems are supposed not just cost-effective, but also sustainable. The DC system inherently is more reliable and robust and could be adopted locally for power delivery. Finally, the idea of a DC microgrid, as a solution for future smart grids has gained attraction due to its several advantages. The DC microgrid can operate based on DC power and They offer all the advantages of DC networks plus the ability to operate grid-connected or off-grid for electrification of remote areas.

Despite all the advantages related to the concept of DC microgrids, there are still challenges regarding their operation and control in the presence of massively integrated renewable energy resources exacerbated by their natural intermittent production characteristics. This issue is more important in microgrids, especially in the off-grid operation mode, which relies mostly on PVs and wind turbines. To overcome this dilemma, employing new control schemes seems necessary for maintaining the balance between consumption and generation. Several solutions are proposed in the literature e.g., demand-side management, load balancing, real-time energy management system, and energy storage.

In this thesis, our focus is on a very modern method proposed in the literature which is the application of electric springs for improving the performance of DC microgrids. We propose an energy-sharing scheme for coordinating the role of a DC electric spring (DCES) and a hybrid battery energy source system (hybrid BESS) for improving the DC bus voltage when the main source of the DC microgrid is a PV system. Then two contingencies are studied: (1)a cloudy situation is simulated in which the production of the main PV system drops, (2) a DC

bus to ground fault. The simulation results prove that DCES can effectively and positively contribute to the steady-state stability of the DC bus, dampen the oscillations, improves the quality of provided power and voltage, and release the stress from the hybrid BESS.

Keywords: electrical spring, distribution energy system, microgrid, direct current system, solar photovoltaic (PV), voltage control, battery energy storage systems (BESS), critical load, non-critical load, coordinated energy-sharing scheme

TABLE OF CONTENTS

Page

LIST OF TABLES

Page

LIST OF FIGURES

Page

LIST OF ABBREVIATIONS

DC	Direct Current
AC	Alternating Current
DER	Distributed Energy Resources
RES	Renewable Energy Sources
PV	Photovoltaic
BESS	Battery Energy Storage Systems
DSM	Demand-Side Management
IEA	International Energy Agency
ACES	AC Electric Spring
DCES	DC Electric Spring
CL	Critical Load
NCL	Non-Critical Load
MPPT	Maximum Power Point Tracking
NREL	National Renewable Energy Laboratory
PCC	Point of Common Coupling
MG	Microgrid
BD	Boosting & Discharging Operation Mode
SD	Suppressing & Discharging Operation Mode
BC	Boosting & Charging Operation Mode
SC	Suppressing & Charging Operation Mode
IGBT	Insulated-Gate Bipolar Transistor
PWM	Pulse-Width Modulation
EDLC	Electric Double Layer Capacitors

LIST OF SYMBOLS AND UNITS OF MEASUREMENT

V	Voltage (V)
P	Active power (KW)
Q	Reactive power (kVAR)
V_{PCC_ref}	Reference value for the voltage of the connection point (V)
P_{ES}	Active power of DCES (KW)
Ir	Irradiance (W/m2)
$Temp$	Temperature (deg. C)
R	Resistance (Ohm)
t	Time (Second)
F	Capacitance(Farad)
Ah	Unit of Electric Charge (Ampere-Hour)

CHAPTER 1

INTRODUCTION

1.1 Context and Motivation

Since the invention of electricity, there has always been a debate between alternating current (AC) and direct current (DC). By the late 19th century, AC-based distribution systems dominated DC-based distribution systems due to several interesting features (Xu et al., 2017). However, recent massive integration of DC loads, distributed energy resources (DERs), energy storage, and electric vehicles into the grids, many researchers start to develop the idea of DC distribution systems.

DC distribution systems have many advantages compared to AC distribution systems as well including longer supply range, bigger power transfer capability, simpler power transfer without needing converters and inverters, less investment, and most importantly no issue with reactive power circulation (Van den Broeck et al., 2018)(Gerber et al., 2018)(van der Blij et al., 2018).

Among different types of DC distribution systems, the concept of DC microgrids has gained more attraction due to their several advantages including the ability to operate grid-connected or off-grid for electrification of remote areas. A DC microgrid is generally defined as a small-scale DC distribution system that comprises 1) DC power generation units such as PVs, Wind turbines, and Energy storages, 2) DC distribution networks such as DC feeders and DC control and protection devices, and 3) DC consumers and prosumers residential, commercial, and small-scale DC industrial loads (Charles & Bagavathy, 2016).

A new challenge for any power system in the 21st century is the rising trend of power generation from renewable energy resources which are naturally intermittent (Abdelilah et al., 2020). This issue is more important in microgrids, especially off-grid microgrids which rely mostly on PVs and wind turbines. To overcome this dilemma, employing new control schemes seems necessary for maintaining the balance between consumption and generation.

Several solutions are proposed in the literature e.g., demand-side management (DSM), load balancing, real-time energy management system, and energy storage (Mahmoud, 2016)(Tiwari et al., 2017)(Faisal et al., 2018). Despite all efforts, these methods are not highly effective and practical. For example, DSMs and load-balancing methods may fail to balance the instantaneous power mismatch. The cost of energy storage is still relatively high, and its response time is not fast in the case of rapid changes.

1.2 DC Distribution Network Issues

Although DC distribution networks have many interesting characteristics, some concerns regarding the voltage of DC bus exist which require attention. A summary of those issues is plotted in Figure 1.2 (Mok et al., 2017).

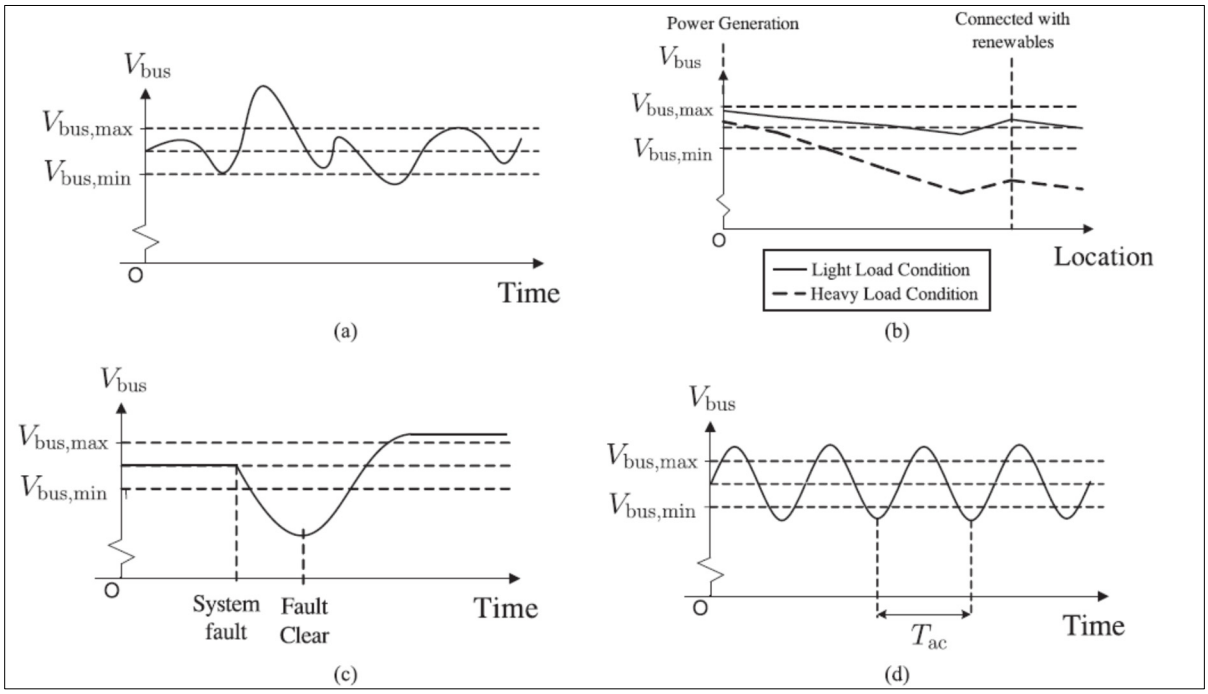

Figure 1.1 A number of common problems in DC distribution system are (a) voltage variation (b) Voltage drop in the DC distribution system, (c) Voltage drop and rise following a system fault, and (d) DC voltage and harmonic component
Taken from Mok et al. (2017, P.8)

1.2.1 Unstable DC Bus Voltage

In real-world applications, the voltage of a DC bus may vary with time due to several factors such as:

- Voltage variation at higher supply-side
- Variation of load power
- Variation of the output power of DERs

In the case of unstable DC bus voltage, the operation of the DC system may create undesired oscillation on the voltage trajectory.

1.2.2 Voltage Drop

The voltage drop across the DC distribution network is an unavoidable fact that happens because of the line impedance. The drop may exacerbate when heavy loads are connected to the network, especially near the end of a line. This issue is studied by (Kakigano et al., 2013), (Loh et al., 2013), and (Anand et al., 2013).

1.2.3 Short Circuit

When a sudden short circuit happens in the DC distribution system, the voltage drop on the dc bus may exceed certain limits, and protection devices may isolate the faulty location. Consequently, the voltage level after the fault might be higher (Cairoli et al., 2013), (Baran & Mahajan, 2007).

1.2.4 Harmonic Circulation

In the microgrid, harmonics can be produced by both the load and power sources. Any nonlinear load injects harmonic to the grid (Guerrero et al., 2011; Leu & Nha, 2013). On the generation side, the PV panels for example inject harmonics.

1.3 Electric Spring

A very modern method proposed in the literature is the application of Electric Springs (ESs). Inspired from the restorative force of an ideal mechanical spring mentioned first with 17th century-old Hooke's law, an ES, an energy management technology, retains the power system stability even if some of the other ESs fail to operate properly (Hui et al., 2012).

The mechanical springs and their equivalent ESs are shown in Figure 1.2 along with different modes of operating. As shown, the operation of a mechanical spring is defined by extending and compressing actions which are understood as voltage step-down or boost actions (Hashem et al., 2018).

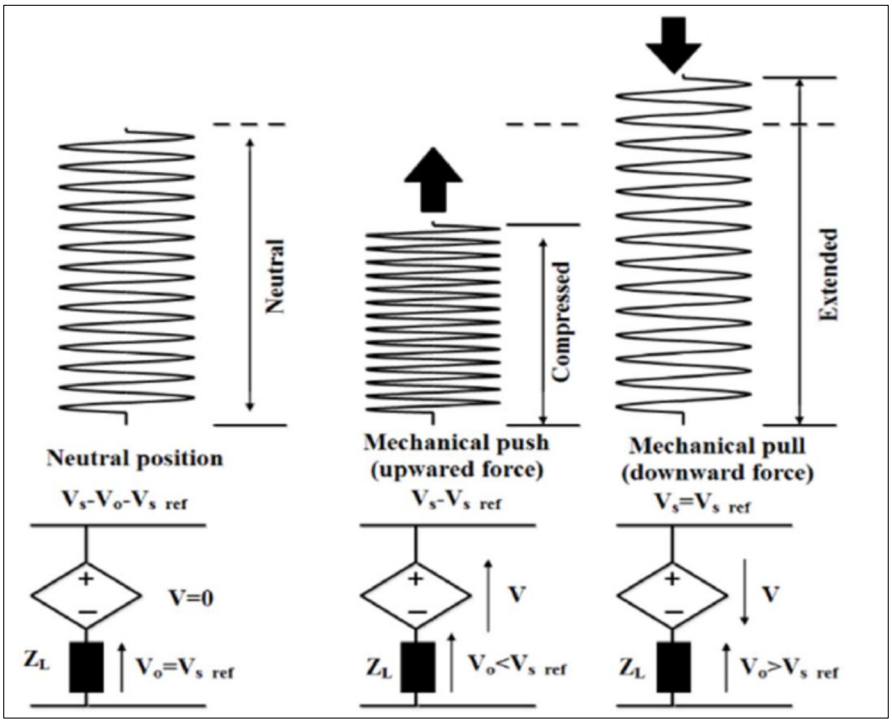

Figure 1.2 Mechanical Spring and equivalent Electrical Spring
Taken from Hashem et al. (2018, P. 1)

ES is a simple and novel method for voltage control that provides effective DSM without any need for communication. The main idea is to modulate the loads of connected system which

are less sensitive to the variations of voltage, so-called non-critical loads, according to the fluctuations of renewable energy resources. To do so, the ES tries to introduce a controllable voltage in series, or controllable current in parallel, with the non-critical loads and control the voltage across the loads which are sensitive to voltage, so-called critical loads. As a result, the power consumed by the non-critical loads is also modulated (Bahrami et al., 2018)(Huang & Abu Qahouq, 2015). The non-critical loads may include thermostatically controlled loads such as electric water heaters, refrigerators, and air conditioning systems, charging stations of electric vehicles.

1.4 Thesis outline

The thesis consists of five chapters. Chapter 2 covers the characteristics of DC-type ESs. All possible operation modes and operation configurations are reviewed. Moreover, different types of the so-called non-critical load (NCL) are reviewed along with corresponding mathematical equations.

Chapter 3 presents a focused literature review and relevant applications of DCES in DC microgrids followed by the fundamental arguments that are needed to understand their advantages and disadvantages.

An energy-sharing scheme for coordinating the role of a DC electric spring (DCES) and a hybrid battery energy source system (hybrid BESS) is proposed in Chapter 4. A DC microgrid including DCES, critical load, and hybrid BESS is constructed where the main source of power is a PV system. The study results simulating a cloudy situation and a dc bus to ground fault situation, show that DCES can effectively and positively contribute to the power shortage compensation process caused by a drop in PV production, dampen the oscillations, and release the stress from the hybrid BESS.

Finally, Chapter 5 concludes the thesis and gives some recommendations about further work on this topic and proposes a road map for development and implementation.

CHAPTER 2

CONCEPT OF ELECTRIC SPRING

In this chapter, the proposed types and configurations of Electric Springs (ESs) in the literature are reviewed:

2.1 The Concept and Configuration of ESs

It has been widely accepted that ESs are conceptually based on two main ideas, the AC system, and the DC system.

2.1.1 AC Electric Spring (ACES)

ESs are used in AC systems as reactive power compensator devices while providing active power compensation (Hui et al., 2012)(Q. Wang et al., 2015). The ESs are usually installed at the distribution level close to the loads. Different types of ACESs are shown in Figure. 2.1.

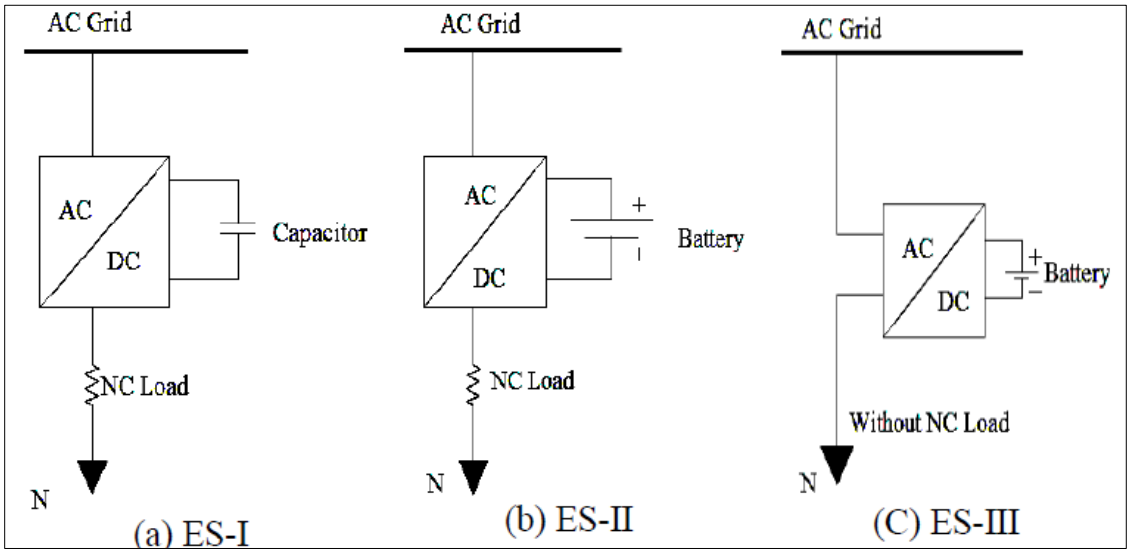

Figure. 2.1 Different types of ACES
Taken from Mok et al. (2017, P. 3)

The ACESs are just briefly mentioned here since the focus of this thesis is on DC types of ESs.

2.1.2 DC Electric Spring (DCES)

DC Electric Springs (DCESs) operate similarly to ACES which helps the non-critical loads of DC systems to consume less power by altering the supplied power (Q. Wang et al., 2016)(Mok et al., 2015) (see Figure. 2.2 and Figure. 2.3).

For the rest of this chapter, the main focus is to review the contents related to DCESs.

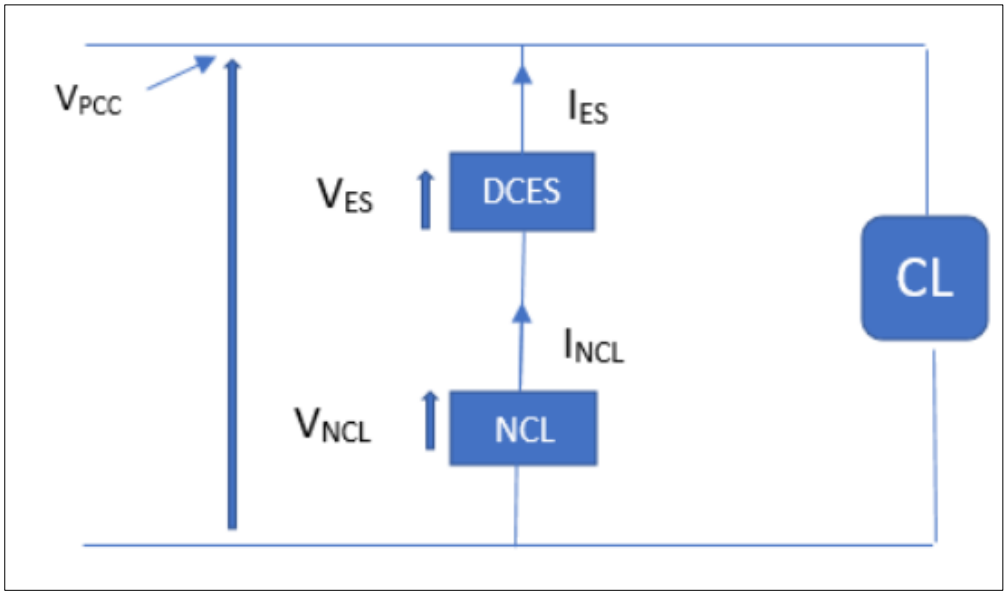

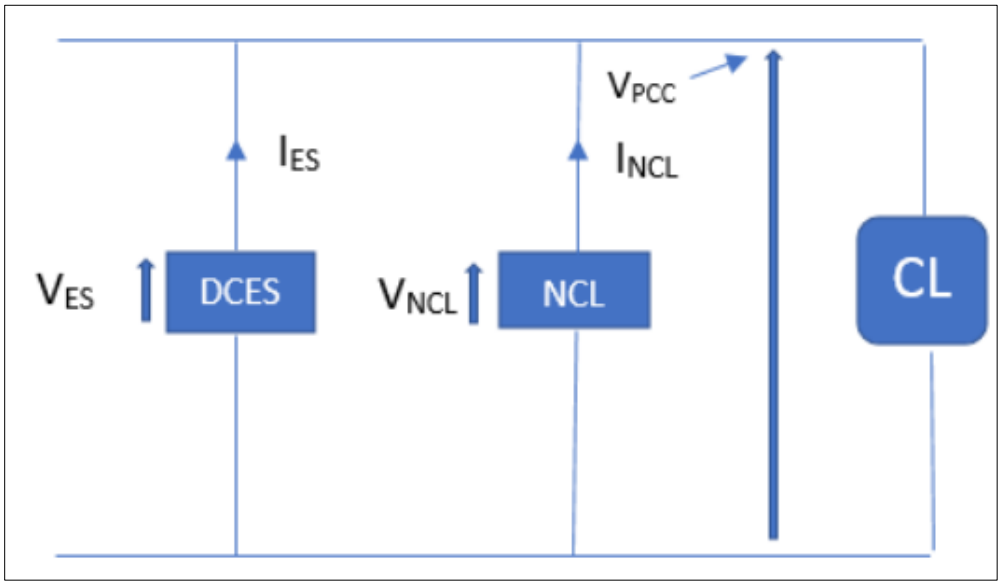

Figure. 2.2 General Block Diagram of DC-Electric Spring

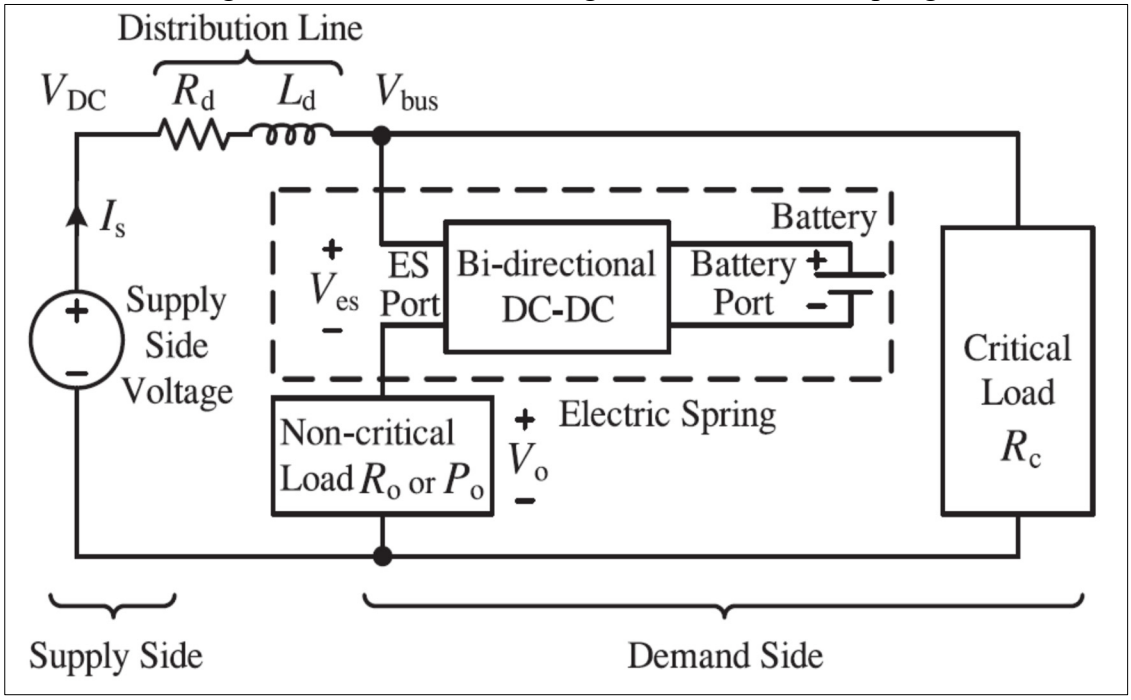

Figure. 2.3 The general configuration of DCES, the demand side, and the supply side
Taken from Mok et al. (2017, P. 3)

2.1.3 General Configuration

A common way of categorizing ESs is based on their connection to the grid and the non-critical load. In this concept, two types of ESs are studied in the literature: shunt and series DCES (Charles & Bagavathy, 2016). Generally speaking, we could define the series and shunt DCES as follows:

- Series DCES can be understood as a voltage source that is controllable and is connected in series with a non-critical load.

- Shunt DCES operate similar to a current source which is controllable and is connected to both positive and negative polarity of the main DC system.

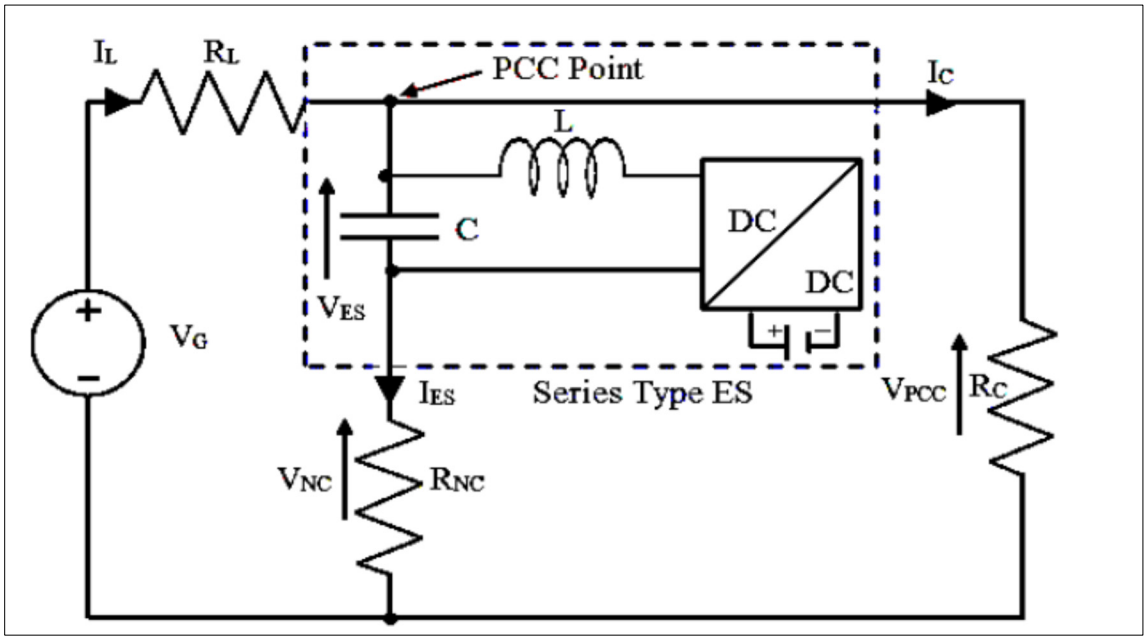

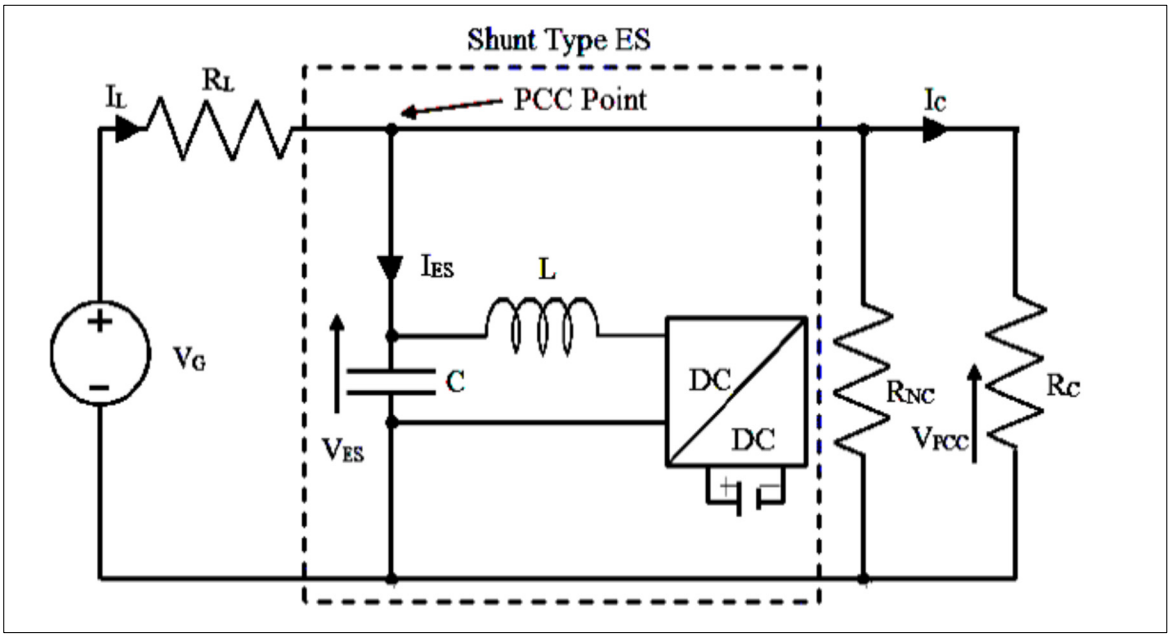

Figure. 2.4 Shunt and the series DCES
Taken from Hashem et al. (2018, P. 2)

The main differences between these two types of DCES are summarized in Table. 2.1 and a simple schematic is given in Figure. 2.4.

Table. 2.1. Comparison between the series and the shunt DCES (Hashem et al., 2018)

Point of comparison	**Series ES**	**Shunt ES**
Type of controller	Voltage source controller	NCL connected in parallel with ES
Type of Connection	NCL connected in series with ES	$V_{ES} = V_{ref}$
Voltage across ES	$V_{ES} = V_{ref} - I_{NC}R_{NC}$	$P_{ES} = V_{ES} I_{ES}$
Power across ES	$P_{ES} = V_{ref} I_{NC} - I_{NC}^2 R_{NC}$	$P_{ES} = V_{ES} I_{ES}$
Compensator	Indirect current compensator	Direct current compensator

In practical applications, both series and shunt DCESs are constructed using power converters, a power energy source such as battery energy storage, and the controlling loop for modulating the voltage of connecting bus.

2.1.4 Classification of the Non-Critical Load

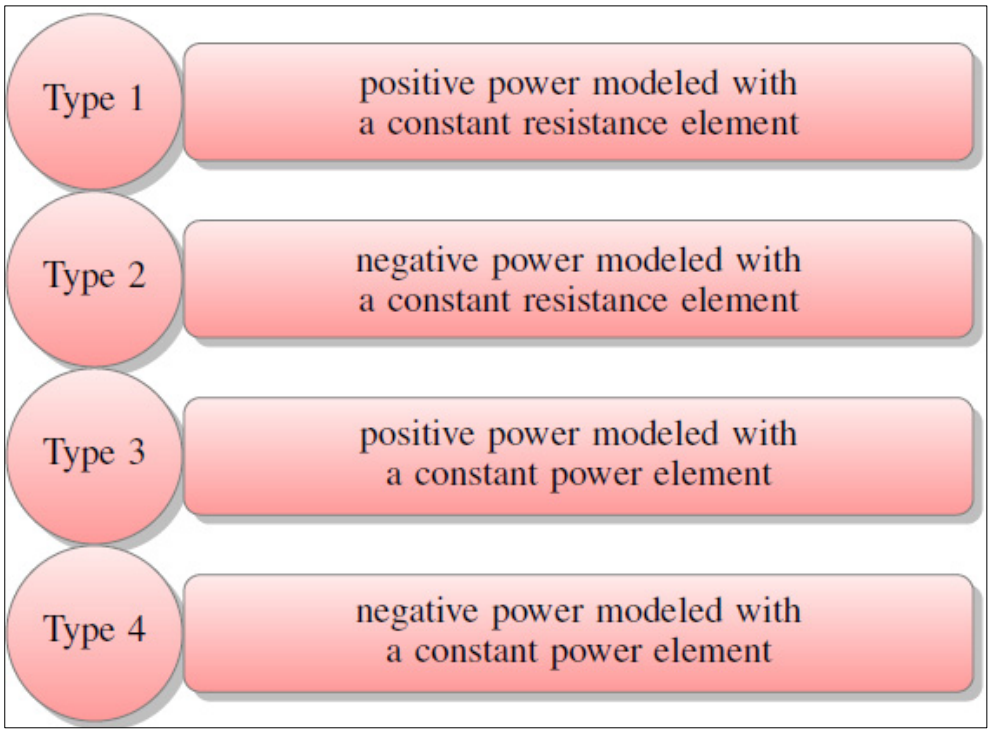

Figure. 2.5 Classification of the Non-Critical Load

Generally speaking, non-critical loads are categorized into the following four main types as shown in Figure. 2.5:

Type 1. positive power modeled with a constant resistance element

Type 2. negative power modeled with a constant resistance element

Type 3. positive power modeled with a constant power element

Type 4. negative power modeled with a constant power element

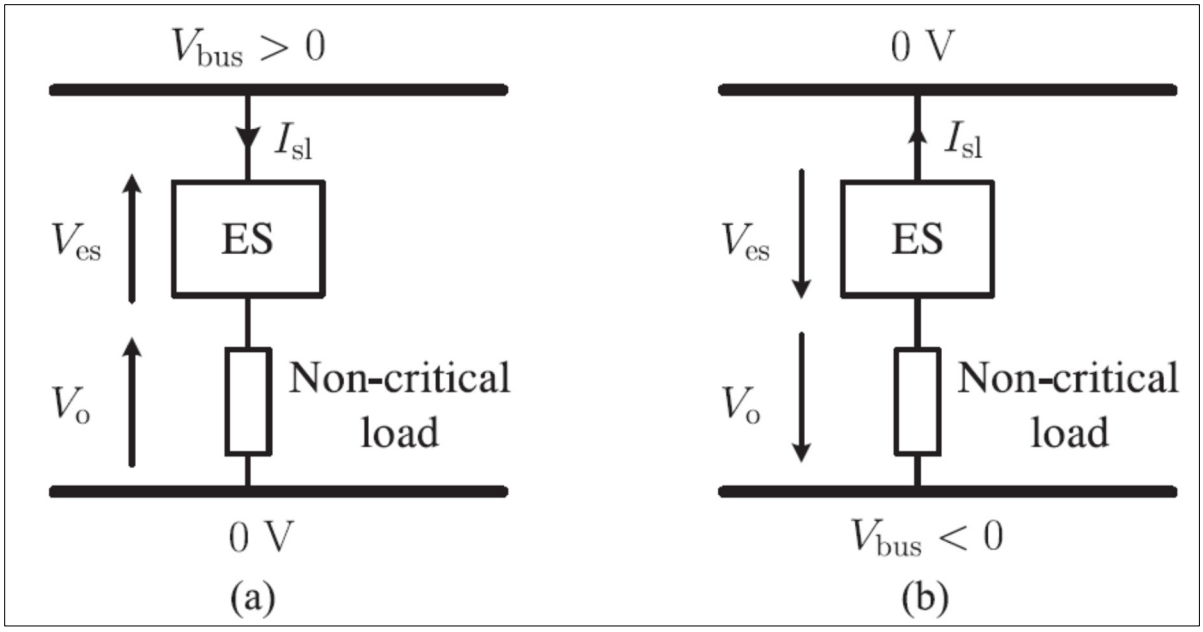

Figure. 2.6 Series connection of DCES & non-critical load (a) DCES supplied by positive side (b) DCES supplied by negative side
Taken from Mok et al. (2017, P. 4)

When positive, it means that it consumes power, and the model represents an actual load. In the case of negative power, the model represents a power generation source (Figure. 2.6). Depending on the type of connected bus there would be eight possible connection configurations (Mok et al., 2017).

2.2 Operation configuration and Operation Modes of DCES

In this section, the possible connection between DCES and non-critical load and the operation modes are reviewed.

2.2.1 Operation Configuration

Depending on the polarity of the connected DC bus and the load type, there are several possible configurations for the DCES connection to the non-critical load and the DC grid, as shown in Figure. 2.7.

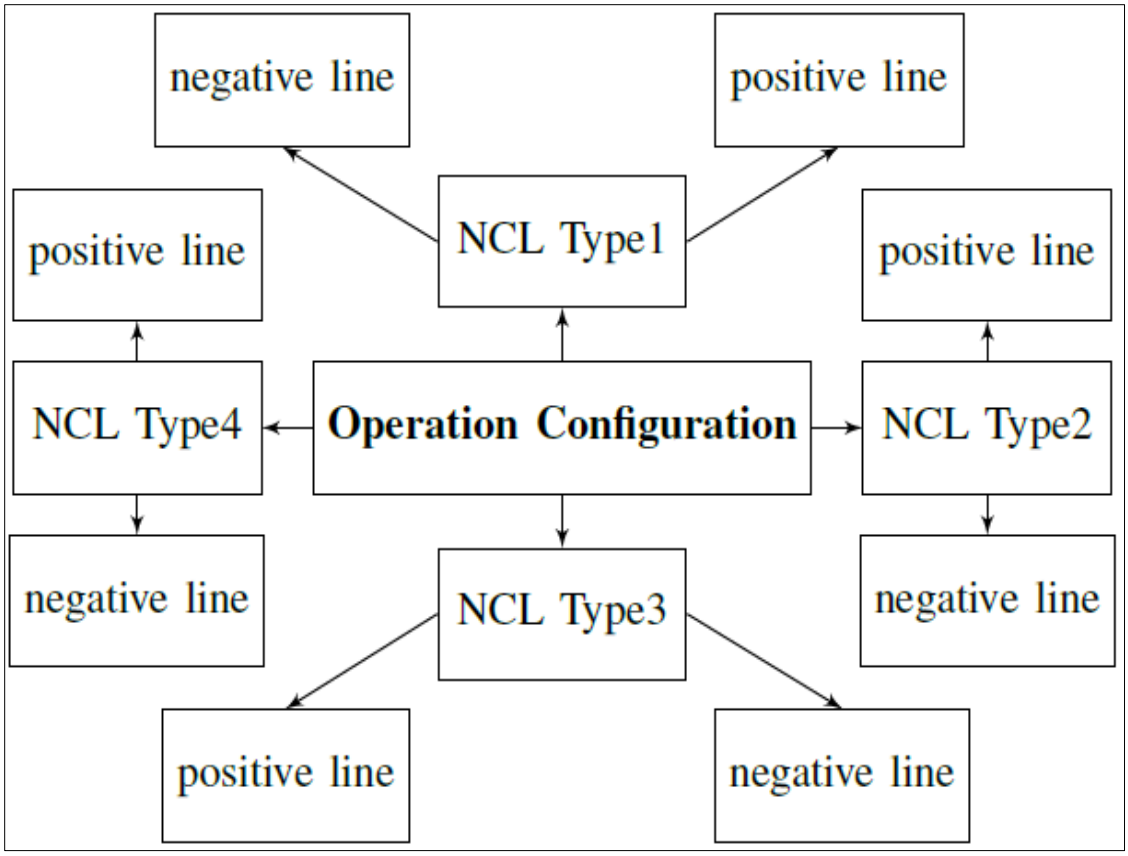

Figure. 2.7 Operation Configuration of DCES

2.2.1.1 Operation Configuration 1: Non-critical load Type 1 connected to the positive bus

In this operation configuration, the DCES is connected in series with a Type 1 non-critical load where the non-critical load is connected itself to the positive line.

2.2.1.2 Operation Configuration 2: Non-critical load Type 2 connected to the positive bus

In operation configuration 2 the DCES is connected in series with a Type 2 non-critical load. Also, the non-critical load is connected itself to the positive line.

2.2.1.3 Operation Configuration 3: Non-critical load Type 1 connected to the negative line

This operation configuration is similar to operation configuration 1 where the DCES is connected in series with a Type 1 non-critical load, however, the non-critical load is connected to the negative line.

2.2.1.4 Operation Configuration 4: Non-critical load Type 2 connected to the negative bus

Similarly, operation configuration 4 is the same as operation configuration 2 where the DCES is connected in series with a Type 2 non-critical load, however, the non-critical load is connected to the negative line.

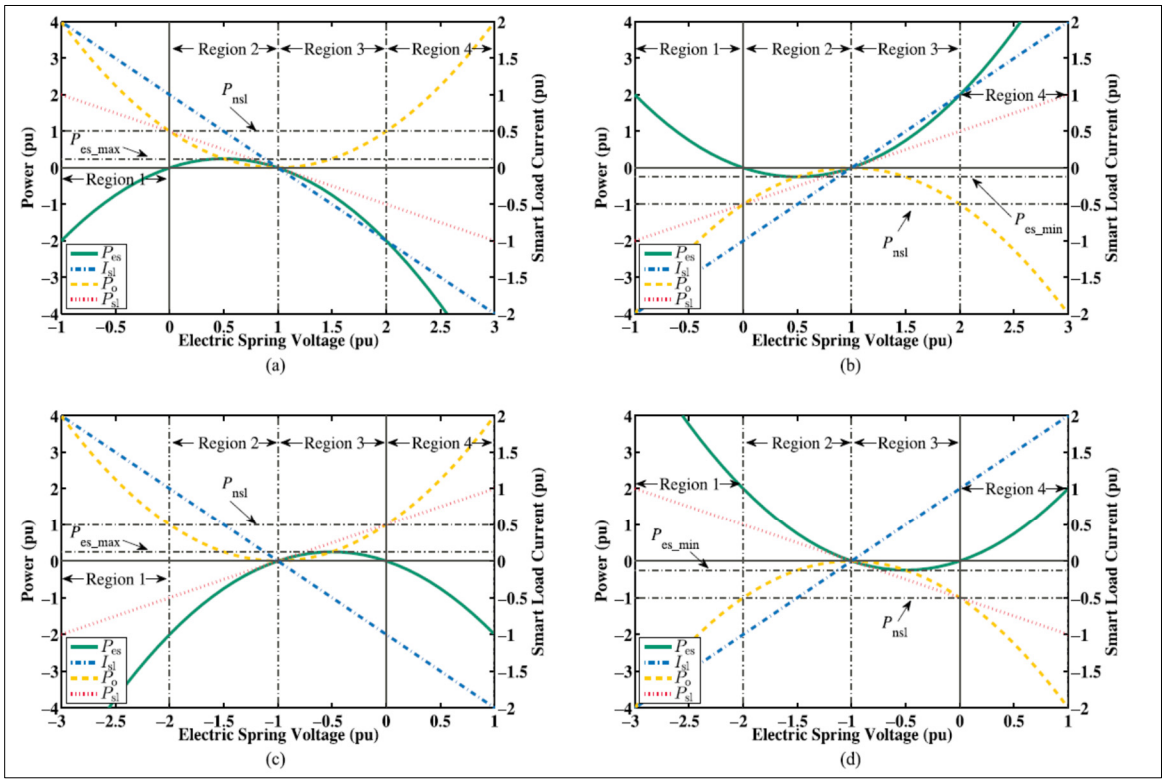

Figure. 2.8 DCES + non-critical load (so-called Smart Load) (a) Type 1 and load is connected to the positive side, (b) Type 2 and load is connected to the positive side, (c) Type

1 and load is connected to the negative side, (d) Type 2 and load is connected to the negative side
Taken from Mok et al. (2017, P. 5)

Table. 2.2. Operation configuration, case: Type 1, load is connected to the positive side
Taken from Mok et al. (2017, P. 5)

Region	V_{es} Range	$\lvert I_{sl}\rvert$	P_{es}	P_o	P_{sl}
1	$V_{es} < 0$	$> \lvert I_{nsl}\rvert$	< 0	$> P_{nsl}$	$> P_{nsl}$
2	$0 < V_{es} < V_{bus\_Ref}$	$< \lvert I_{nsl}\rvert$	> 0	$< P_{nsl}$	$< P_{nsl}$
3	$V_{bus\_Ref} < V_{es}$ and $V_{es} < 2V_{bus\_Ref}$	$< \lvert I_{nsl}\rvert$	< 0	$< P_{nsl}$	$< P_{nsl}$
4	$2V_{bus\_Ref} < V_{es}$	$> \lvert I_{nsl}\rvert$	< 0	$> P_{nsl}$	$< P_{nsl}$

Table. 2.3. Type 2, and load is connected to the positive side
Taken from Mok et al. (2017, P. 5)

Region	V_{es} Range	$\lvert I_{sl}\rvert$	P_{es}	P_o	P_{sl}
1	$V_{es} < 0$	$> \lvert I_{nsl}\rvert$	> 0	$< P_{nsl}$	$< P_{nsl}$
2	$0 < V_{es} < V_{bus\_Ref}$	$< \lvert I_{nsl}\rvert$	< 0	$> P_{nsl}$	$> P_{nsl}$
3	$V_{bus\_Ref} < V_{es}$ and $V_{es} < 2V_{bus\_Ref}$	$< \lvert I_{nsl}\rvert$	> 0	$> P_{nsl}$	$> P_{nsl}$
4	$2V_{bus\_Ref} < V_{es}$	$> \lvert I_{nsl}\rvert$	> 0	$< P_{nsl}$	$> P_{nsl}$

Table. 2.4. DCES Operation configuration, case: Type 1, and load is connected to the negative side
Taken from Mok et al. (2017, P. 5)

Region	V_{es} Range	$\lvert I_{sl}\rvert$	P_{es}	P_o	P_{sl}
1	$V_{es} < 2V_{bus\_Ref}$	$> \lvert I_{nsl}\rvert$	< 0	$> P_{nsl}$	$< P_{nsl}$
2	$2V_{bus\_Ref} < V_{es}$ and $V_{es} < V_{bus\_Ref}$	$< \lvert I_{nsl}\rvert$	< 0	$< P_{nsl}$	$< P_{nsl}$
3	$V_{bus\_Ref} < V_{es} < 0$	$< \lvert I_{nsl}\rvert$	> 0	$< P_{nsl}$	$< P_{nsl}$
4	$0 < V_{es}$	$> \lvert I_{nsl}\rvert$	< 0	$> P_{nsl}$	$> P_{nsl}$

Table. 2.5. DCES Operation configuration, case: Type 2, and load is connected to the negative side
Taken from Mok et al. (2017, P. 5)

Region	V_{es} Range	$\lvert I_{sl}\rvert$	P_{es}	P_o	P_{sl}
1	$V_{es} < 2V_{bus\_Ref}$	$> \lvert I_{nsl}\rvert$	> 0	$< P_{nsl}$	$> P_{nsl}$
2	$2V_{bus\_Ref} < V_{es}$ and $V_{es} < V_{bus\_Ref}$	$< \lvert I_{nsl}\rvert$	> 0	$> P_{nsl}$	$> P_{nsl}$
3	$V_{bus\_Ref} < V_{es} < 0$	$< \lvert I_{nsl}\rvert$	< 0	$> P_{nsl}$	$> P_{nsl}$
4	$0 < V_{es}$	$> \lvert I_{nsl}\rvert$	> 0	$< P_{nsl}$	$< P_{nsl}$

In the case where the non-critical load is modeled using a constant power model, (Type 3 and Type 4), the operation configurations are as follows:

2.2.1.5 Operation Configuration 5: Non-critical load Type 3 connected to the positive bus

In this operation configuration, the DCES is connected in series with a Type 3 non-critical load where the non-critical load is connected itself to the positive line.

2.2.1.6 Operation Configuration 6: Non-critical load Type 4 connected to the positive bus

In operation configuration 6 the DCES is connected in series with a Type 4 non-critical load. Also, the non-critical load is connected itself to the positive line.

2.2.1.7 Operation Configuration 7: Non-critical load Type 3 connected to the negative line

This operation configuration is similar to operation configuration 5 where the DCES is connected in series with a Type 3 non-critical load, however, the non-critical load is connected to the negative line.

2.2.1.8 Operation Configuration 8: Non-critical load Type 4 connected to the negative bus

Similarly, operation configuration 8 is the same as operation configuration 6 where the DCES is connected in series with a Type 4 non-critical load, however, the non-critical load is connected to the negative line.

A summary of all operation configurations od DCES is given in Figure. 2.8 and Figure. 2.9 and Table. 2.2 to Table. 2.9.

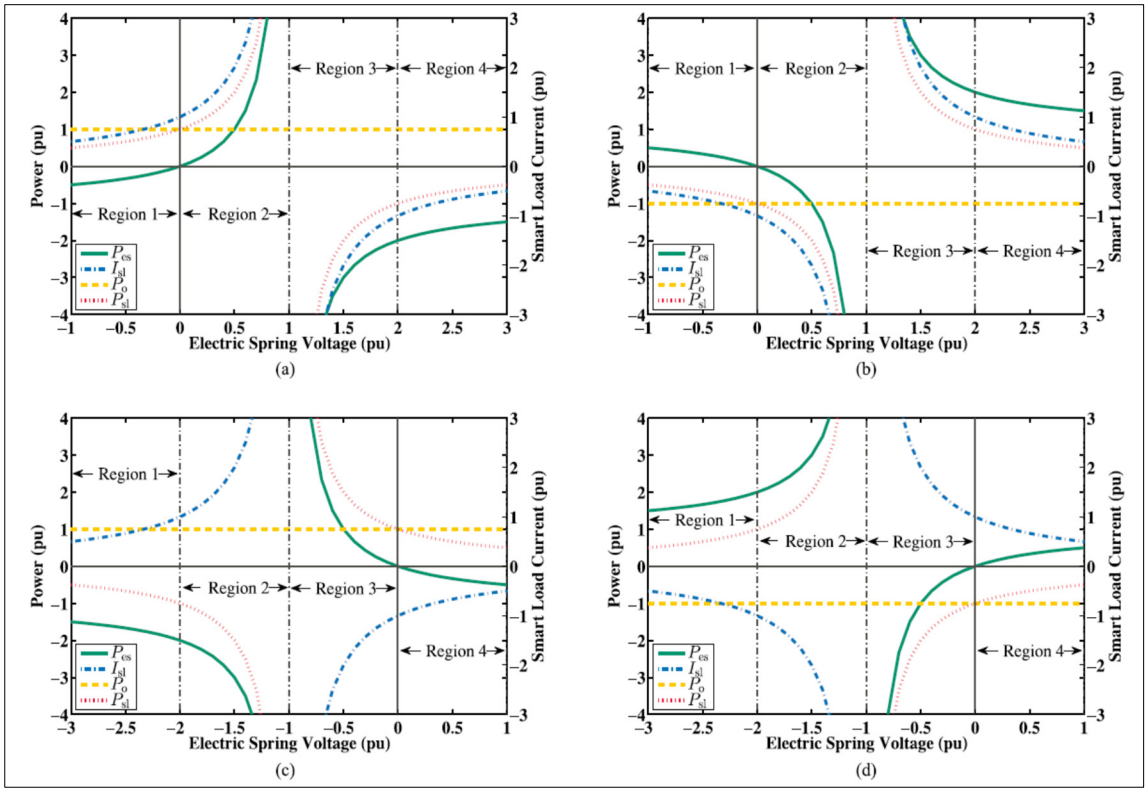

Figure. 2.9 DCES + non-critical load (so-called Smart Load) (a) Type 3 and load is connected to the positive side, (b) Type 4 and load is connected to the positive side, (c) Type 3 and load is connected to the negative side, (d) Type 4 and load is connected to the negative side

Taken from Mok et al. (2017, P. 7)

Table. 2.6. DCES Operation configuration, case: Type 3, and load is connected to the positive side

Taken from Mok et al. (2017, P. 7)

Region	V_{es} Range	$\lvert I_{sl}\rvert$	P_{es}	P_{sl}
1	$V_{es} < 0$	$< \lvert I_{nsl}\rvert$	< 0	$< P_{nsl}$
2	$0 < V_{es} < V_{bus\_Ref}$	$> \lvert I_{nsl}\rvert$	> 0	$> P_{nsl}$
3	$V_{bus\_Ref} < V_{es} < 2V_{bus\_Ref}$	$> \lvert I_{nsl}\rvert$	< 0	$< P_{nsl}$
4	$2V_{bus\_Ref} < V_{es}$	$< \lvert I_{nsl}\rvert$	< 0	$< P_{nsl}$

Table. 2.7. DCES Operation configuration, case: Type 4, and load is connected to the positive side
Taken from Mok et al. (2017, P. 7)

Region	V_{es} Range	$\lvert I_{sl}\rvert$	P_{es}	P_{sl}
1	$V_{es} < 0$	$< \lvert I_{nsl}\rvert$	> 0	$> P_{nsl}$
2	$0 < V_{es} < V_{bus\_Ref}$	$> \lvert I_{nsl}\rvert$	< 0	$< P_{nsl}$
3	$V_{bus\_Ref} < V_{es} < 2V_{bus\_Ref}$	$> \lvert I_{nsl}\rvert$	> 0	$> P_{nsl}$
4	$V_{bus} < V_{es}$	$< \lvert I_{nsl}\rvert$	> 0	$> P_{nsl}$

Table. 2.8. DCES Operation configuration, case: Type 3, and load is connected to the negative side
Taken from Mok et al. (2017, P. 7)

Region	V_{es} Range	$\lvert I_{sl}\rvert$	P_{es}	P_{sl}
1	$V_{es} < 2V_{bus\_Ref}$	$< \lvert I_{nsl}\rvert$	< 0	$< P_{nsl}$
2	$2V_{bus\_Ref} < V_{es} < V_{bus\_Ref}$	$> \lvert I_{nsl}\rvert$	< 0	$< P_{nsl}$
3	$V_{bus\_Ref} < V_{es} < 0$	$> \lvert I_{nsl}\rvert$	> 0	$> P_{nsl}$
4	$0 < V_{es}$	$< \lvert I_{nsl}\rvert$	< 0	$< P_{nsl}$

Table. 2.9. DCES Operation configuration, case: Type 4, and load is connected to the negative side
Taken from Mok et al. (2017, P. 7)

Region	V_{es} range	$\lvert I_{sl}\rvert$	P_{es}	P_{sl}
1	$V_{es} < 2V_{bus\_Ref}$	$< \lvert I_{nsl}\rvert$	> 0	$> P_{nsl}$
2	$2V_{bus\_Ref} < V_{es} < V_{bus\_Ref}$	$> \lvert I_{nsl}\rvert$	> 0	$> P_{nsl}$
3	$V_{bus\_Ref} < V_{es} < 0$	$> \lvert I_{nsl}\rvert$	< 0	$< P_{nsl}$
4	$0 < V_{es}$	$< \lvert I_{nsl}\rvert$	> 0	$> P_{nsl}$

2.2.2 Operation Mode

When a DCES is connected in parallel with the non-linear load, the shunt DCES, the operation of the DCES does not depend on the connection configuration. However, in the case of the series DCES, more operation modes are feasible. All possible operation modes of DCES are shown in Figure. 2.10

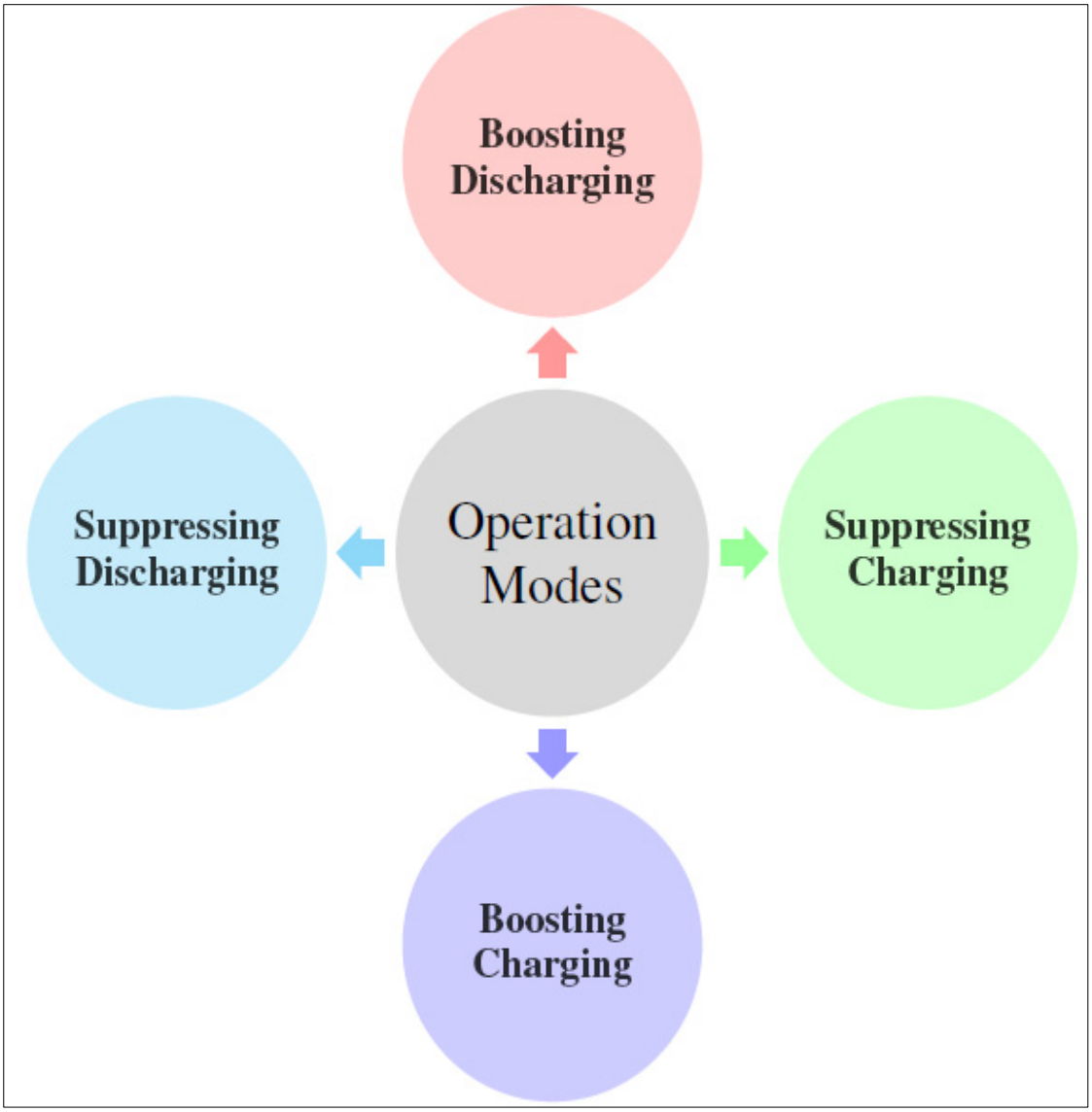

Figure. 2.10 Operation Modes of DCES

According to the configuration of series and shunt DCESs, the KVL rule for each configuration is as follows:

- Series DCES:

$$V_{ES} = V_{PCC\_ref} - I_{NC} \times R_{NC} \quad (2.1)$$

$$P_{ES} = V_{PCC\_ref} * I_{NC} - I^2{}_{NC} \times R_{NC} \quad (2.2)$$

- Shunt DCES

$$V_{ES} = V_{PCC\_ref} \quad (2.3)$$

$$P_{ES} = V_{ES} \times I_{ES} \quad (2.4)$$

where

P_{ES}: the active power of DCES and

V_{PCC_ref}: the reference value for the voltage of the connection point

2.2.2.1 Boosting & Discharging operation mode

This operation mode is called the BD operation mode.

- the series DCES tries to enhance the voltage of the connected DC bus. To do so, the power source has to discharge and provide energy to the DC microgrid. In this case:

$$V_{PCC} < V_{ES} \quad (2.5)$$

$$-I_{OC} < I_{ES} < 0 \quad (2.6)$$

and I_{OC} is the maximum value for the current of the non-critical load.

- The shunt DCES operates similarly to an auxiliary power supply source.

$$V_{ES} = V_{PCC} \quad (2.7)$$

$$I_{Dis\_max} < I_{ES} < 0 \quad (2.8)$$

and I_{Dis_max} is the maximum value for the discharging current of shunt DCES.

2.2.2.2 Suppressing & Discharging operation mode

This operation mode is called the SD operation mode.

- the series DCES tries to suppress the voltage of the connected DC bus and the energy source provides power to the main DC system. In addition:

$V_{ES} < 0$ (2.9)

$I_{NC\_nom} < I_{ES} < I_{OC}$ (2.10)

and I_{NC_nom}: the nominal value for the current of the non-critical load

The shunt DCES is not able to operate in this mode.

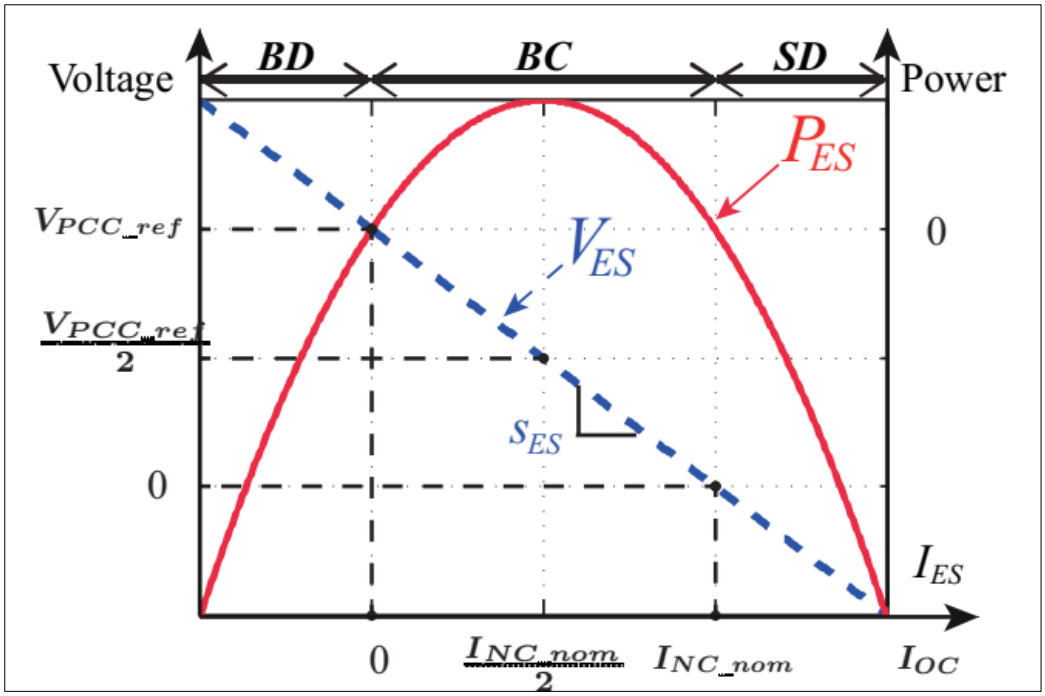

Figure. 2.1 The characteristic curve of operation modes of series DCES
Taken from M. H. Wang et al. (2015, P. 3)

2.2.2.3 Boosting & Charging operation mode

This operation mode is called the BC operation mode.

- The series DCES draws current from the connected DC bus in order to charge its battery and enhances the voltage of the connected load simultaneously. Also,

$0 < V_{ES} < V_{PCC}$ (2.11)

$0 < I_{ES} < I_{NC\_nom}$ (2.12)

- The shunt DCES is not able to operate in this mode.

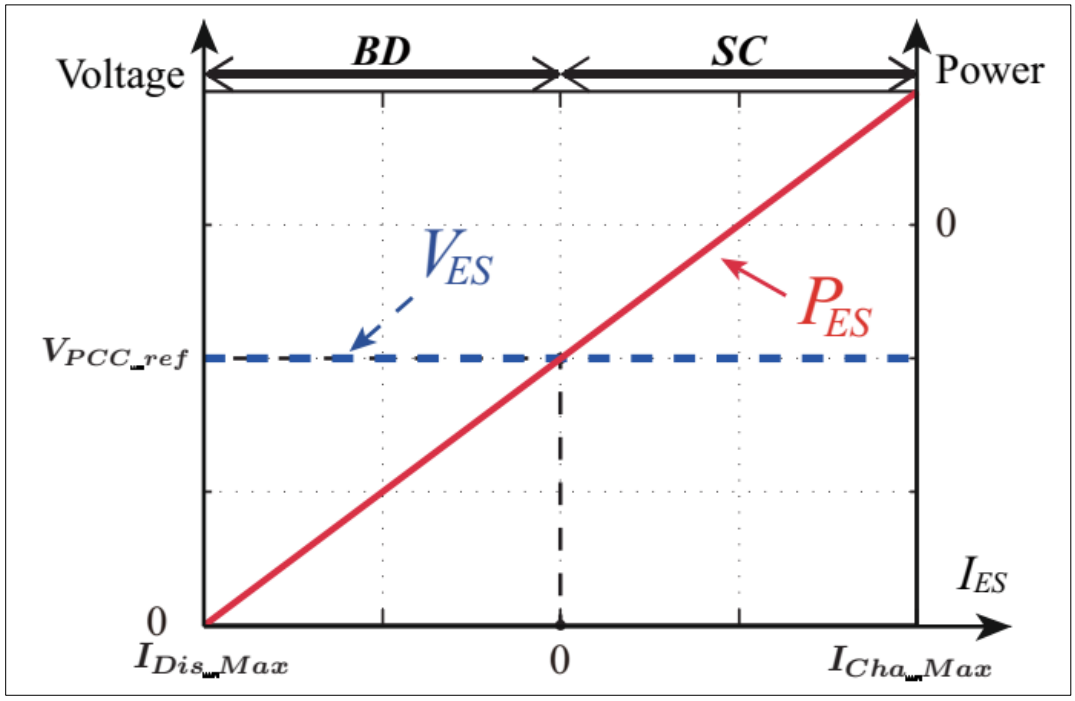

Figure. 2.1 The characteristic curve of operation modes of shunt DCES
Taken from M. H. Wang et al. (2015, P. 3)

Figure. 2.1 Figure. 2.1 and Figure. 2.1 show the different operation modes of series and shunt DCES when the power is plotted against the voltage (M. H. Wang et al., 2015).

2.2.2.4 Suppressing & Charging operation mode

This operation mode is called SC operation mode.

- The series DCES is not able to operate in SC operation mode with a Type 1 non-linear load.
- The shunt DCES aims to suppress the voltage of the connected bus. At the same time, the power source of DCES operates in charging mode by drawing power from the main DC system. Also,

$$V_{ES} = V_{PCC} \tag{2.13}$$

$$0 < I_{ES} < I_{Cha\_max} \tag{2.14}$$

and I_{Cha_max} is the maximum value for the charging current of shunt DCES.

2.3 Conclusion

In this section, the characteristics of DCESs, as well as operation modes, and operation configurations, were reviewed. The so-called non-critical load (NCL) could be categorized into four types in which the positive term means that it consumes power, the model represents an actual load, and the negative term, the model represents a power generation source. According to the configuration of series and shunt DCESs, there are also eight possible configurations for DCES connection to the NCL and the DC grid. Subsequently, the four operation modes of a DCES and corresponding equations were reviewed.

CHAPTER 3

LITERATURE REVIEW

In this section, we try to review several proposed applications of DCES in the literature. Each application is studied separately, and the advantages and disadvantages are listed.

3.1 Suppression of unbalanced voltage situation in DC Distribution System

Refs. (Liao et al., 2020a) and (Liao et al., 2020b) propose a technique for the suppression of unbalanced voltage situations in a bipolar DC distribution network using DCES and decoupling controlling variables (see Figure. 3.1). With the help of KCL and KVL rules, the equations of a bipolar DC microgrid are developed. Then, the coupling equations of positive and negative buses of the DC microgrid are extracted based on the equivalent resistances of lines and loads. Later on, assuming that non-critical load and the converter can be modelled with a load and a controllable voltage source, the coupling equations of positive and negative buses are given as follows:

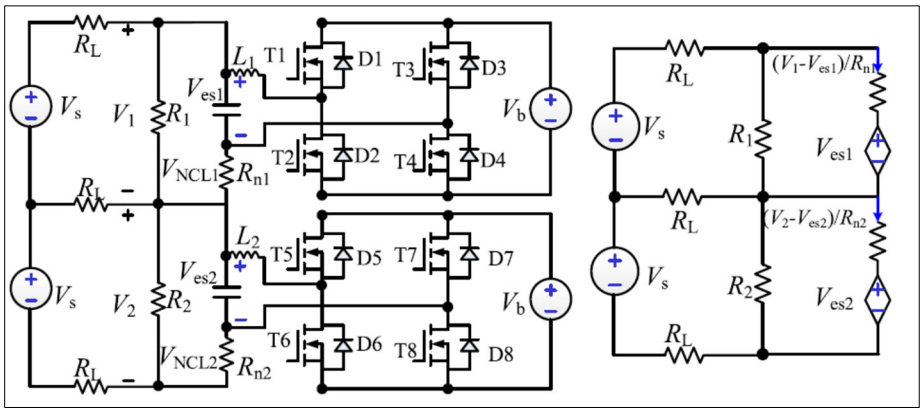

Figure. 3.1 The topology of DCESs in the bipolar DC distribution systems (left), and equivalent model (right)
Taken from Liao et al. (2020, P. 2)

$$V1 = a11Ves1 + a12Ves2 + c1Vs \quad (3.1)$$

$$V2 = a21Ves1 + a22Ves2 + c2Vs \quad (3.2)$$

where the coefficients are functions of modeled resistances.

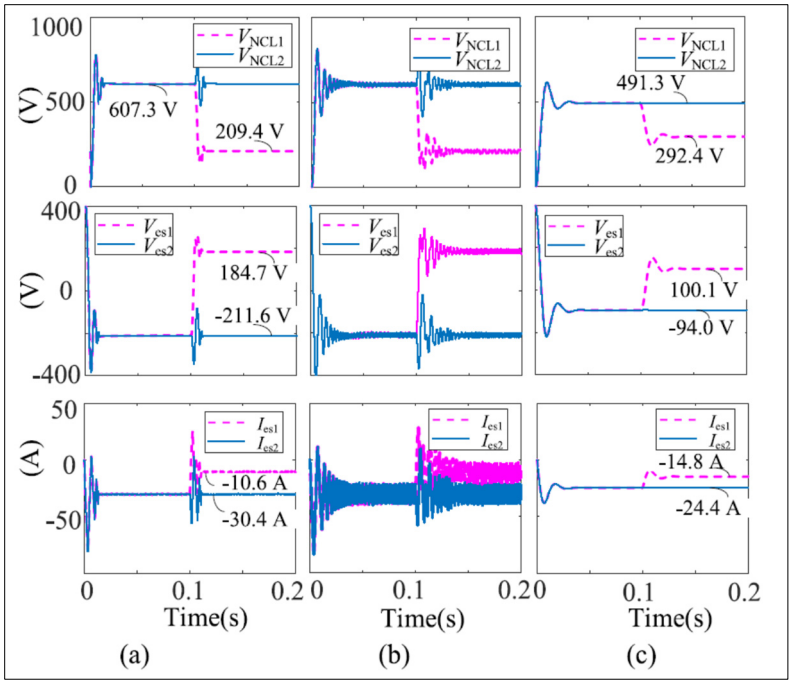

Figure. 3.2 Voltage & current of DCESs (a) with the proposed control method, (b) without the proposed control method, and (c) when the battery has a limited range of voltage
Taken from Liao et al. (2020, P. 9)

Finally, it is proven that by modulating the voltage of non-critical load, the unbalanced voltage of the main system is controlled. The factor for an unbalanced problem of voltage in a DC microgrid is defined as follows (Liao et al., 2020a):

$$\varepsilon\% = \frac{V_1 - V_2}{(V_1 + V_2)/2} \tag{3.3}$$

which can be expressed as:

$$\varepsilon\% = \frac{|RL(R_2 - R_1)|}{2RL(R_1 + R_2) + 4R1R2/3} \tag{3.4}$$

To evaluate the proposed idea, the small signal equivalent of the studied system is constructed while the output voltage of DCES is among the state variables. Next, the concept of the decoupling control method is formulated to control the voltages of negative and positive lines independently.

The simulation and experimental results (Figure. 3.2 and Figure. 3.3) show that when the decoupling controller approach is implemented on a DCES, the unbalanced voltage situations and the power loss will reduce considerably.

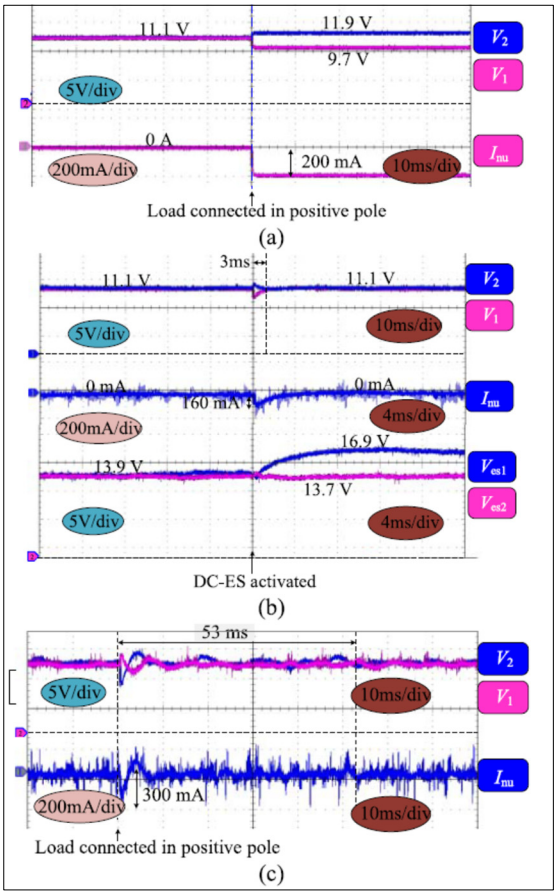

Figure. 3.3 Experimental results: (a) without DCES, (b) DCESs with proposed control method (c) DCESs without proposed control method
Taken from Liao et al. (2020, P. 11)

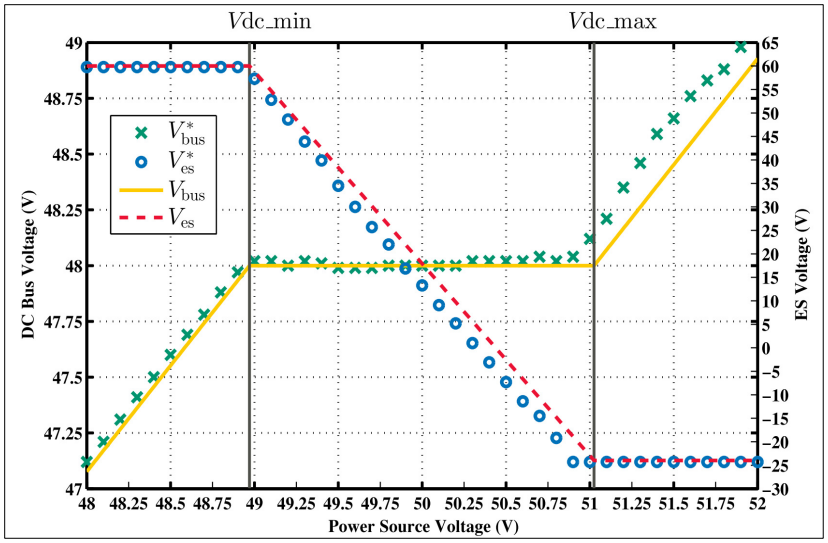

Figure. 3.4 Analytical analysis results versus experimental results for Type 1 noncritical load, * means measured values
Taken from Mok et al. (2017, P. 12)

This approach has the following advantages and pitfalls:

Pros:

- ✓ The proposed method is based on strong mathematical concepts and is a robust scheme
- ✓ An easy approach to develop the small-signal equivalent of the main microgrid.

Cons:

- × Difficult to implement
- × The effectiveness of the proposed method is to be evaluated in the case of other types of non-critical loads.
- × The proposed method to be evaluated in the presence of multiple DCESs.

3.2 DC Power Distribution Systems Stabilizing

Ref. (Mok et al., 2017) proposes the application of DCES as an active suspension tool for dynamic voltage regulation. This work starts with the analysis of a series DCES with/without the resistance of the main system. Then, an experimental setup is built for evaluating the performance of the studied series DCES under different conditions. Several cases are simulated and tested such as unstable supply-side voltage variation and voltage drop.

In the case of standalone series DCES, it is assumed that the voltage of the main grid is fixed. Some results of this analysis were presented in the previous section. However, in actual DC microgrids, the amplitudes of voltages across the buses vary with time and are not constant. A DCES can provide voltage stability service when properly controlled. For the case in which the voltage of the main DC system is not stable, the simulation and test scenarios are conducted over both Type 1 and Type 3 non-critical loads. From analytical study and it is shown that:

For Type 3 non-critical load:

$$\boldsymbol{V}_{bus} = \frac{R_o R_c}{R_o R_c + R_c R_d + R_d R_o} \times (V_{DC} + \frac{R_d}{R_o} V_{es}) \tag{3.5}$$

For Type 1 non-critical load:

$$\boldsymbol{V}_{bus} = \frac{\mathrm{RcV}_{DC} + \mathrm{RcV}_{es} + \mathrm{RdV}_{es} \pm \sqrt{(\mathrm{RcV}_{DC} + \mathrm{RcV}_{es} + \mathrm{RdV}_{es})2 - 4(\mathrm{Rc} + \mathrm{Rd})(\mathrm{RcV}_{DC}\mathrm{V}_{es} + \mathrm{RdRcPo})}}{2(Rc + Rd)} \tag{3.6}$$

where *Po* is the power of the non-critical load.

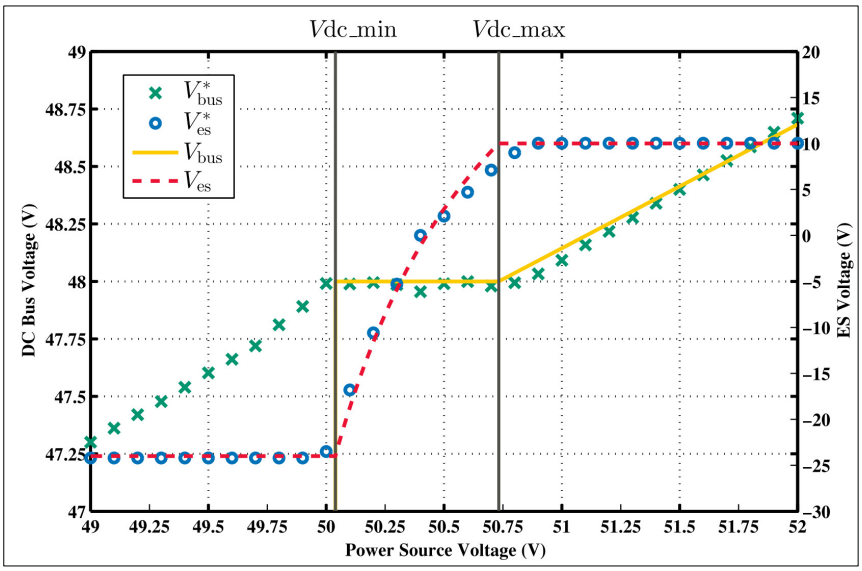

Figure. 3.5 Analytical analysis results versus experimental results for Type 3 noncritical load, * means measured values
Taken from Mok et al. (2017, P. 13)

With the help of the above equations, V_{bus} can be controlled. The comparison between the analytical results and the experimental results proves the precision of the analytical approach (see Figure. 3.4 and Figure. 3.5).

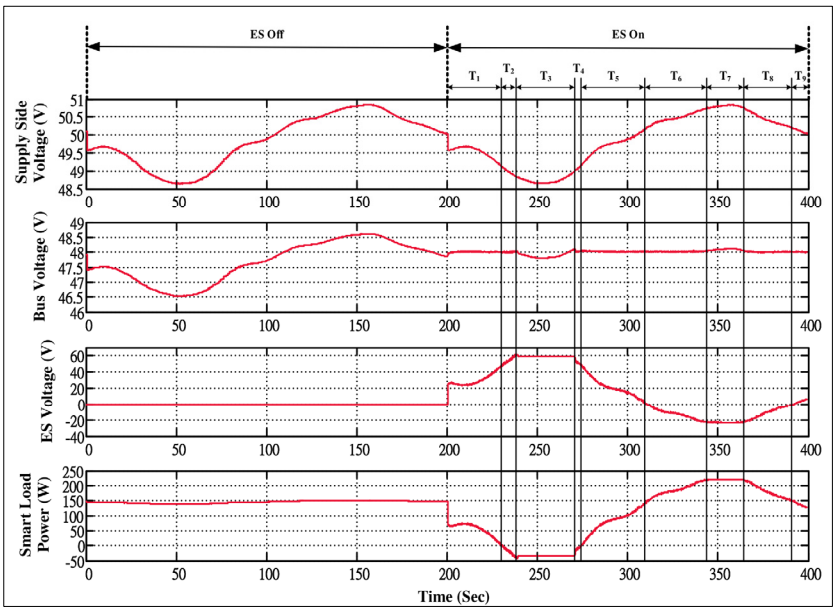

Figure. 3.6 Experimental results with Type 1 non-linear load (DCES turns on at t= 200ms)
Taken from Mok et al. (2017, P. 14)

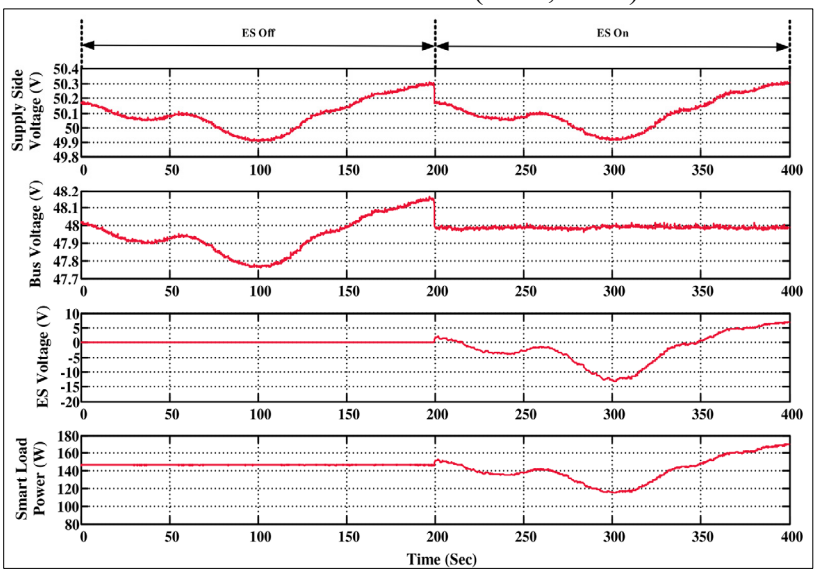

Figure. 3.7 Experimental results with Type 3 non-linear load (the DCES system turns on at t= 200ms)
Taken from Mok et al. (2017, P. 15)

For the experimental scenarios, the main voltage source of DC micro fluctuates with time. The performance of series DCES is tested for regulating the voltage. The achieved results show that a series DCES when turns on, can effectively enhance voltage stability (see Figure. 3.6 and Figure. 3.7).

As the last result, the impact of series DCES on the voltage drop of the DC microgrid is studied using the benchmark shown in Figure. 3.8.

simulation and experimental results prove that with a DCES the voltage amplitudes across the system are increased and stabilized around acceptable points of operations under heavy-load conditions (Figure. 3.9).

The advantages and disadvantages of the proposed application for stabilizing the DC system could be summarized as follows:

Pros:

- ✓ highly recommended for any further study in this domain.
- ✓ Several aspects of DCES are studied.
- ✓ the proposed method is based on strong mathematical concepts.
- ✓ Experimental results are remarkably close to analytical results.

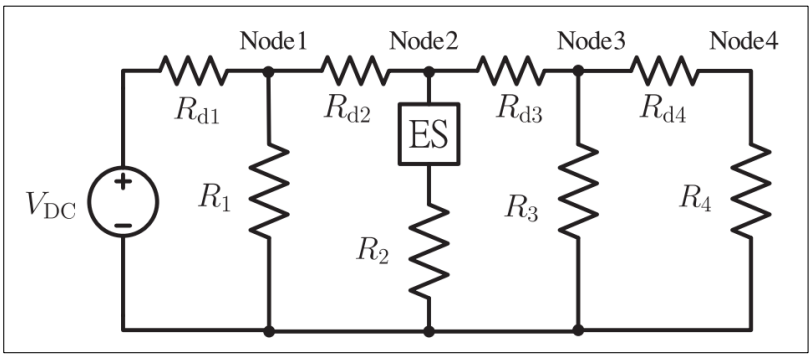

Figure. 3.8 The benchmark for voltage drop study
Taken from Mok et al. (2017, P. 15)

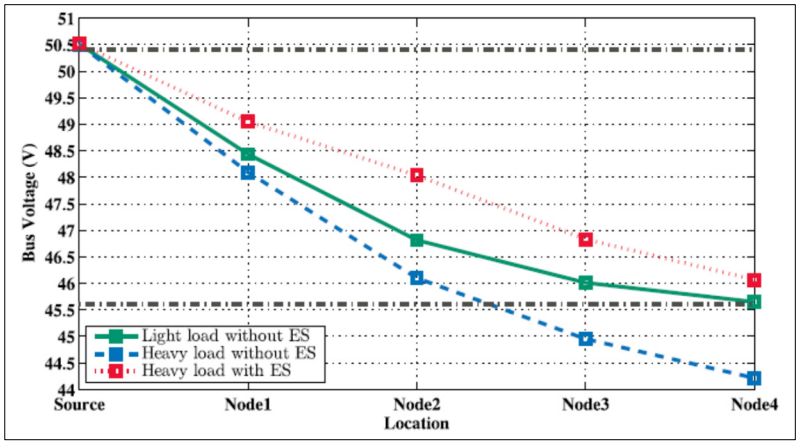

Figure. 3.9 The voltage level of each node with experiment results
Taken from Mok et al. (2017, P. 16)

Cons:

- × Difficult to implement the experimental setup
- × The effectiveness of the proposed method is to be evaluated in the case of other types of non-critical loads.
- × The proposed method to be evaluated in the presence of multiple DCESs

3.3 Active Damping Control of DC Microgrids

The role of distributed DCES as equipment for active damping control in DC microgrids is studied in (Hosseinipour & Hojabri, 2020). The studied single-bus DC microgrid is shown in Figure. 3.10.

To determine the dominant frequencies of a microgrid, the small-signal equivalent model is extracted. The studied series DCES is a full-bridge bipolar PWM-controlled converter and battery energy storage. The linearized equivalent block diagram model of the series DCES controller is shown in Figure. 3.11 where:

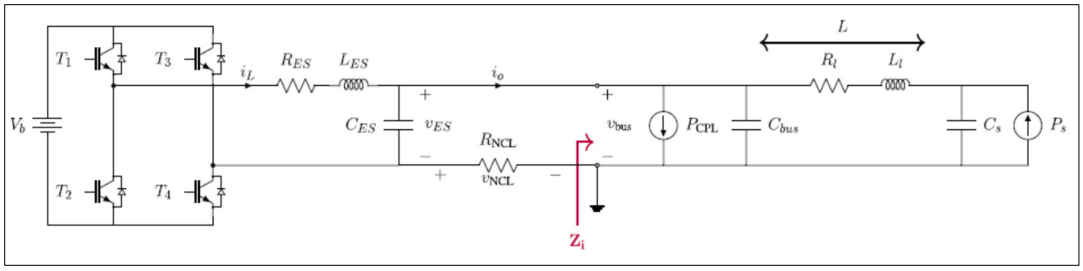

Figure. 3.10 Studied single-bus DC microgrid with a series DCES
Taken from Hosseinipour & Hojabri. (2020, P. 3)

$G_{vd}(s)$: open-loop function

$Z_{out}(s)$: open-loop function

$G_v(s)$: voltage compensator (PID controller)

$GM(s)$: modulator gain

Two major concerns regarding the control approaches of common series DCES are the need for an auxiliary circuit and the adverse effect on the power quality of some power constant loads. To overcome these issues, the proposed scheme applies the so-called virtual R&C damper impedance, Gvir(s) in Figure. 3.11, for enhancing the response of DCES and supporting the DC microgrid stabilization (see Figure. 3.12 and Figure. 3.13).

$$G\text{vir}(s) = \frac{1}{\text{Zvir}(s)}\left(RdGv(s) + \frac{\text{Zout}(s)}{Gvd(s)}\right) \qquad \text{s} \qquad (3.7)$$

and $Zvir(s) = Rvir + \frac{1}{sCvir}$

The results of the analysis show that:

- ✓ The proposed scheme can be applied to multiple DCESs.
- ✓ the more DCESs employed, the more low-frequency damping improves.
- ✓ The adverse impact of two close DCESs is insignificant.

Regarding the proposed scheme, the following points could be mentioned:

Pros:

- ✓ Several technical aspects of DCES are addressed.
- ✓ the proposed method is based on strong mathematical concepts.
- ✓ The possibility of installing several DCES is studied.

Cons:

- × The effectiveness of the proposed method is to be evaluated in the other types of NCL.
- × Difficult to be implemented.
- × The effectiveness of the proposed scheme is to be validated against other proposed methods in the literature.

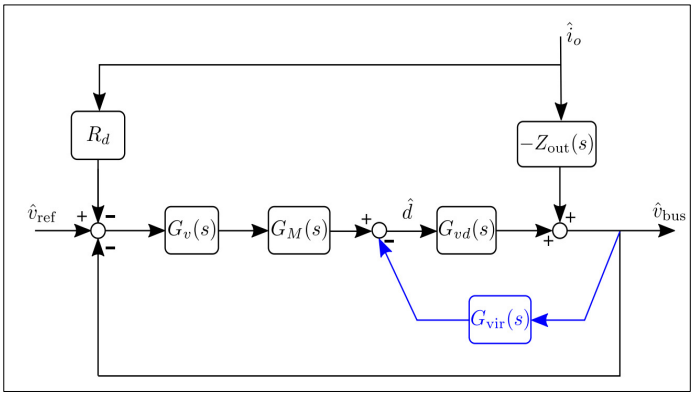

Figure. 3.11 linearized equivalent model of series DCES controller
Taken from Hosseinipour & Hojabri. (2020, P. 3)

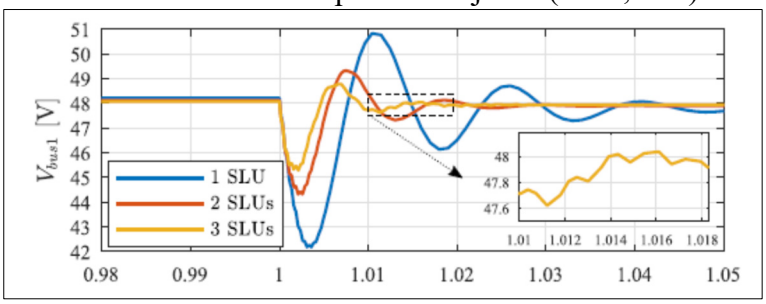

Figure. 3.12 Performance of multiple smart loads and the behavior of the DC bus voltage
Taken from Hosseinipour & Hojabri. (2020, P. 9)

3.4 Reducing Dependency of DC Microgrids to Main Grid

The impact of DCES on the dependability of DC microgrids to the main grid is studied in Ref. (Charan Cherukuri et al., 2019). Using MATLAB software, a microgrid including a DCES in series with a non-critical load is developed (see Figure. 3.14)

To decrease drawn power from the main grid, the power consumption of the non-critical load is partially reduced by modulating its voltage. To do so, first, the power equation is developed:

$P_S+P_G=P_C+P_{NC}+P_{loss}$

where

P_S: the power of modeled renewable energy source

P_G: power drawn from the main grid

P_C: the demand of the critical load

P_{NC}: the demand of the non-critical load

P_{loss}: active power loss of the microgrid

Then, the energy drawn from the main grid is calculated as follows:

$$E_G = \int_0^T P_G dt = \int_0^T P_C dt + \int_0^T P_{NC} dt + \int_0^T P_{loss} dt - \int_0^T P_S dt \quad (3.8)$$

finally, it is shown that:

$$E_G - E_G^{ES} = \begin{pmatrix} \int_0^T P_{NC} dt \geq \int_0^T P_{NC}^{ES} dt, \\ \int_0^T P_{loss} dt \geq \int_0^T P_{loss}^{ES} dt, \end{pmatrix}, E_G \geq E_G^{ES} \quad (3.9)$$

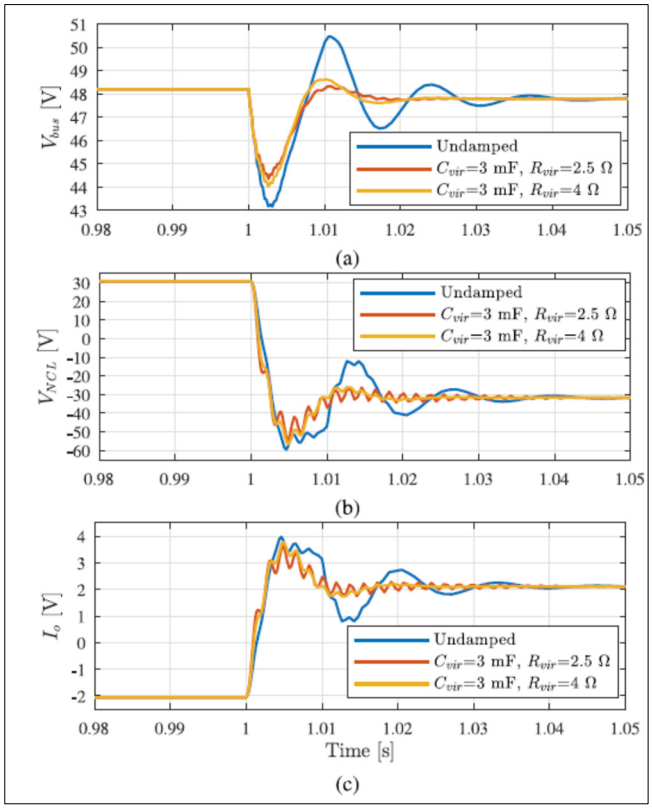

Figure. 3.13 Impact of virtual RC impedance scheme on DC bus and non-critical load
Taken from Hosseinipour & Hojabri. (2020, P. 9)

which means with employing DCES, the required energy reduces. As shown in Figure. 3.15, simulation results also confirm that DCES can be employed to minimize the dependency on the main power network.

Pros:

- ✓ the proposed method can be employed easily to prove the idea.
- ✓ The possibility of installing several DCES is studied.

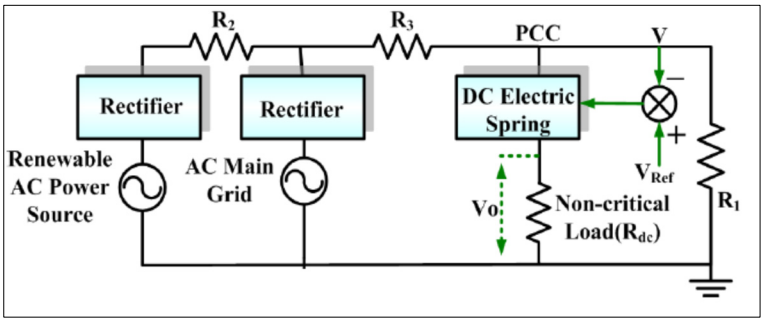

Figure. 3.14 Schematic of studied DC microgrid
Taken from Charan Cherukuri et al. (2019, P. 3)

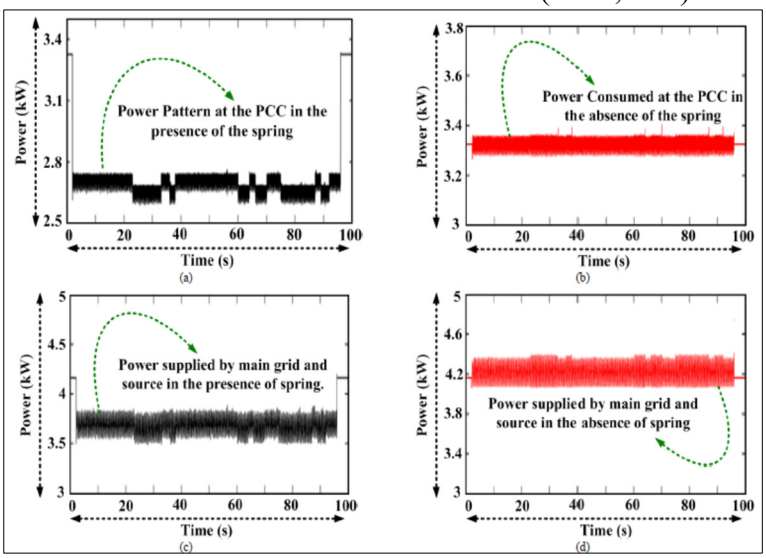

Figure. 3.15 (a) PCC Power pattern (with DCES) (b) PCC power (without DCES) (c) Power exchange with the main grid (with DCES) (d) Power exchange with the main grid (without DCES)
Taken from Charan Cherukuri et al. (2019, P. 5)

Cons:

- × Several assumptions were made for simplifying the problem.

× The effectiveness of the proposed scheme is to be validated against other proposed methods in the literature.

3.5 DCES Energy Management System for Voltage Stability of connected DC Bus

A topology for household application of DCES is proposed in Refs. (Zha et al., 2019)(Q. Wang et al., 2020) (see Figure. 3.16) for power quality and voltage stability issues in DC microgrids. It comprises an energy storage system and a DC/DC three-port converter. The three-port converter supplies a PV and both non-critical and critical loads (see Figure. 3.17). For the studied DCES, four operation modes are defined:

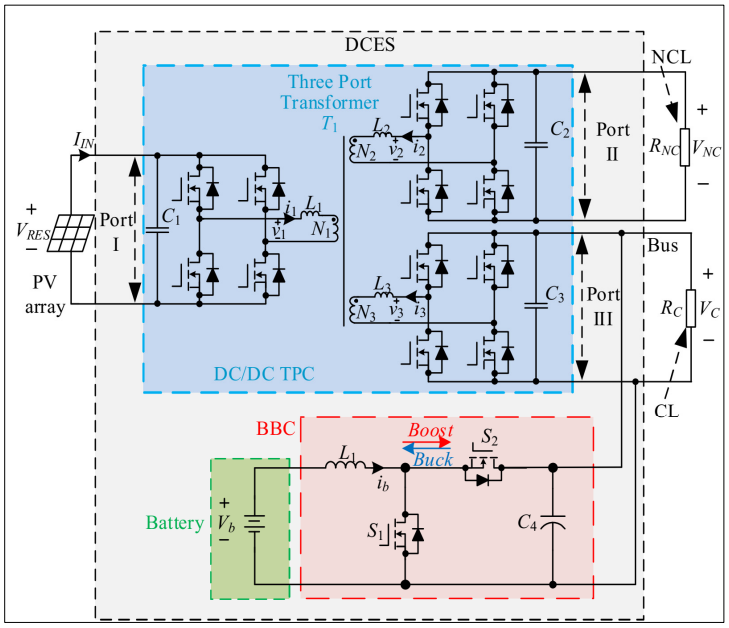

Figure. 3.16 Proposed DCES topology
Taken from Q. Wang et al. (2020, P. 3)

- Mode 1: BES Discharging

The PV is unable to provide completely the load. DCES also operates at its maximum capability. The BES is discharged to compensate for mismatch power.

- Mode 2: BES Balancing

The PV produces its maximum power, and the voltage of the critical load is within an acceptable range. The BES absorbs a little power to maintain its SOC level.

- Mode 3: BES Charging

In this mode, the power generated by PV is more than the demand of the critical and non-critical loads. Therefore, the BES operates in charging mode and establishes a balance between generation and consumption.

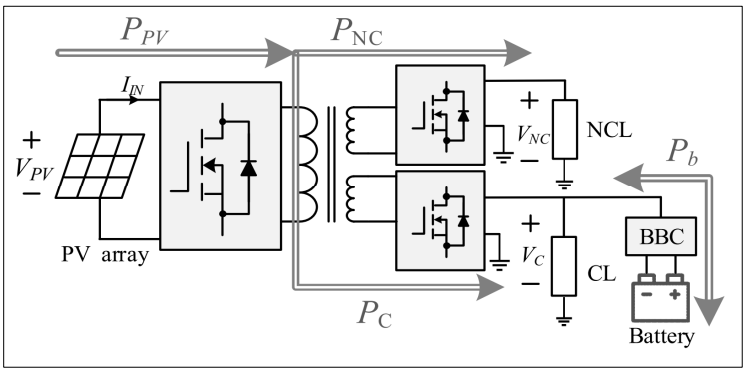

Figure. 3.17 The general structure of PV, DCES, and battery energy storage connection
Taken from Q. Wang et al. (2020, P. 3)

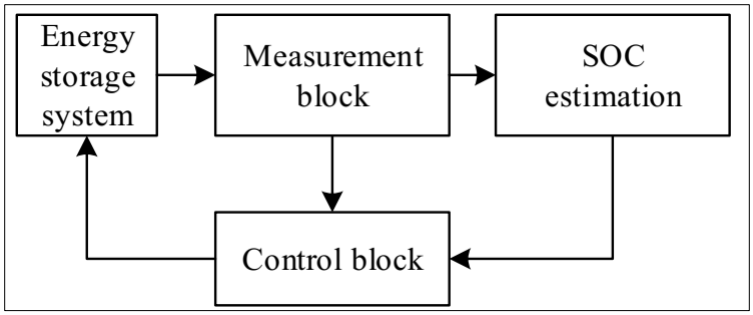

Figure. 3.18 The schematic of the proposed energy management system
Taken from Q. Wang et al. (2020, P. 4)

All these actions are controlled using a so-called energy management system which its general structure and the operation control logic are shown in Figure. 3.18 and Figure. 3.19 where the logic values Q1 and Q2 are considered for controlling the operation modes as defined in Table. 3.1.

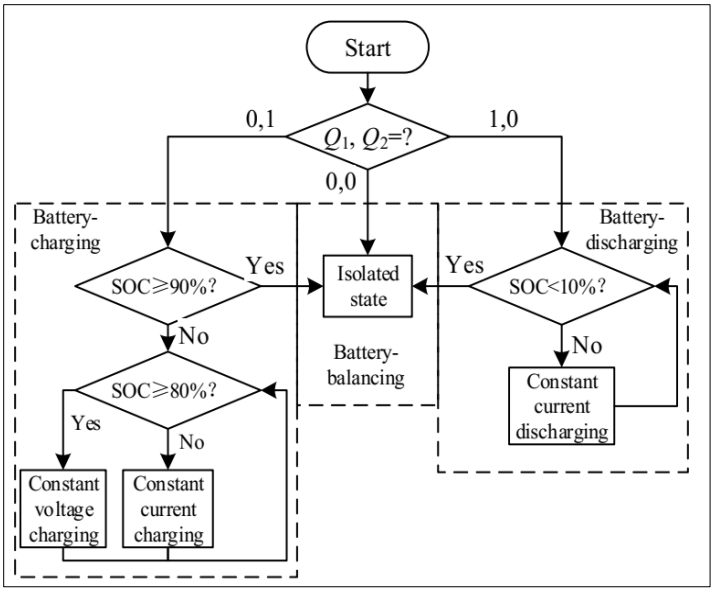

Figure. 3.19 Proposed switching scheme of the energy management system.
Taken from Q. Wang et al. (2020, P. 6)

A battery energy storage and a bi-directional buck-boost converter (BBC) are placed in parallel with the DC bus. The PI controller is also modeled to control the actions of the battery. The main goal is to guarantee the voltage stability and power quality of the critical load. Simulation and experimental results confirm that the proposed topology can provide better power quality for the connected critical load (see Figure. 3.20).

Table. 3.1. Definition of switching mode logic.
Taken from Zha et al. (2019, P. 5)

Q_1, Q_2	S_1	S_2	BBC	Battery
Q_1=1, Q_2=0	PWM	OFF	Boost	Discharging
Q_1=0, Q_2=1	OFF	PWM	Buck	Charging
Q_1=0, Q_2=0	OFF	OFF	Standby	Balancing

Regarding this work, the following points are important:

Pros:

- ✓ highly recommended for any further study in this domain.
- ✓ the proposed method is based on strong mathematical concepts.

- ✓ Integration of a renewable energy resource

Cons:

- × The effectiveness of the proposed method is to be evaluated in the case of other types of non-critical loads.
- × Difficult to be implemented.
- × The effectiveness of the proposed scheme is to be validated against other proposed methods in the literature.

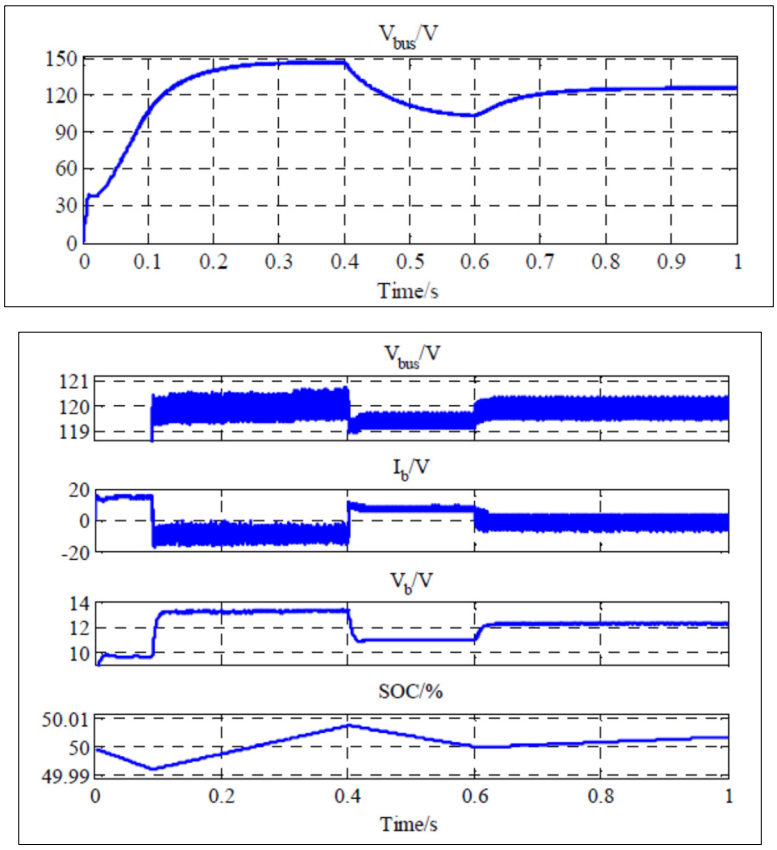

Figure. 3.20 Simulation results with/without the proposed energy management system
Taken from Zha et al. (2019, P. 4)

3.6 Voltage Regulation in DC Microgrid and Multiple DCES

Ref. (Z. Chen et al., 2020) proposes to implement multiple DCES for the purpose of voltage regulation in DC microgrids (see Figure. 3.21).

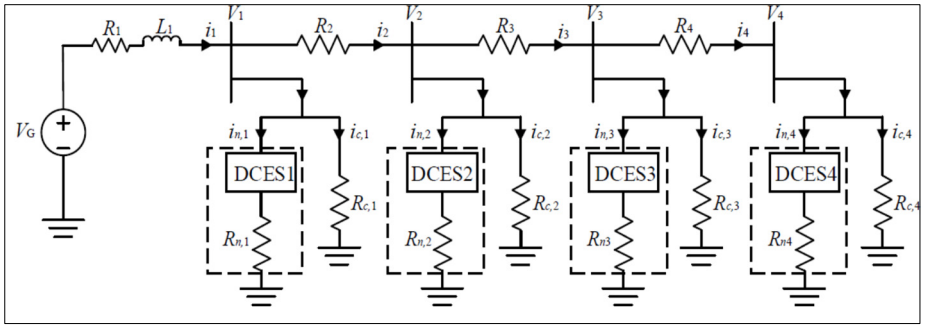

Figure. 3.21 Schematic of studied DC microgrid with multiple DCES
Taken from Z. Chen et al. (2020, P. 2)

For the primary control, it is considered that the operation of DCES is controlled with a DC/DC converter. Using Figure. 3.22, it is shown that for each series DCES following equation can be written:

$$L\frac{di_L}{dt} = V_{es} - v \tag{3.10}$$

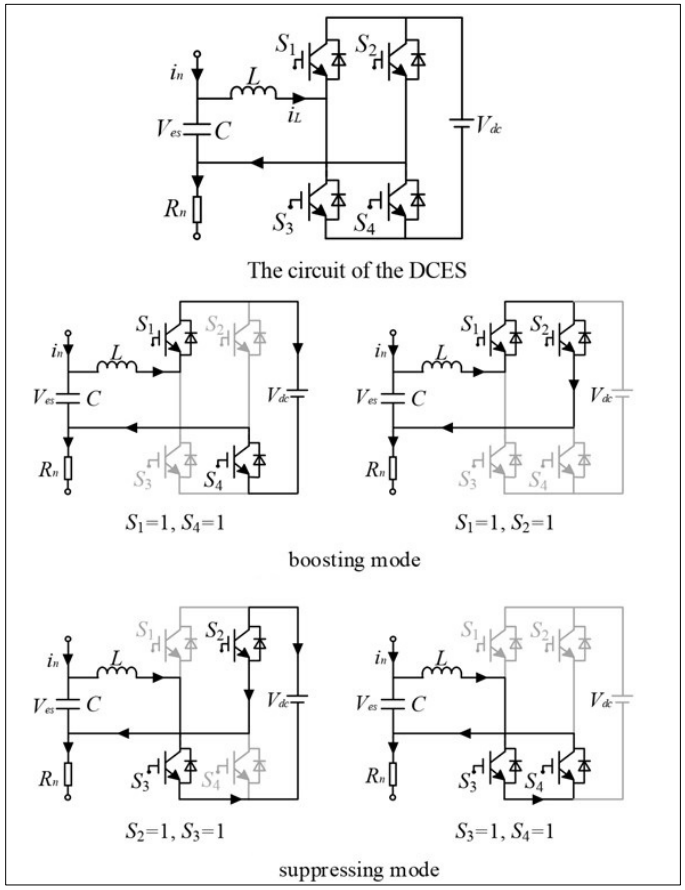

Figure. 3.22 Switching sequence of studied DCES
Taken from Z. Chen et al. (2020, P. 2)

where its discrete-time equivalent with the sampling time (T_s) is:

$$i_L(k+1) = \frac{T_s}{L}\left(V_{es}(k) - v(k)\right) + i_L(k) = \frac{T_s}{L}\left(V_{dc}(k).w - v(k)\right) + i_L(k) \quad (3.11)$$

For the purpose of voltage modulation, the following objective function is set to be minimized:

$$J = |i_L^* - i_L(k+1)| \quad (3.12)$$

where i^*_L is the reference for the current generated by the second control loop.

A consensus-based distributed control scheme is designed and formulated for the sake of coordinating the operation of multiple DCESs and regulating the voltage of the DC bus as shown in Figure. 3.23. The reference of voltage is generated by the secondary control which takes benefit from a consensus algorithm. To do so, a straightforward communication system is modeled to minimize the inaccuracy of decentralized control and the cost of communication.

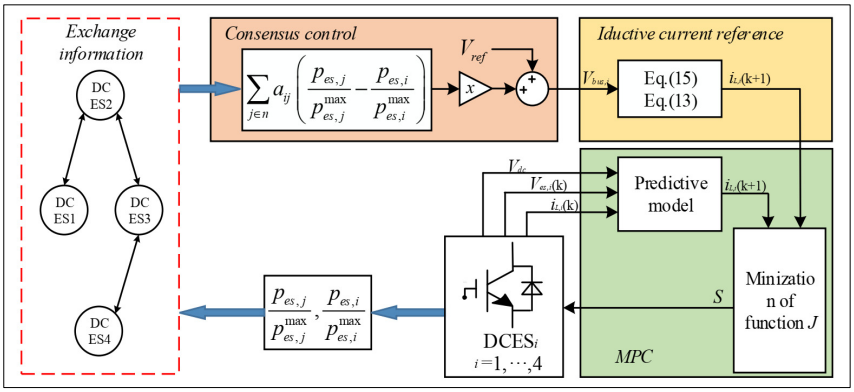

Figure. 3.23 Proposed control scheme
Taken from Z. Chen et al. (2020, P. 3)

Finally, it is proven that:

$$i^*_{L1} = \frac{V_G - V_{bus1}}{R_1} - \frac{V_{bus1}}{R_{c1}} - \frac{V_{bus2} - V_{bus1}}{R_2} \quad (3.13)$$

$$i^*_{Lx,(x=2,3,4)} = \frac{V_{bus,x-1} - V_{bus,x}}{R_x} - \frac{V_{bus,x}}{R_{cx}} - \frac{V_{bus,x} - V_{bus,x+1}}{R_{x+1}} \quad (3.14)$$

The results show that the proposed consensus-based distributed scheme is able to regulate the voltages properly when the source voltage varies with time and several DCESs are installed across the DC microgrid (see Figure. 3.24, Figure. 3.25, and Figure. 3.26).

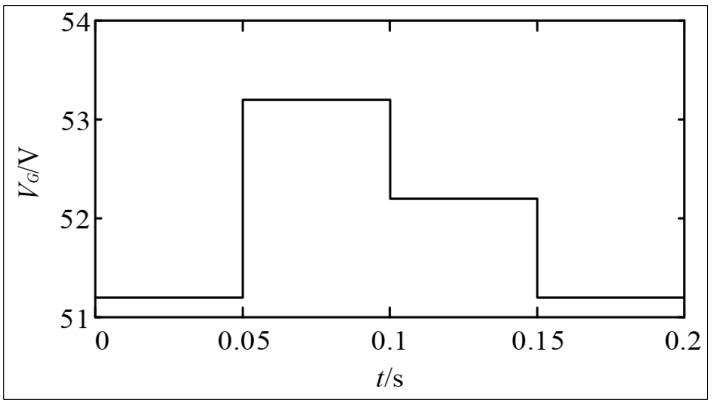

Figure. 3.24 Variation of voltage at the main power source
Taken from Z. Chen et al. (2020, P. 4)

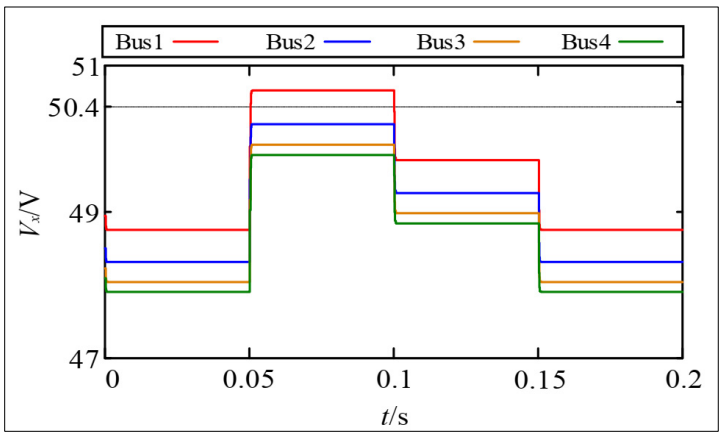

Figure. 3.25 Voltage amplitudes of buses without DCESs
Taken from Z. Chen et al. (2020, P. 4)

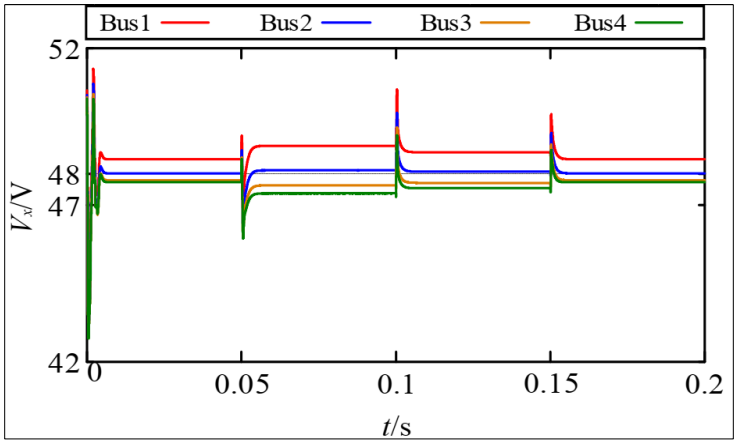

Figure. 3.26 Voltage amplitudes of buses with DCESs
Taken from Z. Chen et al. (2020, P. 4)

(X. Chen et al., 2018) also uses a distributed cooperative control approach for several DCESs in a DC microgrid getting only neighbor-to-neighbor information (see Figure. 3.27). For coordinating the DCESs, the primary layer formulates a droop control technique. Adjusting the state-of-charge (SOC) and the DC bus voltage reference among DCESs, the secondary control takes benefit from a consensus algorithm (Figure. 3.28). Simulation and experimental studies, as shown in Figure. 3.29 confirm the improved performance of the studied microgrid under different operating situations.

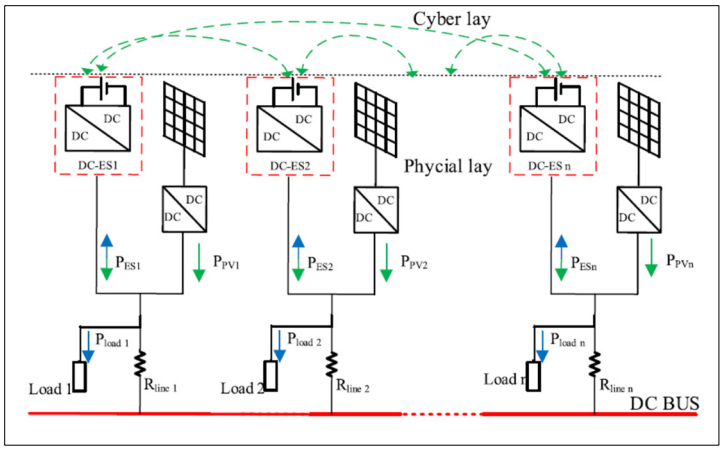

Figure. 3.27 General schematic of the simulated benchmark
Taken from X. Chen et al. (2018, P. 2)

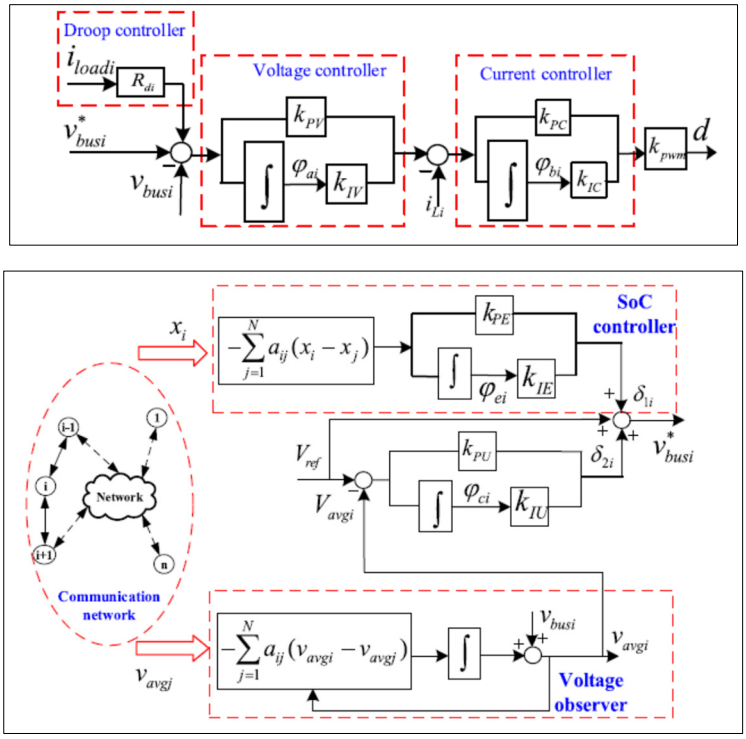

Figure. 3.28 Primary and secondary control loops
Taken from X. Chen et al. (2018, P. 3)

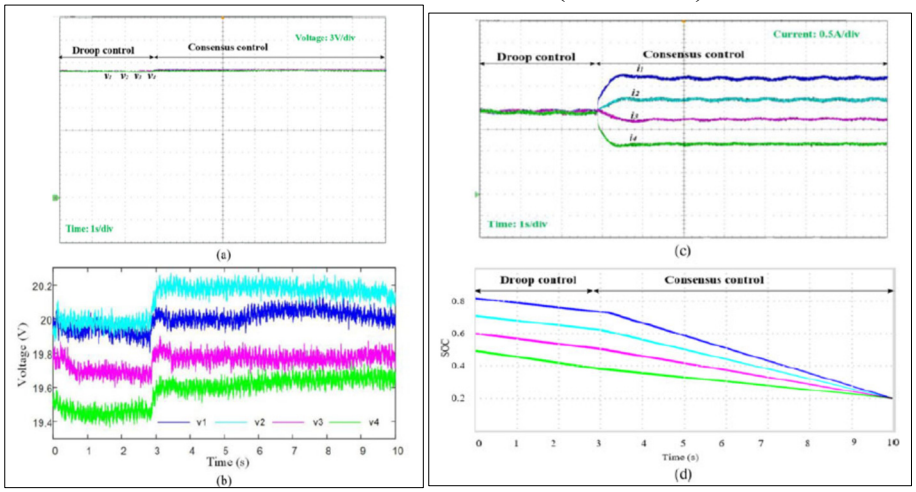

Figure. 3.29 Results of experimental tests (a) DCES voltage (b) Snapshot of the various time interval for voltages (c) DCES current (d) SOC of Batteries
Taken from X. Chen et al.(2018, P. 11)

Regarding the above works, the following points are captured:

Pros:

- ✓ recommended for any further study in this domain.
- ✓ the proposed method is based on strong mathematical concepts .
- ✓ Studying the impact of Multiple DCES

Cons:

- × The effectiveness of the proposed method is to be evaluated in the case of other types of non-critical loads.
- × Difficult to be implemented.
- × The effectiveness of the proposed scheme is to be validated against other proposed methods in the literature.
- × High Computation effort

3.7 Enhancing Power Quality in DC Microgrid

A proportional-Integral (PI) controller is modeled to control and modulate a DCES and four-quadrant DC-DC converter in Ref (Hashem et al., 2018). The small-signal model of the developed microgrid with DCES is given in Figure. 3.30.

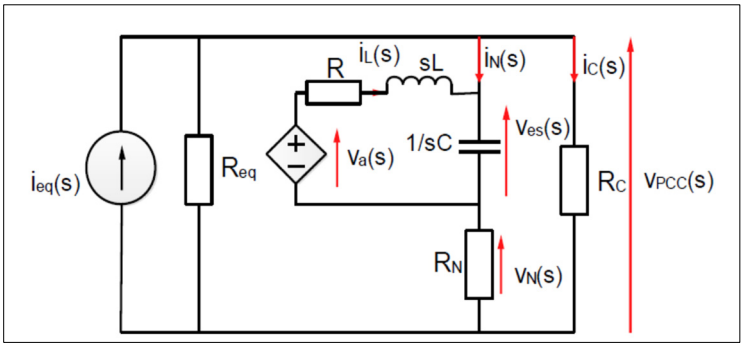

Figure. 3.30 The schematic of the developed microgrid in small-signal mode
Taken from Hashem et al. (2018, P. 5)

A PI controller is generally defined as:

$$K(s) = K_p(1 + \frac{1}{T_i s}) \tag{3.15}$$

If the voltage of DCES and the point of connection define as follow

$$V_{es}(s) = \frac{v_a(s)}{1+CLs^2+CR_s} + \frac{i_N(s)[Ls+R]}{1+CLs^2+CRs} \quad (3.16)$$

$$V_{PCC}(s) = \frac{V_a(s)}{1+CLs^2+CRs} + \frac{i_N(s)[Ls+R+R_N+R_NCLs^2+R_NRCs}{1+CLs^2+CRs} \quad (3.17)$$

Then, the following transfer function can be extracted:

$$\frac{V_{PCC}}{V_{PCC-ref}} = \frac{K_ps+K_I}{LCs^3+CRs^2+(K_P+1)s+K_i} \quad (3.18)$$

Simulation and experimental results show that the applied control scheme is able to regulate the voltage even in the presence of fluctuations (see Figure. 3.31)

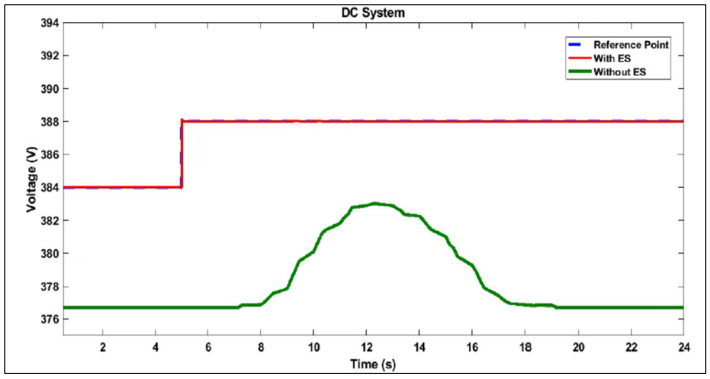

Figure. 3.31 The output voltage of the PCC in different scenarios
Taken from Hashem et al. (2018, P. 5)

The following points can be concluded about this work:

Pros:

- ✓ Easy implementation
- ✓ Studying the impact of a PV system

Cons:

- × The effectiveness of the proposed method is to be evaluated in the case of other types of non-critical loads.
- × Not a strong mathematical background
- × The effectiveness of the proposed scheme is to be validated against other proposed methods in the literature.

3.8 Battery Storage Reduction in DC Microgrids

DCES can be used to reduce the total size of the required battery for a DC microgrid. The more integrated, the less battery is needed (See Figure. 3.32).

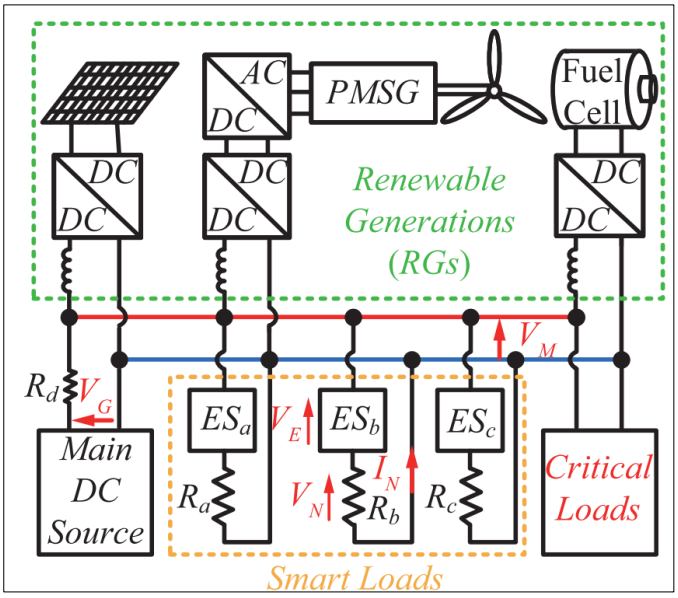

Figure. 3.32 Studied DC microgrid.
Taken from M. H. Wang et al. (2020, P. 2)

However, the main question is how to coordinate multiple DCESs. Ref. (M. H. Wang, Yan, et al., 2018) proposes a decentralized controller for reducing the total storage capacity and improving the voltage stability of a DC microgrid.

First, a mathematical analysis is conducted to find the maximum and minimum amount of required power of DCESs. It is proven that the rated power of DCESs, P_{rate}, can be calculated using the following equation:

$$P_{rate} \geq P_{nom} \frac{V_{min}(V_M - V_{mon})}{V_M^2} \quad (3.19)$$

where

P_{nom}: The nominal power of the non-critical load

V_{min} Minimum voltage of DCES

Next, a simplified diagram of the study system is constructed (Figure. 3.33), the state-space equivalent model is developed, and the proposed decentralized controller is designed to guarantee the stability of the whole system (Figure. 3.344).

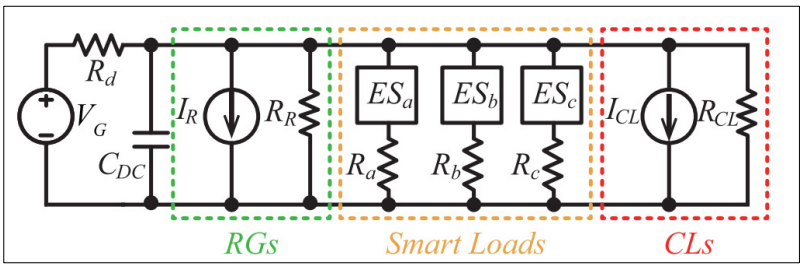

Figure. 3.33 Simplified model of the studied system
Taken from M. H. Wang et al. (2020, P. 6)

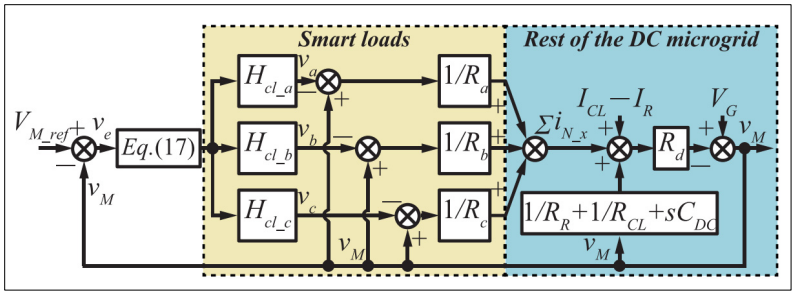

Figure. 3.34 The block diagram of the decentralized control scheme
Taken from M. H. Wang et al. (2020, P. 6)

The stability of the system, dynamic response, and voltage response to a grid fault are simulated and verified with a real experiment. As shown in Figure. 3.35, Figure. 3.36, and Figure. 3.37 , the proposed scheme is effective in coordinating the operations of multiple DCESs and minimizing the total battery storage capacity.

The authors of this work claim that the proposed scheme leads to battery storage reduction. Regarding this work following points are observed:

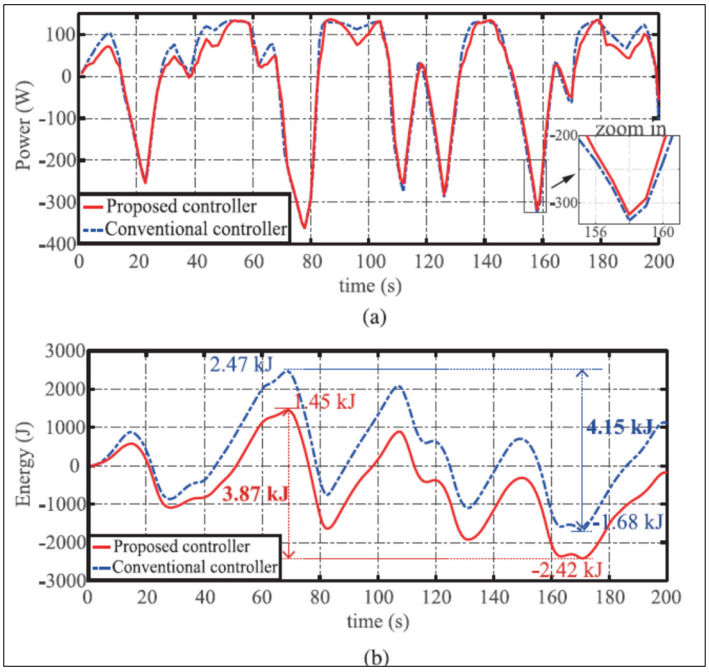

Figure. 3.35 Experiment results for (a) power of the battery (b) energy of the battery
Taken from M. H. Wang et al. (2020, P. 10)

Pros:

- ✓ Strong mathematical concept and highly recommended for any work in this domain.
- ✓ Studying the impact of renewable energy resources.
- ✓ The effectiveness of the proposed scheme is to be validated against other proposed methods in the literature.

Cons:

- × The effectiveness of the proposed method is to be evaluated in the case of other types of non-critical loads.
- × High computational effort

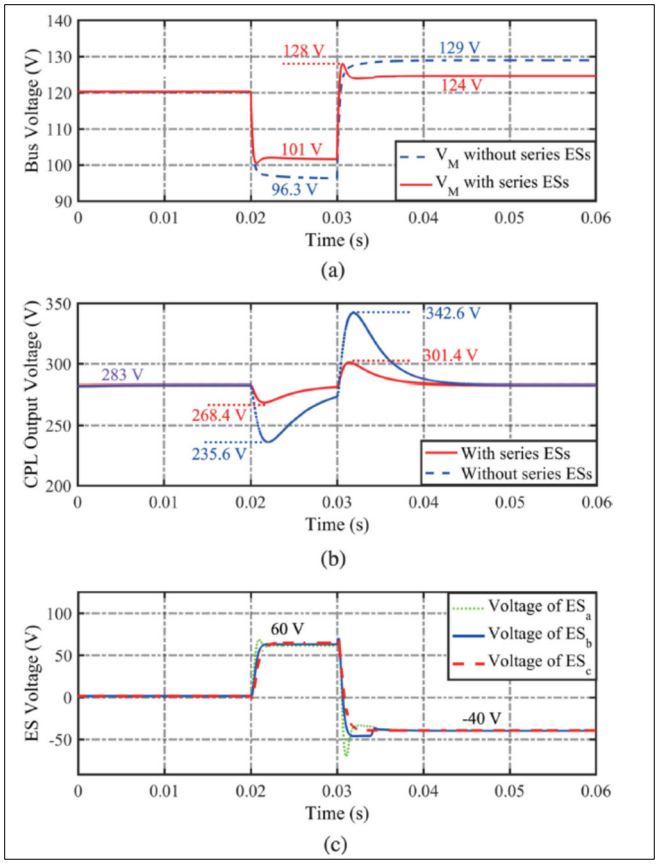

Figure. 3.36 Simulated voltage waveforms of positive constant-power load with/without the DCES (a) Voltage of DC bus (b) Voltage of positive constant-power load (c) ES output voltages

Taken from M. H. Wang et al. (2020, P. 11)

3.9 Simultaneous voltage compensation and optimal power balancing with shunt DCES

The voltage synchronization and optimal operation of multiple shunt DCESs in a DC microgrid are studied in Ref. (Jena & Padhy, 2019) The studied benchmark is given in Figure. 3.38. The communication Layer of the studied benchmark is set to establish a data exchange link between different elements. To achieve cooperative operating, a distributed secondary control based on a consensus algorithm is developed (Figure. 3.39). For enhancing the capabilities of shunt DCESs, a so-called primary reverse droop controller is assigned. It is well-known that to minimize the associated costs and to assure unified operation, every DCES should follow the cost-generation characteristic curve and operate at its optimal operating point.

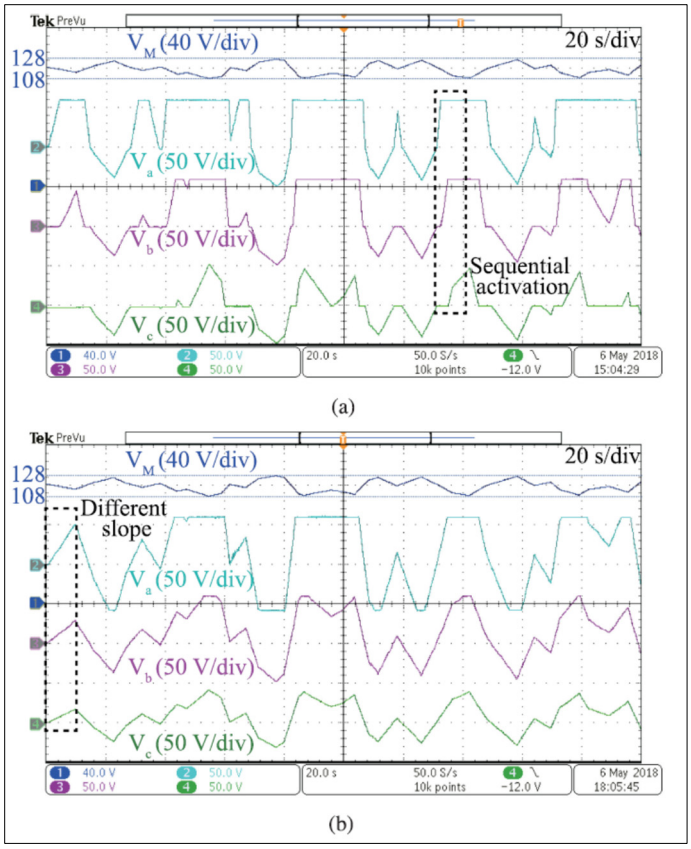

Figure. 3.37 Experiment results for voltages and DCES (a) with the proposed scheme (b) with the conventional method
Taken from M. H. Wang et al. (2020, P. 10)

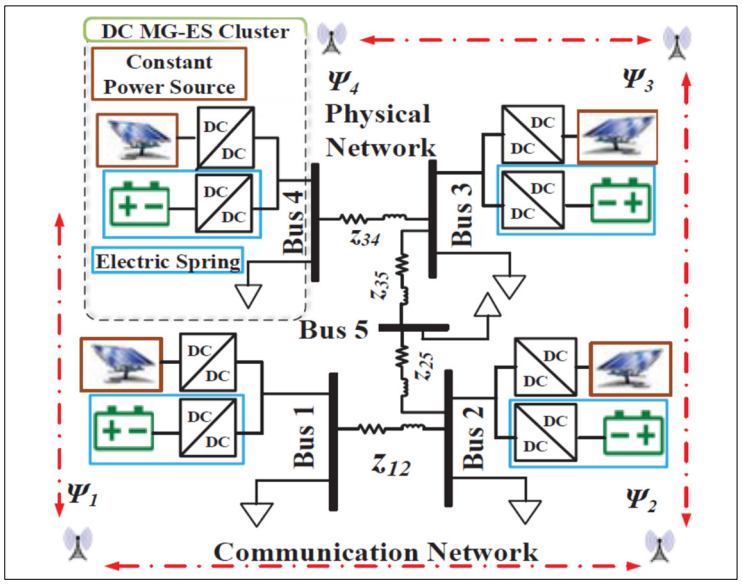

Figure. 3.38 Studied test case

Taken from Jena & Padhy. (2019, P. 2)

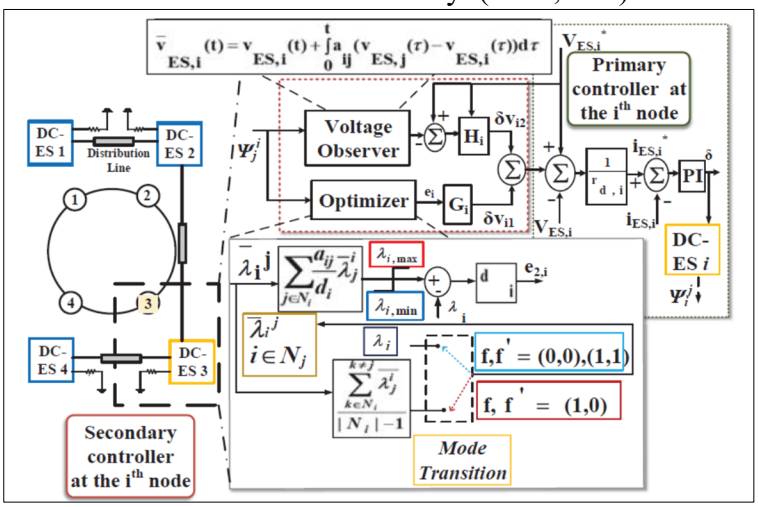

Figure. 3.39 Proposed scheme for controlling multiple shunt DCESs
Taken from Jena & Padhy. (2019, P. 2)

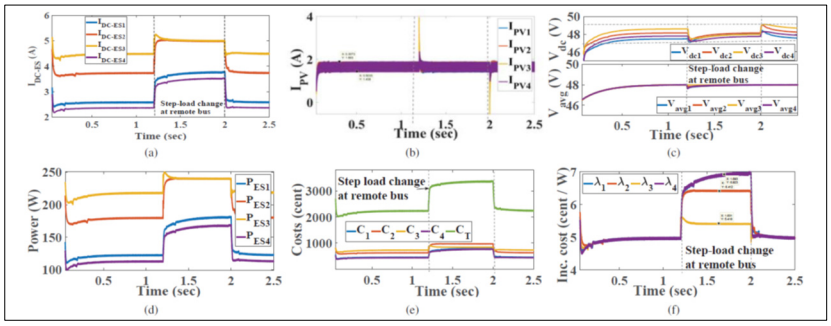

Figure. 3.40 (a) Participation of DCESs (b) the current of constant power source (c) voltage of DC bus(d) Active power (e) Costs (f) Load variation incremental costs & evaluation of limit violation
Taken from Jena & Padhy. (2019, P. 4)

This work also examined some other aspects as well as:

- convergence analysis for proving that average voltages tent to reach global pre-defined setpoints.
- plug and play capability.
- Robustness to ambiance condition variation
- Communication delay

Simulation results show that the proposed algorithm is highly effective in the operational coordination of multiple shunt DCES (Figure. 3.40).

Regarding this work, we could list the following items:

Pros:

- ✓ Highly recommended for any work in this domain
- ✓ Strong mathematical concept
- ✓ Studying shunt DCES

Cons:

- × The effectiveness of the proposed method is to be evaluated in the case of other types of non-critical loads.
- × High computational effort
- × The effectiveness of the proposed scheme is to be validated against other proposed methods in the literature.

3.10 Active Power Loss reduction in DC microgrids

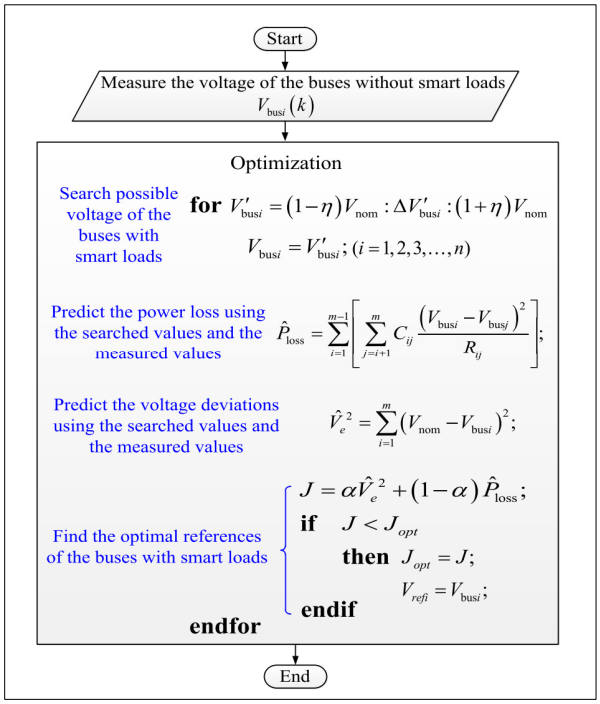

Figure. 3.41 Proposed a centralized model predictive control approach
Taken from Yang et al. (2018, P. 4)

DCES might be used to reduce the power loss on the distribution lines. For this purpose, a centralized model predictive control approach is formulated in Ref (Yang et al., 2018) which controls multiple DCESs. The general flowchart of the proposed approach is given in Figure. 3.41 The objective function of the proposed centralized model predictive control is as follows:

$$minJ = \alpha \sum_{i=1}^{m}(V_{nom} - V_{busi})^2 + (1-\alpha)\sum_{i=1}^{m-1}\left[\sum_{j=i+1}^{m} cij \frac{(V_{busi}-V_{busj})^2}{R_{ij}}\right] \quad (3.20)$$

$$0 \le \alpha \le 1, (1-\eta)V_{nom} \le V'_{busi} \le (1+\eta)V_{nom} \quad (3.21)$$

The weighting factor (α) of the approach is either adaptive or non-adaptive. For example, in the case of adaptive tuning of the weighting factor, the procedure is described using a flowchart (see Figure. 3.42)

The authors take benefit from a previously verified DCES model and run simulation studies over a DC microgrid setup (Figure. 3.43). For the purpose of voltage regulation, each DCES is equipped with a PI controller as shown in Figure. 3.44.

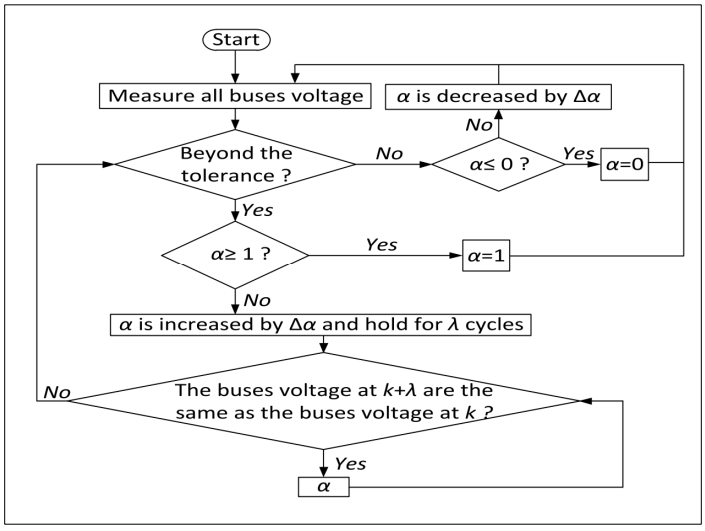

Figure. 3.42 Calculating the weighting factor (adaptive approach)
Taken from Yang et al. (2018, P. 5)

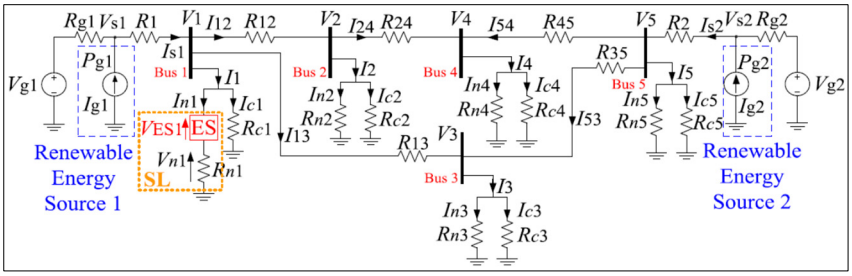

Figure. 3.43 Studied benchmark
Taken from Yang et al. (2018, P. 5)

Simulation results confirm saving energy goals can be achieved with different sets of tunning (See Figure. 3.45 and Figure. 3.46).

In general, the following points can be mentioned regarding this work:

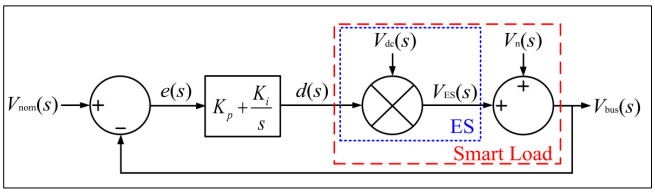

Figure. 3.44 The proposed local control scheme
Taken from Yang et al. (2018, P. 3)

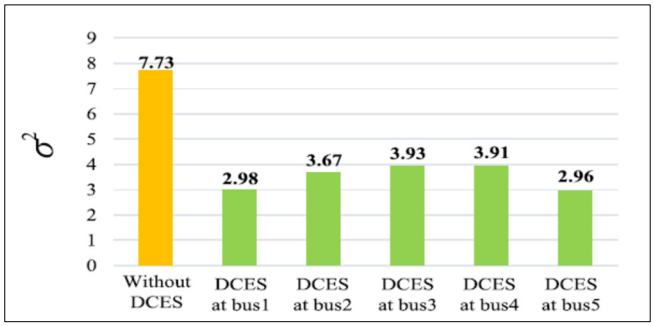

Figure. 3.45 Defined voltage index
Taken from Yang et al. (2018, P. 7)

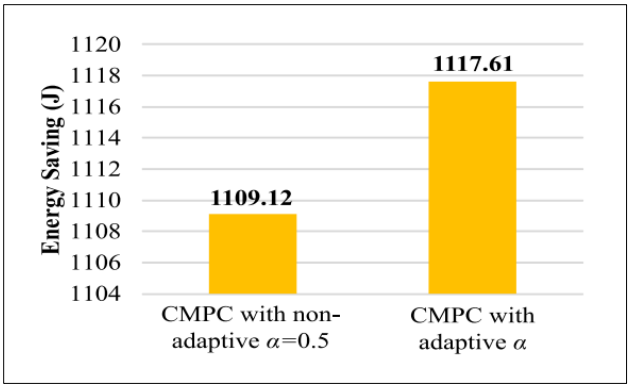

Figure. 3.46 Energy saving with adaptive and non-adaptive weighting factors
Taken from Yang et al. (2018, P. 9)

Pros:

- ✓ recommended for any work in this domain.
- ✓ a simple and effective mathematical concept
- ✓ Studying multiple DCESs

Cons:

- × The effectiveness of the proposed method is to be evaluated in the case of other types of non-critical loads.

The effectiveness is to be validated against other proposed methods in the literature.

3.11 Enhancing the Quality of Voltage in DC Microgrids

A combination of objective functions including fault-ride-through support, double-line frequency harmonic compensation, and DC bus voltage regulation is studied using either series or shut DCES (M. H. Wang, Mok, et al., 2018). The experimental setups for each test are given in Figure. 3.47 and Figure. 3.48.

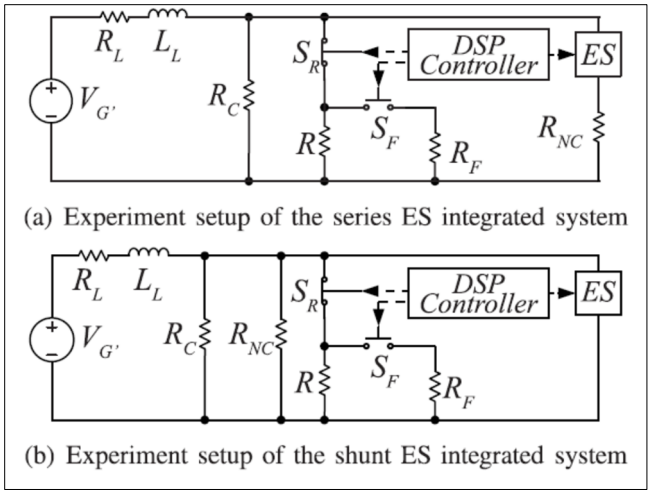

Figure. 3.47 The setup for fault-ride-through support experiment
Taken from M. H. Wang, Mok, et al. (2018, P. 8)

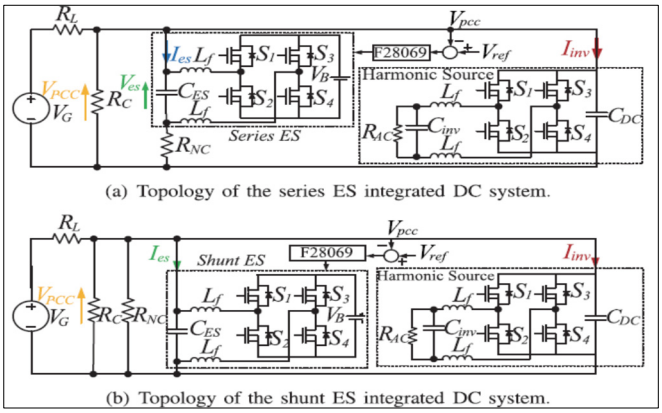

Figure. 3.48 The setup for double-line frequency harmonic compensation
Taken from M. H. Wang, Mok, et al. (2018, P. 7)

It is concluded that the series DCES is capable of manipulating the power consumption of non-critical load and reducing the required size of storage in the DC microgrid but cannot target the current harmonics. The shunt DCES can eliminate the current harmonics of the system without using extra energy and has a better dynamic response compared to series DCES, which is appreciated for fault-ride-through support (See Figure. 3.49 and Figure. 3.50).

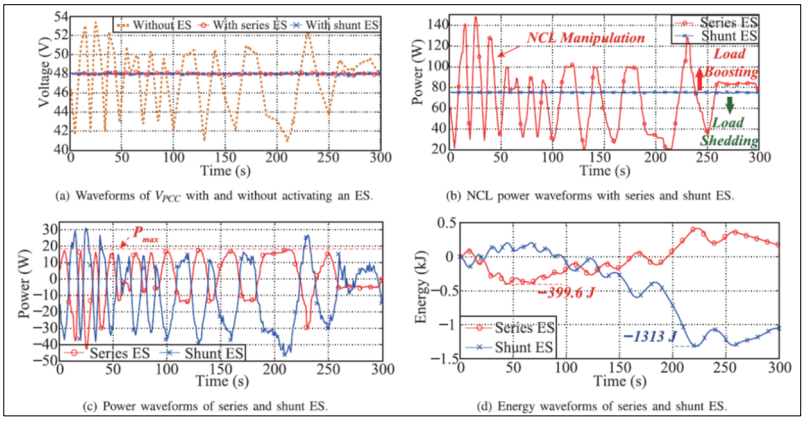

Figure. 3.49 Experimental results for bus voltage regulation goal
Taken from M. H. Wang, Mok, et al. (2018, P. 7)

3.12 conclusion

In this section, several applications in DC microgrids were studied. Each application and proposed control scheme are reviewed separately and their advantages and pitfalls are listed. The literature review findings are summarized in Table. 3.2 based on some criteria, e.g. the technical level, proposed control scheme, the type of DCES, etc.

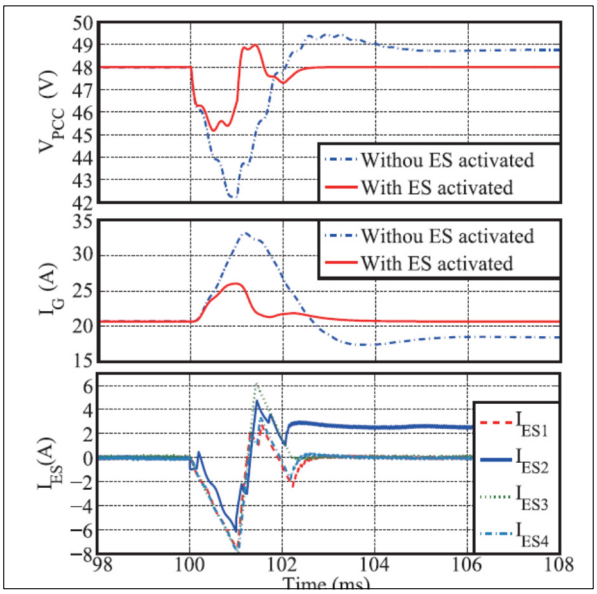

Figure. 3.50 Simulation results for multiple shunt DCESs riding through a fault
Taken from M. H. Wang, Mok, et al. (2018, P. 10)
Table. 3.2. Proposed Applications in Literature

Application	Simulation	Experiment	Control Scheme	Analytical Proof	Single or Multiple	Series or Shunt
Suppression of Unbalanced Voltage Situations (Liao et al., 2020a)-(Liao et al., 2020b)	✓	✓	Decoupling controlling variables	✓	Single	series
DC Distribution System Stabilizing (Kakigano et al., 2013)	✓	✓	DC Distribution System Stabilizing	✓	Single	Series
Active Damping Control (Hosseinipour & Hojabri, 2020)	✓	✓	virtual R&C damper impedance	✓	Single Multiple	Series
Reducing Dependency to Main Grid (Charan Cherukuri et al., 2019)	✓	×	Developed energy equation between DCES and grid & power of NCL	✓	Single	Series
Power Quality & Voltage Stability Improvement (Zha et al., 2019)-(Z. Chen et al., 2020)	✓	✓	Energy management system	✓	Single	series
Voltage Regulation with Multiple DCES (Z. Chen et al., 2020)-(X. Chen et al., 2018)	✓	✓	consensus-based distributed control	✓	Single Multiple	Series
Enhancing Power Quality (Hashem et al., 2018)	✓	✓	proportional Integral (PI) controller	✓	Single	Series
Reduction of Required Battery Energy Storage (M. H. Wang, Yan, et al., 2018)	✓	✓	Decentralized controller	✓	Single Multiple	Series
voltage compensation and optimal power balancing (Jena & Padhy, 2019)	✓	×	Primary reverse droop controller+ distributed secondary control based consensus algorithm	✓	Single Multiple	Shunt
Active Power Loss reduction (Yang et al., 2018)	✓	×	centralized model predictive control	✓	Single	Series
Enhancing the Quality of Voltage (M. H. Wang, Mok, et al., 2018)	✓	✓	hybrid quasi-proportional resonant integral (PRI) hysteresis controller	✓	Single Multiple	Series Shunt
DC bus voltage regulation and FRT Support (Gawande et al., 2020)	✓	×	droop control using the virtual resistor	×	Single	Shunt
DC Voltage Regulation and Harmonic Cancellation with Hybrid DCES (M. H. Wang, Yan, et al., 2018)	✓	×	Power decoupling controller	✓	Single	Series Shunt

.

CHAPTER 4

Coordinated Energy-Sharing Scheme for DC Electric Spring and Hybrid Battery Energy Storage Source in Modern DC Microgrids

4.1 Abstract

In this chapter, we propose an energy-sharing scheme for coordinating the role of a DC electric spring (DCES) and a hybrid battery energy source system (hybrid BESS) for improving the DC bus voltage when the main source of the DC microgrid is a PV system. Despite all the advantages related to the concept of DC microgrids, there are still challenges regarding their operation and control in the presence of massively integrated naturally intermittent renewable energy resources. The hybrid BESS, including a Li-Ion chemical battery and a supercapacitor, provides the capability of responding to any production command signal. The simulation results conducted on a test case show that DCES can effectively and positively contribute to the power shortage compensation process caused by a drop in PV production, dampen the oscillations, and release the stress from the hybrid BESS.

4.2 Introduction

Combating climate change and achieving resilient and green socioeconomic systems require cost-effective pathways for decarbonizing human societies and changing the patterns of energy supply and consumption. In the transition toward carbon neutrality by 2050 (Position & Planet, 2018), (IEA, 2021), (House of Commons of Canada, 2020), (McKinsey, 2022), reducing greenhouse gas

emissions is a big challenge that is exacerbated following the emergency of the COVID-19 pandemic (Kikstra et al., 2021). In this way, all public and private sectors should contribute and propose viable solutions (McKinsey and Company, 2022),(IRENA, 2021). Meanwhile, the imperative of energy transition to decarbonize the economy of tomorrow is increasing the

penetration of distributed energy resources (DERs), especially in distribution systems which have a positive impact on the environmental issues arising from conventional power plants while reducing the dependency on energy prices on fossil fuel availability. In this way, an interesting concept is microgrids which are proposed as an effective solution for reaching the future resilient grid (Farrokhabadi et al., 2020),(Olivares et al., 2014). Microgrids have been considered a key element in future smart grids. According to the Department Of Energy (DOE) (Ton & Smith, 2012), the microgrid is defined as "a group of interconnected loads and distributed energy resources within clearly defined electrical boundaries that acts as a single controllable entity with respect to the grid. A microgrid can connect and disconnect from the grid to enable it to operate in both grid-connected and island mode." However, several challenges should be addressed in alternating current (AC) electrical systems before real implementation. The main challenge is the power quality issues caused by the electronically interfaced DERs at the common coupling point to the AC side of the power system (Stoyanov et al., 2019),(Liang & Andalib-Bin-Karim, 2018),(Ahsan & Khan, 2022),(Chidurala et al., 2014),(Gimenes et al., 2022). To overcome this critical challenge, direct current (DC)-type microgrids are proposed that have several promising features and can operate grid-connected or off-grid for electrification of remote areas without the need for installing smart inverters (van der Blij et al., 2018),(Van den Broeck et al., 2018),(Charles & Bagavathy, 2016),(Gerber et al., 2018). Despite all the interesting characteristics, some concerns still must be addressed regarding the voltage of DC microgrids such as voltage variation, voltage drop, short circuit, etc.

Several methods are proposed in the literature for addressing the common issues observed in DC microgrids, e.g., demand side management (DSM), load balancing, real-time energy management systems, energy storage, and DC electric springs (DCES) (Guerrero et al., 2011),(Anand et al., 2013),(Baran & Mahajan, 2007),(Kakigano et al., 2013),(Mok et al., 2017),(Loh et al., 2013),(Cairoli et al., 2013),(M. Wang et al., 2021),(Faisal et al., 2018).

4.3 Steady-State Stable DC bus of DC Systems

The stability problem is a big and critical issue with the AC system since all AC generators should be kept synchronized and the balance between the generation and consumption should be maintained around the system's nominal frequency (Farrokhabadi et al., 2020).

In the case of the DC system, the voltage and current remain the only observable variables for stability analysis. The stability criteria are reviewed by Riccobono & Santi, 2014. There are different types of classifications regarding the nature of stability itself. Generally speaking, a DC system is considered steady-state stable via time-domain simulations and studies if the voltage of the DC bus returns to the initial operation point after an imposed disturbance and the oscillations are limited to ±5% of the rated value (Adly & Strunz, 2021; Ghanbari et al., 2018; Riccobono & Santi, 2014; Toro et al., 2021; J. Wang et al., 2020).

In this work, we will monitor the voltage of the DC bus and the currents regarding each studied scenario to evaluate the steady-state stability of the whole system including the DCES.

4.4 Power Quality of DC Systems

The quality of supplied power to the clients may affect the life span and operation of corresponding electrical equipment. These phenomena are of importance in the case of critical loads that are highly dependant on the quality of provided power. The power quality of AC systems is a well-known issue and is addressed by several standards. For example, the IEEE Guide for Identifying and Improving Voltage Quality in Power Systems addresses in detail the common characteristics of power quality by covering several subjects such as different levels of power quality, important key factors deteriorating the quality of supplied power, and solutions to identify and improve power quality (IEEE Std 1250, 2018).

In the case of DC systems, a different viewpoint is needed to analyze the power quality issue (H. Wang et al., 2021). As a matter of fact, the main idea behind the design and utilization of DC systems is to avoid all those power quality concerns which are related to AC systems.

(Guerrero et al., 2011; Zhang et al., 2000) The sources of power in the DC system operate with a frequency equal to zero, and the generation at other frequencies does not exist. All the connected equipment is DC powered and there is no power electronic-based element that may produce harmonics. Therefore, it could be assumed that with a system fully operatable with DC equipment, there will not be any harmonics (Mariscotti, 2021; Mayoral et al., 2021; Mohamad & Mohamed, 2019; Veneri, 2016; Zuo et al., 2016).

Another challenging power quality issue applicable to DC systems is the fault current. In the domain of AC systems, the impact of any type of fault on a system's characteristics such as voltage, current, and power is well-known to researchers and operators. Several types of solutions, preventive or corrective, exist in the real world for mitigating the consequences of any fault in the AC system. The applicability of such approaches is tested and validated effectively.

When dealing with a DC system, a fault could be interpreted as the extra current drawn from the main source of energy. Usually, the contribution to the fault is limited to the nominal capacity of energy resources and installed converters. Yet, a fault on a DC bus could be a serious issue especially when it leads to a sustaining arc in that its detection is complex (Kwasinski, 2011; Uriarte et al., 2012; Whaite et al., 2015).

4.5 Proposed Coordination Scheme and Studied System

The technical characteristics of a proposed controller of series DCES, Hybrid Energy storage, and main PV system are given. The schematic of the developed DC system is given in Figure. 4.1.

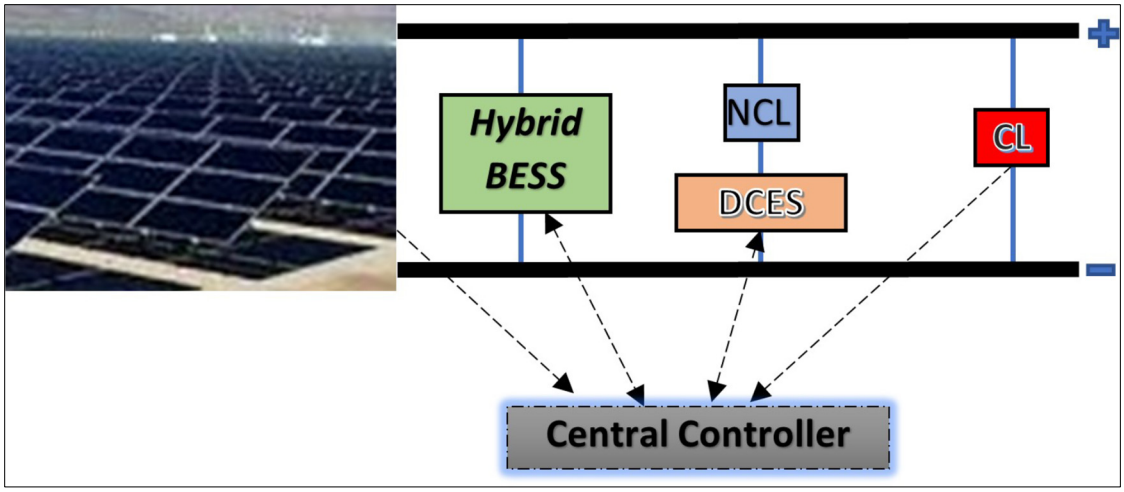

Figure. 4.1 Schematic of Modeled test system

4.5.1 Main Energy Source

The main energy source of the modeled DC microgrid is a PV system. The idea behind using PV panels is to support the decarbonization target and to have a sustainable system that can be installed in remote areas. The simulated PV system has four PV arrays in parallel each connected to a separate DC/DC controller for reliability reasons. The operation power of the whole PV system is 180KW and the operating voltage of the PV system is 130V.

The so-called PV Array block models an array of PV modules connected in parallel. This block allows modeling a wide variety of present PV modules from the National Renewable Energy Laboratory (NREL) System Advisor Model and the user-defined modules. The model also accepts temperature (deg. C) and irradiance (W/m2) as inputs. The DC/DC controller itself, as shown in Figure. 4.2 mainly comprises a maximum power point tracking (MPPT) controller based on the Perturb Observe algorithm for generating the duty cycle of the boost converter and a boost converter (average model).

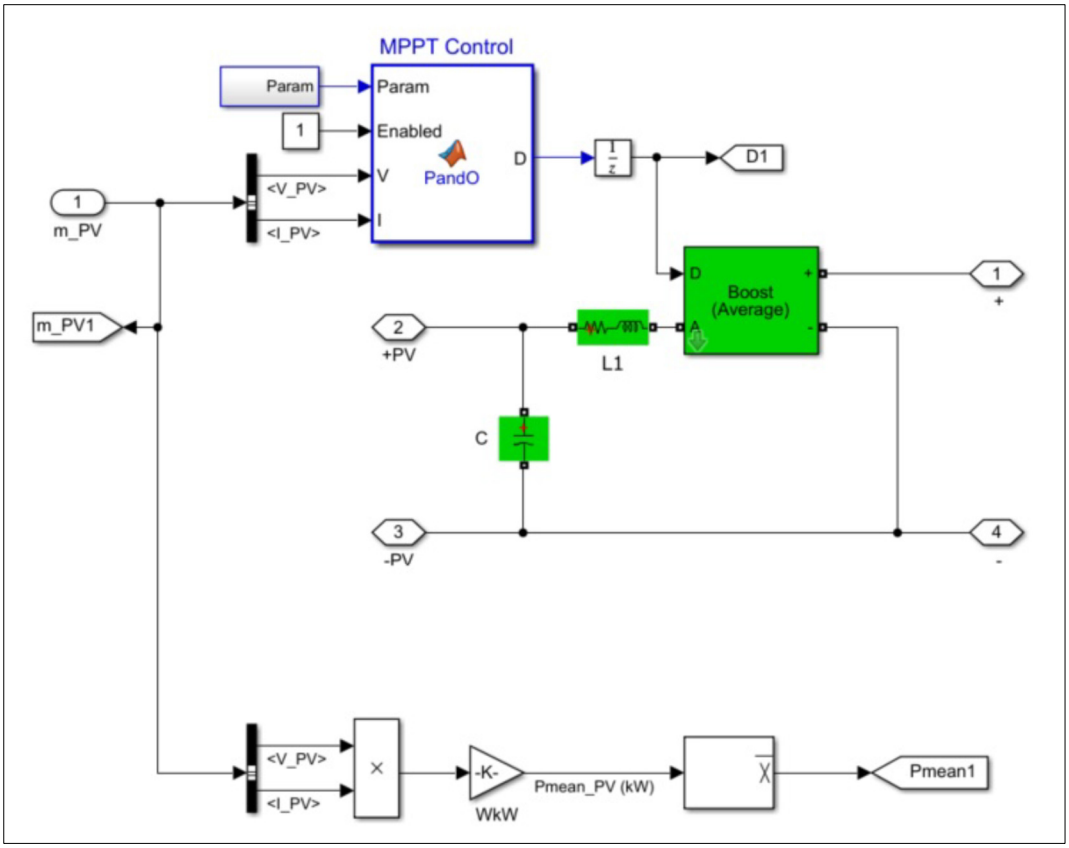

Figure. 4.2 The modeled DC/DC controller for PV arrays

4.5.2 Hybrid BESS

The hybrid battery energy storage system (BESS) as shown in Figure. 4.3 is developed by the following sources: (1) a generic lithium-ion battery model which accepts, and (2) a generic supercapacitor model for simulating the electric double layer capacitors (EDLCs). The reason for having two types of energy sources is that the chemical-type BESS is not usually an extremely fast response device, however, the supercapacitors may react almost instantly to the given modulation signal. On other hand, the energy volume of supercapacitors is not large which is commonly not an issue with chemical BESS since the current technology permits building large-scale storage. In this work, the nominal voltage of the chemical battery is 100V, the rated capacity is 100Ah, and the response time is set to one sec. For the supercapacitor, the rated capacitance is 500F and the rated voltage is 100V.

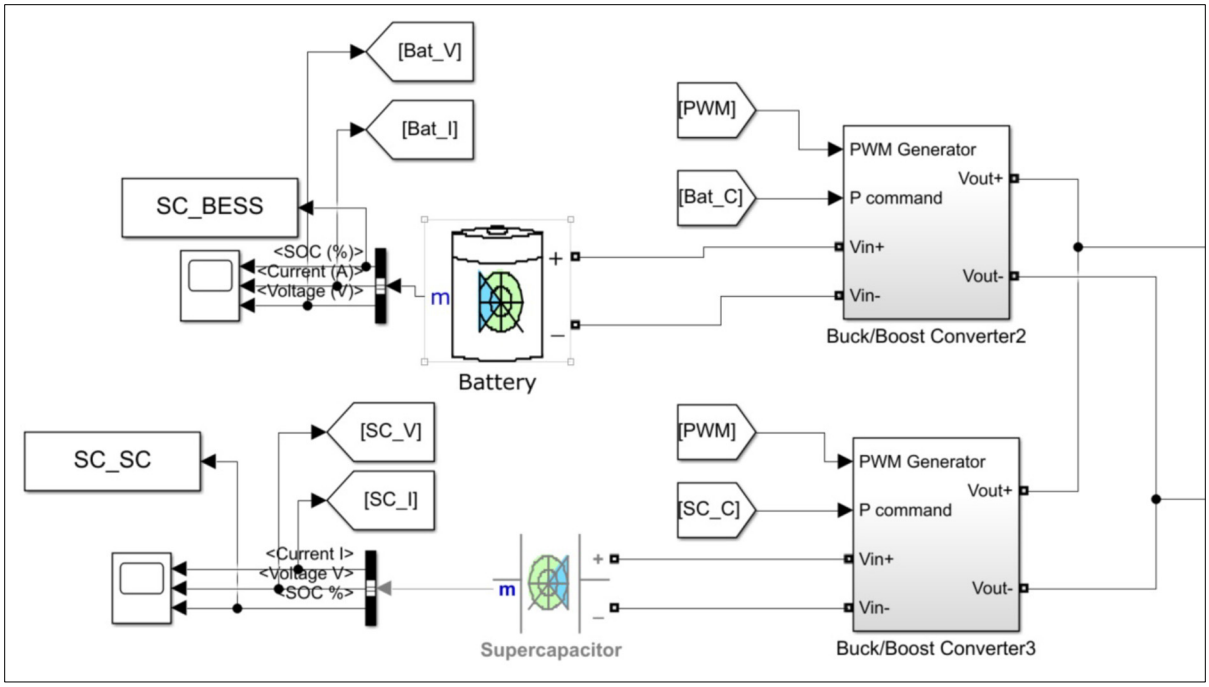

Figure. 4.3Simulink Model of Hybrid BESS

4.5.3 Series DCES

The series DCES is modeled with a voltage source and a two-quadrant DC/DC power converter (see Figure. 4.4The two-quadrant DC/DC power converter uses the so-called switching devices model type in which the converter is modeled with pairs of IGBT and diode pairs and is operated by firing pulses produced by a PWM generator. The PWM generator is set to create a gating signal, the pulses to the

electronic switch of a two-quadrant DC to DC Converter. In this work, the given duty cycle to the PWM generator is calculated based on the difference between the real voltage and a nominal voltage.

4.5.4 Non-Critical Load (NCL)

Non-critical load (NCL) is an adjustable load whose power consumption can be modulated via either its current or voltage. In this work, the NCL is modeled by a resistive load equal to 0.2 Ohm.

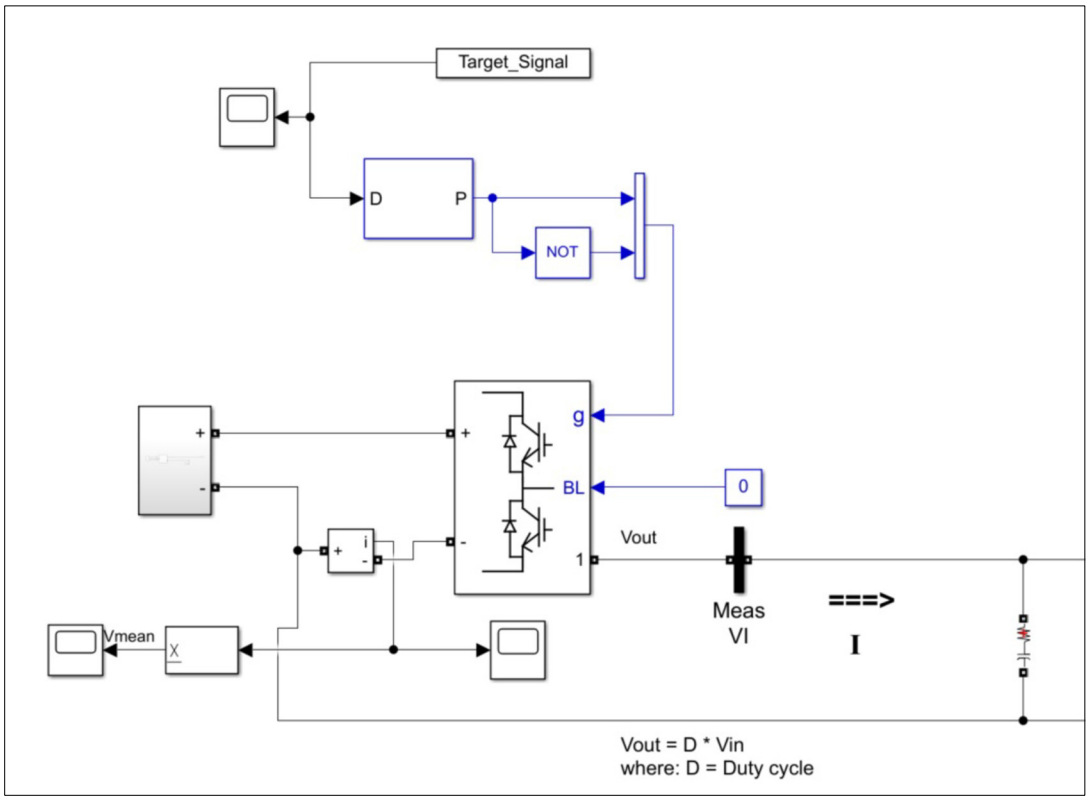

Figure. 4.4 Modeled series DCES

4.5.5 Critical Load (CL)

It is a widely accepted definition that critical loads (CLs) should be continuously supplied with very good power quality. Any system may have critical parts which cannot tolerate deviation from a nominal voltage or current amplitude. In this work, CL is modeled via a resistive load, similarly, 0.2 Ohm, and its voltage, current, and power are monitored constantly.

4.5.6 Energy Sharing Coordinator

The modeled controller is an intelligent energy-sharing block that generates the modulation signal for both the Hybrid BESS and the series DCES. The observatory role of the central

controller is to monitor continuously the status of PV arrays, hybrid BESS, DCES, and NCL. Whenever there is an oscillation in the voltage of the DC bus, the controller is supposed to take an action and turn it back to a pre-determined amplitude by properly distributing the required actions among controllable devices while considering their limits. Depending on the rated values of the system, the operator may tune the setting for the share of hybrid BESS in the case of power shortage. For example, one might limit the participation to a certain level for the sake of preserving the energy of hybrid BESS for later use. Therefore, the DCES will take more responsibility. Once the share of hybrid BESS is defined, the DCES will follow the voltage amplitude and damps the variations.

In this work, the assigned required power signal to the hybrid BESS passes first by a filter, and then a rate limiter for generating the production signal for the chemical storage. The filter is used to filter out high frequencies in the required power signal and avoid any sudden changes or steps introduced to hybrid BESS. The rate limiter is also employed to extract the fast-changing part of the required power signal and assign it to the supercapacitor. The remaining part of the signal that has a slower rate of change is sent to the chemical storage. In general, it could be said that the difference between the chemical storage production signal and the main signal, the share of hybrid BESS, is assigned to the supercapacitor (see Figure. 4.5). The setting of series DCES is generated once there is an oscillation in the voltage of the system. To be more realistic and better observe the impact, a delay of 0.2 seconds is considered for the operation of DCES. Once activated, it measures the target signal, the difference between the voltage of the DC bus and pre-determined nominal voltage and generates the new duty cycle for its two-quadrant DC/DC power converter.

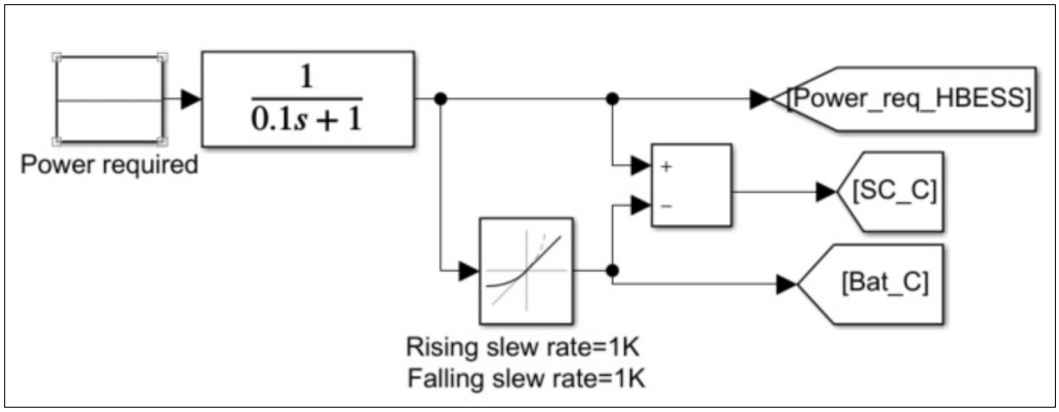

Figure. 4.5 Schematic of sharing energy mechanism between chemical storage and supercapacitor of Hybrid BESS

4.6 Simulation and Discussion

In this section, the findings of simulation results are studied and the responses of each key part of modeled system are presented. All the simulations are conducted in the MATLAB SIMULINK environment.

Three configurations are considered to deal with each simulated contingency:

1. **Only PV system**:

Regarding this scenario, both Hybrid BESS and DCES are deactivated. This scenario could be understood as the base or normal operation of the microgrid.

2. **PV system + Hybrid BESS:**

In this scenario, only the control loop of the Hybrid BESS is activated and the DCES remains inactive. The goal behind this scenario is to determine the capacity of Hybrid BESS in damping voltage oscillation.

3. **PV system + Hybrid BESS + DCES:**

Both Hybrid BESS and DCES are activated. By simulating this scenario, we would be able to know the additional gain in voltage damping given by the DCES.

4.6.1 Cloudy situation and reduced PV generation

In a given scenario, the generation of the PV system reduces by 30% at t=2 sec which simulates a clouding situation. The Hybrid BESS is set to produce 30KW and series DCES compensates for the rest of the power shortage.

The voltage of critical load, as shown in Figure. 4.6 drops significantly when the PV production reduces. Regarding scenario 2, the green curve, a part of the demand is supplied and thus avoids further voltage drop and experiences less oscillation with Hybrid BESS. By the moment DCES is activated, the remaining demand for energy is responded and the voltage of the critical load returns to its default value.

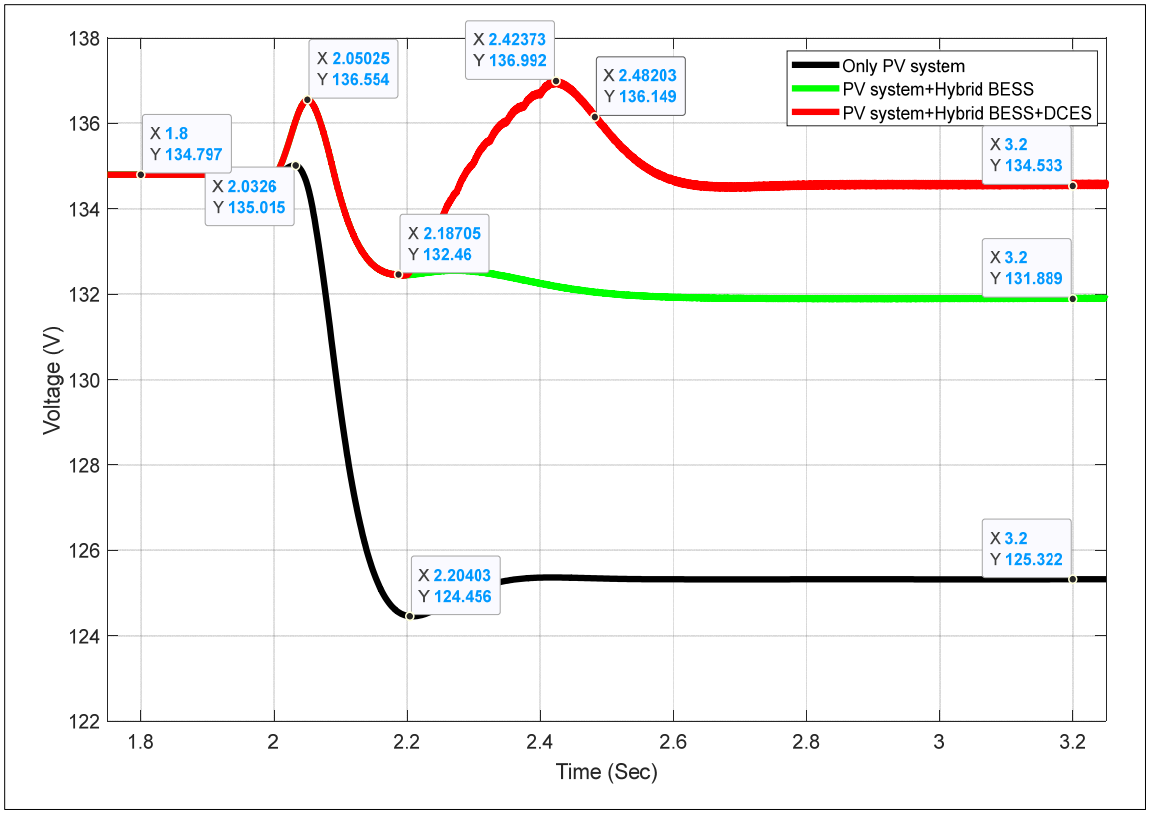

Figure. 4.6 The voltage of the Critical Load [cloudy situation scenario]

Based on the DC bus voltage curves, the voltage final values (V_f) and voltage steady-state values (V_s) are extracted, and the final error is calculated based on the following equation:

$$Error(\%) = \frac{(V_f - V_s)}{V_f} \times 100$$

Table. 4.1. Steady-state stable analysis of DC bus voltage following simulated cloudy situation

Steady-state value= 134.8 V	Only PV system	PV system + Hybrid BESS	PV system + Hybrid BESS + DCES
Final Value (V)	125.3	131.9	134.5
Error (%)	-7.0	-2.2	-0.2

The simulation and calculation results are given in Table. 4.1. If we consider a five percent error as the acceptance criterion for a stable DC bus, we could conclude that the DC bus is not stable without Hybrid BESS. The PV system cannot guarantee the steady state stability of the DC system without a hybrid BESS and DCES. Also, the third configuration, (PV+Hybrid BESS+DCES) has a 0.2% error and is more stable than other configurations.

Regarding the power quality of the studied contingency, the post-contingency voltage overshoot (V_{os}), post contingency voltage undershoot (V_{us}), and post-contingency voltage final value (V_f) for each configuration is extracted based on Figure. 4.6 and the settling time T_s is calculated as shown in Table. 4.2. Note that the settling time is defined as the time when the voltage signal enters the ±1% boundary.

Table. 4.2. Quality of DC bus voltage following simulated cloudy situation

Steady-state value= 134.8 V +1% Error=136.15 V -1% Error=133.45			
	Only PV system	PV system + Hybrid BESS	PV system + Hybrid BESS + DCES
V_{os}	135 V	136.6 V	137 V
V_{us}	124.5 V	131.9 V	132.5 V
T_s	n.a.	n.a.	0.48 Sec

With a boundary of ±1% as the approval index for good power quality, the DC-bus voltage amplitude is not validated unless with the third configuration. Without the DCES the voltage amplitude never returns the defined boundary. The settling time for the third configuration is considerably low (0.48 seconds) which means the quality of the voltage of the critical load is guaranteed. It should be also noted that depending on the critical load characteristics and designed DC microgrid, the system operator may accept other values for settling time. for example, with ±2% index for power quality, the second configuration could be approved as an acceptable configuration.

To see how the operation of series DCES impacts its connected load, the power consumption of NCL is also depicted in Figure. 4.7 It is clear that the contribution of NCL in damping the oscillations is not very significant. By reducing the voltage at the connection points, the total consumption is reduced smoothly.

The share of the supercapacitor and chemical storage in producing energy is shown in Figure. 4.8. The supercapacitor contributes more to the required power signal thanks to its fast response character. The storage starts more slowly to take action and produce energy. Such a response requires smaller chemical storage in terms of charging and discharging rates. It should be noted that the supercapacitor loses around 1% of its energy in two seconds and which is quite significant.

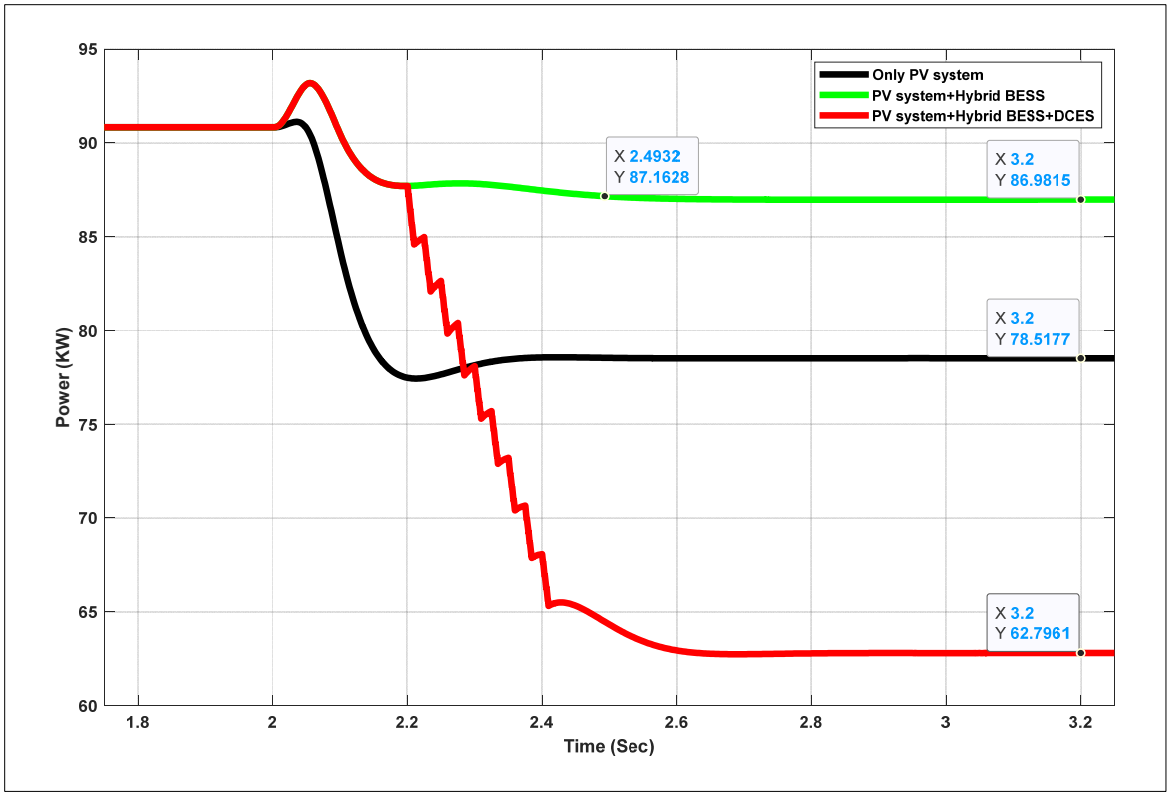

Figure. 4.7 The consumption of Non-Critical Load [cloudy situation scenario]

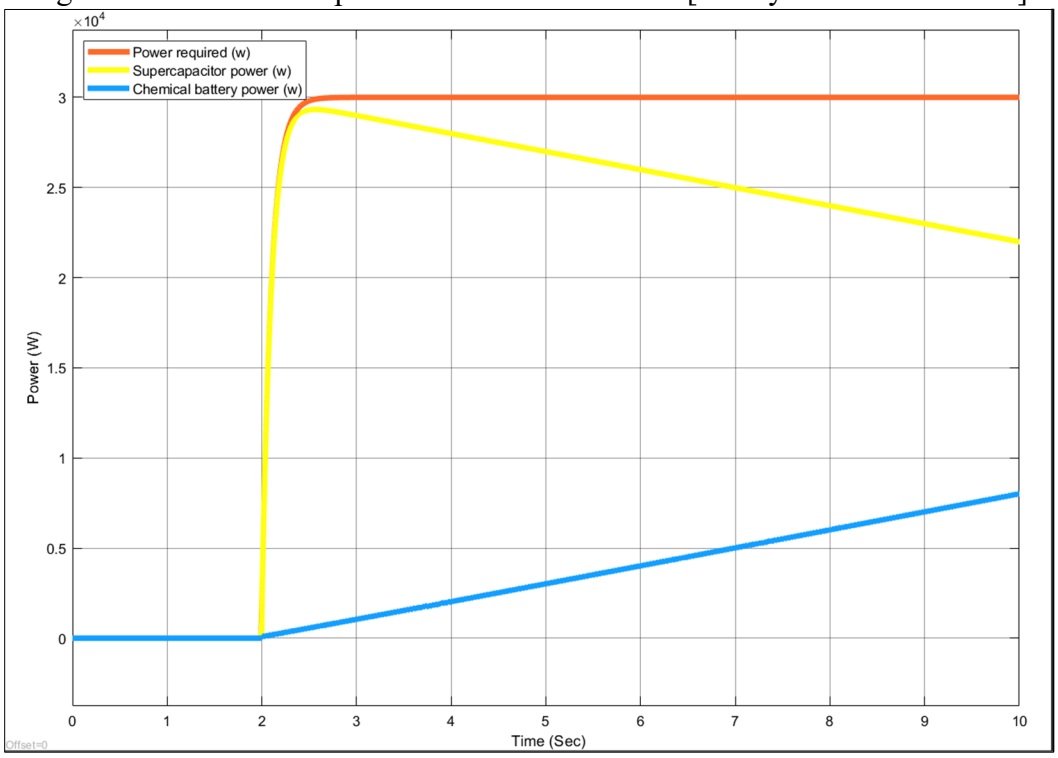

Figure. 4.8 Produced power by supercapacitor and chemical battery storage [cloudy situation scenario]

4.6.2 DC Bus to Ground Fault

In this simulated contingency, a direct ground fault is applied on the DC bus at t=2 seconds and cleared after 0.5 seconds without any equipment outage. Both hybrid BESS and DCES are set off during the fault for avoiding any contribution to the fault current. A delay of 100ms is considered as response time for hybrid BESS and DCES meaning that at t=2.6 sec their reactions to the voltage oscillation begin.

The voltage of the DC bus is shown in Figure. 4.9. As illustrated, the voltage drops to almost zero volts during the fault period and recovers after clearing the fault.

The computation results are given in Table. 4.3. As mentioned earlier, based on the assumption of considering a five percent error as the acceptance criterion for a stable DC bus, we could say that the DC bus is stable in all three simulated configurations and show a 0.3% error. The designed system is naturally resilient to the introduced contingency. By using the Hybrid BESS the response of the system from the steady-state stability point of view has not deteriorated. The same argument applies to the DCES.

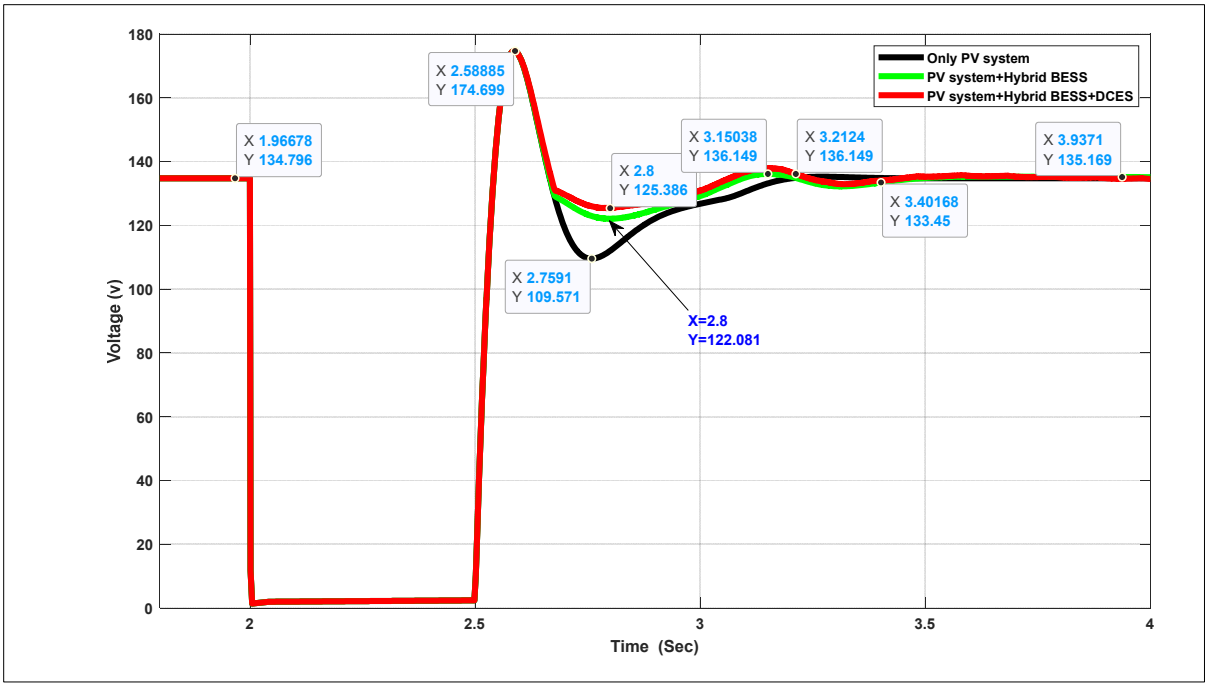

Figure. 4.9 The voltage of the Critical Load [DC bus to ground fault scenario]

Table. 4.3. Steady-state stability analysis of DC bus voltage following simulated faulty situation

Steady-state value= 134.8 V	Only PV system	PV system + Hybrid BESS	PV system + Hybrid BESS + DCES
Final Value (V)	135.2	135.2	135.2
Error (%)	0.3	0.3	0.3

Similar to the previous study, if we consider a boundary of ±1% as the approval index for good power quality in the case of DC system response after the fault, the DC-bus voltage amplitude respects the criteria under the three studied configurations. After clearing the fault at t=2.5 seconds, the voltage of the DC bus raises to over 174 volts. When only the PV system operates, the voltage drops again to less than 110 volts and then turns back smoothly to the pre-fault amplitude and falls inside the defined ±1% approval index at t=3.2 seconds.

Table. 4.4. Quality of DC bus voltage following simulated faulty situation

Steady-state value= 134.8 V +1% Error=136.15 V -1% Error=133.45

	Only PV system	PV system + Hybrid BESS	PV system + Hybrid BESS + DCES
V_{os}	174.7 V	174.7 V	174.7 V
V_{us}	109.6 V	122.1	125.4
T_s	0.6 Sec	0.8 Sec	0.8 Sec

When the hybrid BESS is activated, the second configuration, no impact on the DC bus voltage peak after the fault is observed but it well damps the oscillation and increases the undershoot voltage to 122 volts. Next, the voltage curve inters the +1% deviation at 3.15 Seconds and -1% deviation at 3.4 seconds. In general, the voltage amplitude looks smoother compared to the first configuration.

With the DCES, the third configuration, a similar behavior as the second configuration is observed. The post-contingency DC bus voltage undershoot increases to 125.4 volts and the voltage amplitude enters the +1% deviation at 3.2 Seconds and -1% deviation at 3.4 seconds. The DCES smooths more the voltage curve after the fault. Even though both the second and third configurations improve the quality of voltage after the fault, the corresponding settling times are higher than the first configuration. When only the PV system operates, the voltage enters 0.2 seconds earlier than the pre-defined +1% deviation.

Like the first scenario, the power consumption of NCL is depicted in Figure. 4.10. With the first configuration, the power consumption of NCL drops about 60 KW from the pre-fault consumption of 91 KW. Once the hybrid BESS is activated in the second configuration, the power consumption of NCL stops declining and further tries to reach its initial consumption. In the case of DCES, more drop in NCL power consumption is observed that is represents the capability of DCES in modulating the NCL power and releasing extra power for the CL load connected to the DC bus.

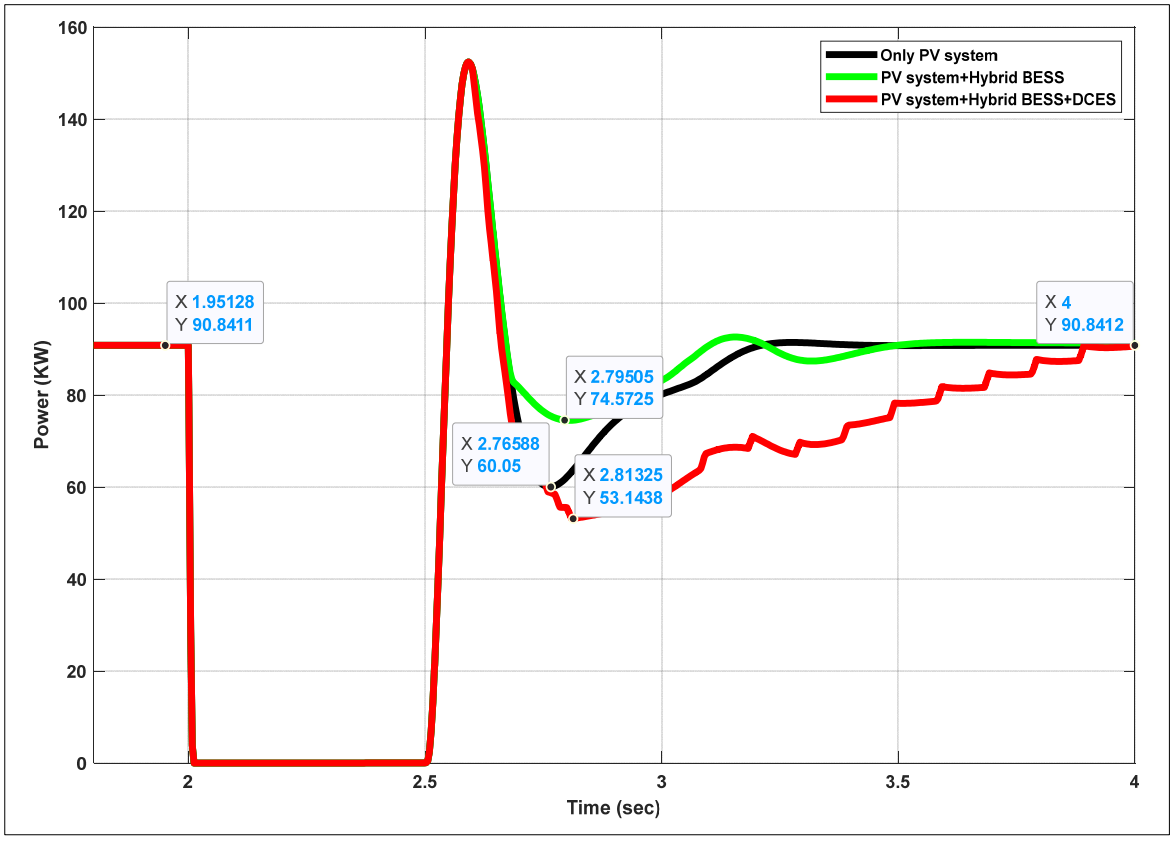

Figure. 4.10 The consumption of Non-Critical Load [DC bus to ground fault scenario]

4.6.3 Ambient Temperature Variation

In this simulated study, the effect of temperature variation on the DC system is studied. To do so, the ambient temperature introduced to the PV system is increased from 35 deg C to 40 deg C at t=2 seconds. The central controller detects the power reduction on the PV sides and tries to compensate for the required power by critical load and bring back the DC voltage to its previous value.

As shown in Figure. 4.11 with the only PV system in place, the DC microgrid experiences a DC voltage drop down to 132.8 volts. Once the hybrid BESS is also activated, the central controller assigns an active power signal to both the chemical battery and the supercapacitor and manages to enhance the DC bus voltage to 134.4 volts. Finally, by activating the DCES at t=2.2 sec, the critical load DC voltage return to the initial value of 134.7 volts.

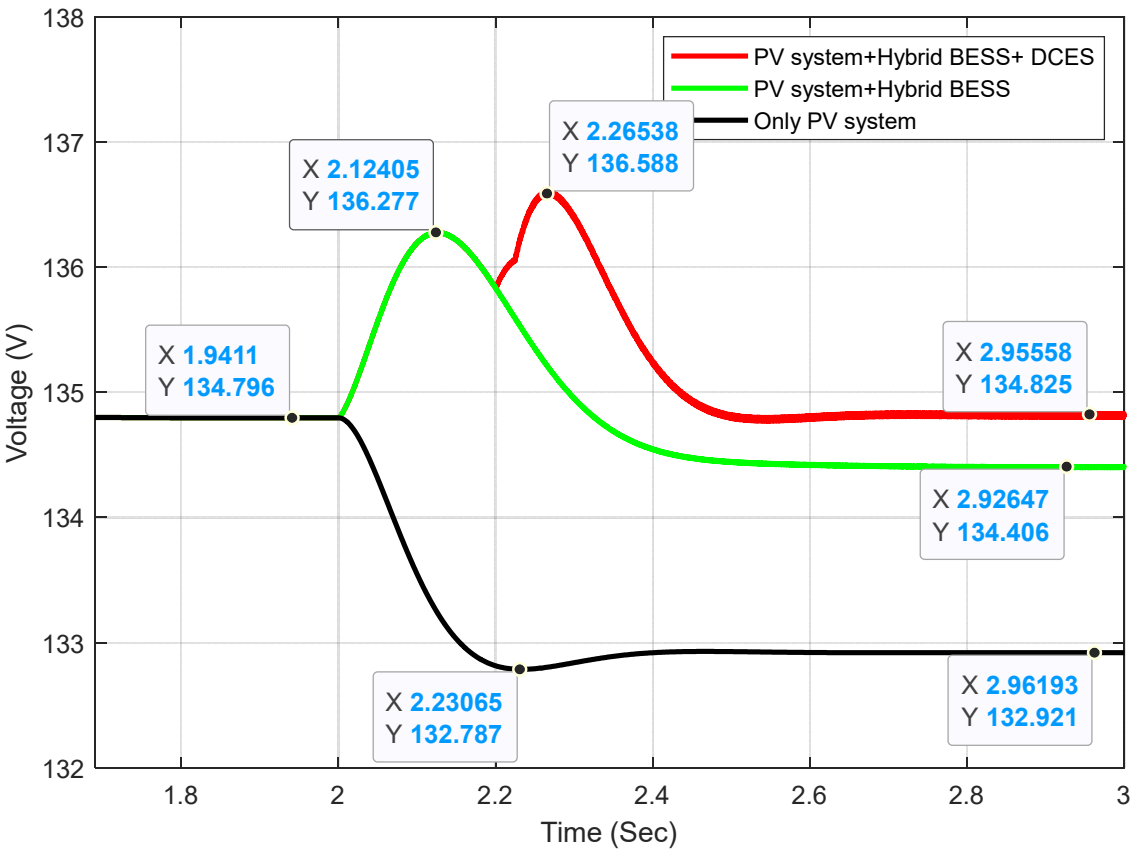

Figure. 4.11 The voltage of the Critical Load [Ambient temperature variation scenario]

Table. 4.5. Stable DC bus analysis of DC bus voltage following simulated ambient temperature variation

Steady-state value= 134.8 V	Only PV system	PV system + Hybrid BESS	PV system + Hybrid BESS + DCES
Final Value (V)	132.9	134.4	134.8
Error (%)	1.4	0.3	0.0

The computation results for the steady-state error of DC bus voltage are given in Table. 4.3Table. 4.5. As mentioned earlier, based on the assumption of considering a five percent error as the acceptance criterion for a steady-state stable DC bus, it is observed that all three simulated configurations have stead-state stability. The designed system is naturally resilient to the introduced contingency. By using the Hybrid BESS the response of the system from the

steady-state stability point of view has not deteriorated. Once the DCES is activated, the DC bus voltage reaches the initial setpoint.

Similar to the previous scenarios, the power consumption of NCL is depicted in Figure. 4.12. When the central controller uses only the PV system, the consumption power of the non-critical load decreases to 88.4 KW. If the hybrid BESS is also considered for controlling the DC bus voltage, then the power of the non-critical load decreases to 90.3 which is very close to its initial value. Once the DCES is employed by the central controller for compensating the error in DC bus voltage, the power consumption of non-critical load is reduced which reflects the activation of the role of non-critical load in voltage enhancement.

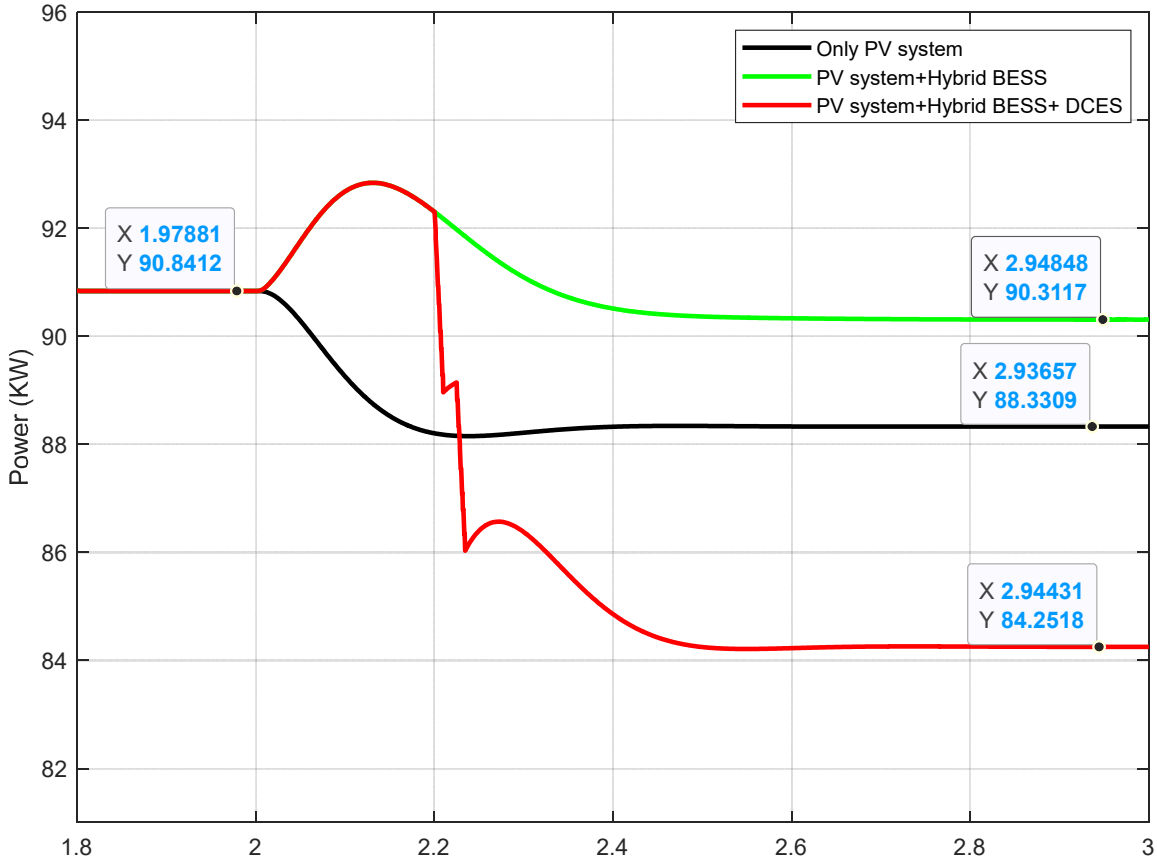

Figure. 4.12 The power of Non-Critical Load [Ambient temperature variation scenario]

Table. 4.6. Quality of DC bus voltage following ambient temperature variation situation

Steady-state value= 134.8 V +1% Error=136.15 V -1% Error=133.45

	Only PV system	PV system + Hybrid BESS	PV system + Hybrid BESS + DCES
V_{os}	n.a.	136.3 V	136.6 V
V_{us}	132.8 V	1344.4	n.a.
T_s	n.a.	n.a.	0.3 Sec

Regarding the quality of the DC bus when the ambient temperature increases, it is shown that the DC microgrid may not be able to respect the boundary of ±1% as the approval index for good power quality. When the PV system operates without additional support, the DC bus voltage has no overshoot and decreases to 132.9 volts. Therefore, it does not fall insight the defined boundary. When the central controller activates the hybrid BESS, the DC bus voltage experiences an overshoot voltage equal to 136.3 volts and an undershoot voltage of 134.4. Again, the DC bus voltage quality is not respected. Finally, with the help of DCES, it is observed that the DC bus voltage falls within the ±1% approval index in about 0.3 seconds (see Table. 4.6).

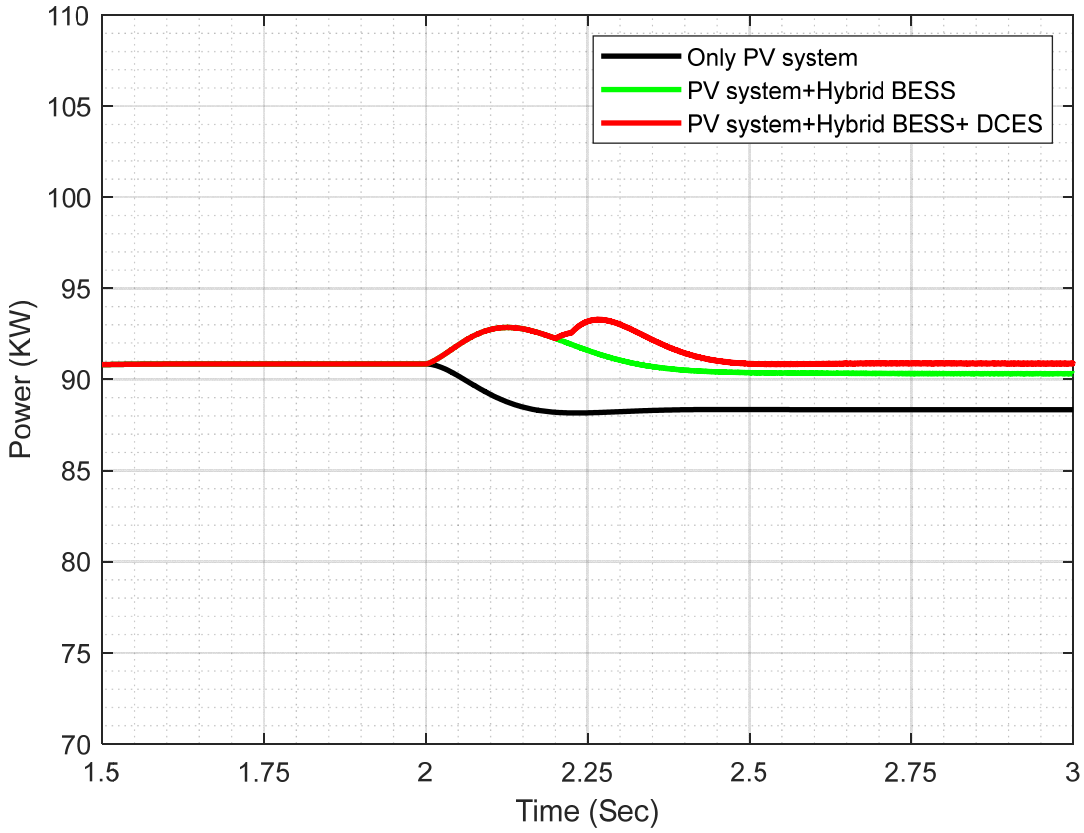

Figure. 4.13 The power of Critical Load [Ambient temperature variation scenario]

The power consumption of CL is also depicted in Figure. 4.13. As shown, the critical load is fed with a more constant power when both DCES and hybrid BESS are controlled by the central controller.

Figure. 4.14 shows the power generation of the supercapacitor and the chemical storage versus the required power signal that is calculated by the central controller. As discussed before, the supercapacitor is set to respond to the fast accelerating part of the required power while the storage increases gradually to take full control.

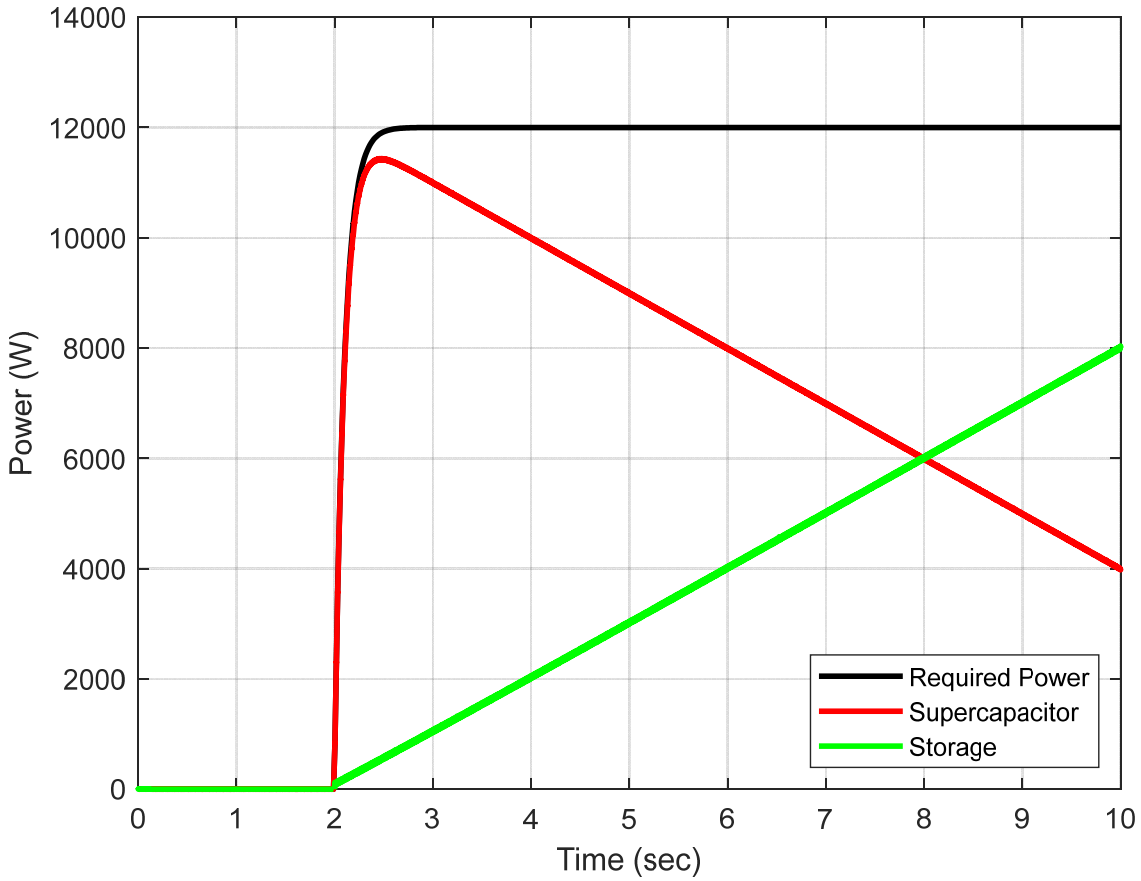

Figure. 4.14 Produced power by supercapacitor and chemical battery storage [Ambient temperature variation scenario]

4.7 Conclusion

DC electric springs (DCES) are considered an effective tool for controlling the oscillations and enhancing the operability of DC microgrids. In this section, a coordination scheme for joint control of series DCES and hybrid battery energy storage (Hybrid BESS) in a DC microgrid is proposed. The hybrid BESS itself comprises a chemical battery storage and a supercapacitor. The main objectives of the proposed coordination scheme are to facilitate the integration of variable renewable energy resources, limit the size and usage of chemical energy storage, activate the share of flexible non-critical load (NCL) in the process of damping voltage oscillation, and maintain the voltage of critical load (CL). The simulation results of the case

with a cloudy situation and the case with a DC bus-to-ground fault confirm the effectiveness of the proposed coordinated energy-sharing scheme in improving the performance of the DC microgrid and supporting the critical load.

CHAPTER 5

CONCLUSIONS AND RECOMMENDATIONS

This chapter concludes the thesis and gives some recommendations about further work on this topic and proposes a road map for development and implementation.

The pathway toward decarbonization of all energy sectors and climate change mitigation are among the main targets set by the Paris agreement for the 21st century. Canada, as one of the participants in this agreement, committed to reducing its greenhouse gas (GHG) emissions by 30 percent by 2030 and achieving net-zero emissions by 2050. The Quebec province is highly involved in this initiative with the plan called" 2030 Plan for a Green Economy" which aims to reach a 37.5 percent reduction compared with 1990 levels, and carbon neutrality by 2050.

The electricity sector is one of the biggest sectors to be decarbonized which is conventionally based on large pollutant fossil-based power plants. As a solution, the load profile is controlled by solutions such as demand-side management programs, load leveling, and battery energy storage. An alternative solution is to supply energy demand from clean energy resources such as renewable energy resources (RESs). A wide variety of technologies including PVs and wind turbines are considered as RESs which are highly integrated at the distribution level. Apart from several advantages, their natural stochastic and intermittent characteristic imposes more oscillations to the balancing equation of generation and consumption and may deteriorate the voltage profile of critical loads.

AC-based distribution systems are widely accepted as the solution for distributing energy among clients. However, recent massive integration of DC loads, distributed energy resources (DERs), energy storage, and electric vehicles into the grids, many researchers start to develop the idea of DC distribution systems. A DC distribution system has many interesting features as well as: simpler power transfer without needing converters and inverters, less investment, and most importantly no issue with reactive power circulation. Among different types of DC distribution systems, the concept of DC microgrids has gained more attraction due to their

several advantages including the ability to operate grid-connected or off-grid for electrification of remote areas.

Despite all the promising features of DC microgrids, the rising trend of power generation from renewable energy resources which are naturally intermittent may cause disturbances especially off-grid microgrids which rely mostly on PVs and wind turbines. To overcome this dilemma, employing new control schemes seems necessary for maintaining the balance between consumption and generation. Several solutions are proposed in the literature e.g., demand-side management (DSM), load balancing, real-time energy management systems, and energy storage.

In this thesis, we used the concept of DC electric spring (DCES) units in modern distribution test systems. First, the characteristics of DCESs, as well as operation modes, and operation configurations, were reviewed and their several applications in DC microgrids are studied and summarized in a table based on some criteria, e.g. the technical level, proposed control scheme, the type of DCES, etc. Next, we proposed a coordination scheme for joint control of series DCES and hybrid battery energy storage (Hybrid BESS) in a DC microgrid. The modeled DCES was employed to optimally modulate the demand of non-critical loads and to support and guarantee the continuous operation of the critical loads with an acceptable range of voltage in the presence of RESs. The results prove the effectiveness of the proposed coordinated energy-sharing scheme in improving the performance of the DC microgrid and supporting the critical load.

5.1 Recommendations

In this section, a number of research gaps are mentioned accompanied by a list of research ideas for future research and development roadmap.

5.1.1.1 Possible Research Ideas

Despite all the ideas explored by the researchers, there are still some gaps in the application of DCES in DC microgrids that can be studied in any future work:

- Developing larger microgrids with different types of DC loads, for example, G2V, DC motors, different types of constant I, constant P, zip, dynamic loads, etc.

- Developing a DC microgrid supplied with several types of DC generation sources, e.g., PV, wind turbine, V2G, mechanical and electrical energy storages.

- Optimal operation of a complex microgrid over a longer period of time. The main goal would be optimizing the utilization of the limited energy source of DCES.
- Employing a controllable renewable energy resource to mimic the role of NCL.
- Coordinated energy sharing with other energy sources for maximizing efficiency.
- Evaluating the possibility of modulating several NCLs with one DCES. The key motivation is to minimize the adverse impact on NCLs.

5.1.1.2 Proposed Roadmap

Last, a roadmap is proposed that illustrates all the phases from simulation to PHIL test before real implementation. The last two phases are of importance from the industrial point of view.

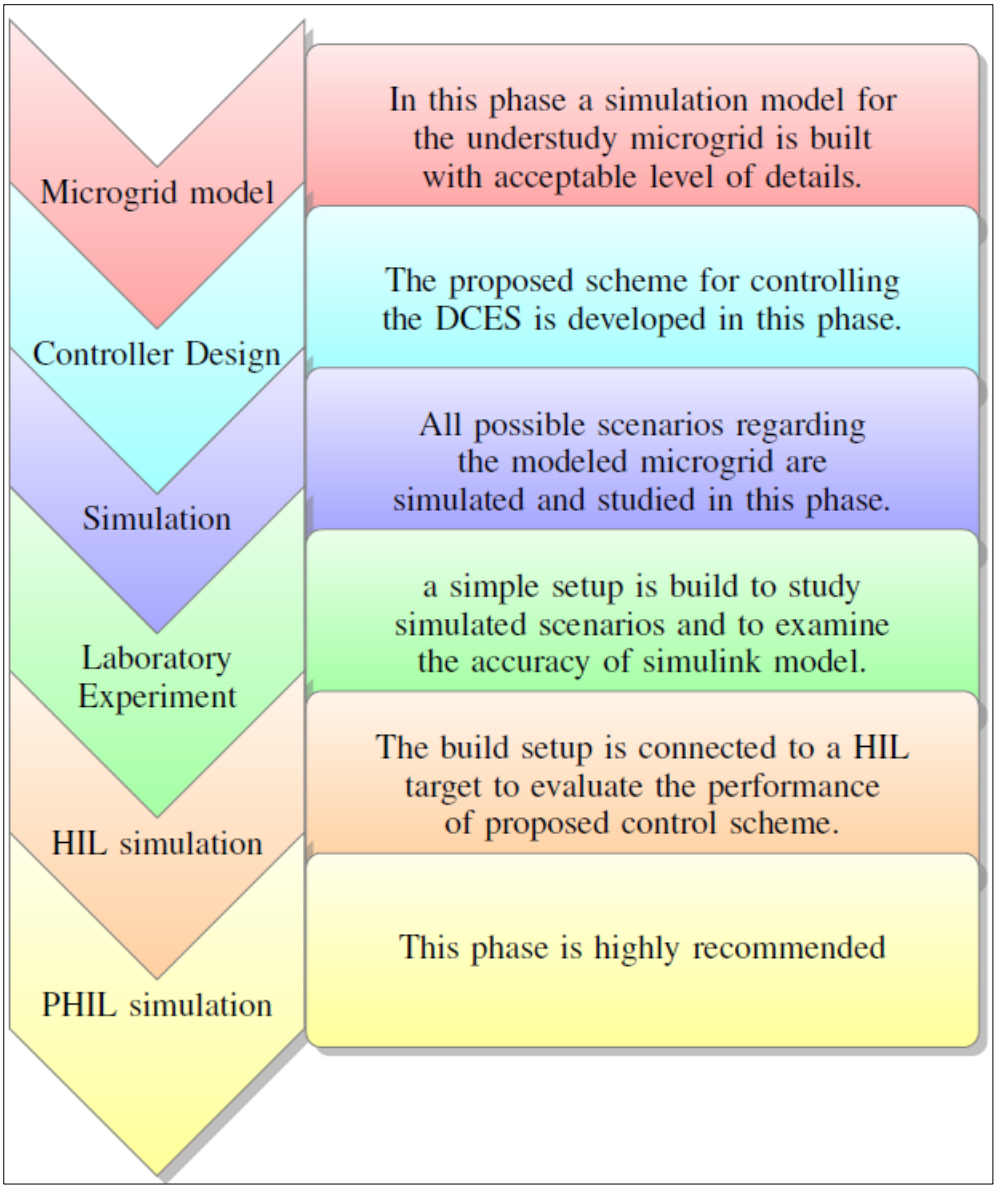

Figure. 5.1 Proposed roadmap for successful DCES integration into modern DC microgrids

LIST OF BIBLIOGRAPHICAL REFERENCES

Abdelilah, Y., Bahar, H., Criswell, T., Bojek, P., Briens, F., & Le Feuvre, P. (2020). Analysis and forecast to 2025. *Renewables 2020*, *74*(9), 1–172. En ligne. < https://iea.blob.core.windows.net/assets/1a24f1fe-c971-4c25-964a-57d0f31eb97b/Renewables_2020-PDF.pdf>

Adly, M., & Strunz, K. (2021). DC microgrid small-signal stability and control: Sufficient stability criterion and stabilizer design. *Sustainable Energy, Grids and Networks*, *26*, 100435. En ligne. <DOI: 10.1016/J.SEGAN.2021.100435>

Ahsan, S. M., & Khan, H. A. (2022). LV Harmonic Analysis of Single-Phase Rooftop Solar PV Systems with Non-Linear Loads. *IEEE Green Technologies Conference*, *2022-April*, 1–6. DOI: 10.1109/GreenTech52845.2022.9772022

Anand, S., Fernandes, B. G., & Guerrero, J. M. (2013). Distributed control to ensure proportional load sharing and improve voltage regulation in low-voltage DC microgrids. *IEEE Transactions on Power Electronics*, *28*(4), 1900–1913. DOI: 10.1109/TPEL.2012.2215055

Bahrami, H., Farhangi, S., Iman-Eini, H., & Adib, E. (2018). A New Interleaved Coupled-Inductor Nonisolated Soft-Switching Bidirectional DC-DC Converter with High Voltage Gain Ratio. *IEEE Transactions on Industrial Electronics*, *65*(7), 5529–5538. DOI: 10.1109/TIE.2017.2782221

Baran, M. E., & Mahajan, N. R. (2007). Overcurrent protection on voltage-source-converter-based multiterminal DC distribution systems. *IEEE Transactions on Power Delivery*, *22*(1), 406–412. DOI: 10.1109/TPWRD.2006.877086

Cairoli, P., Kondratiev, I., & Dougal, R. A. (2013). Coordinated control of the bus tie switches and power supply converters for fault protection in DC microgrids. *IEEE Transactions on Power Electronics*, *28*(4), 2037–2047. DOI: 10.1109/TPEL.2012.2214790

Charan Cherukuri, S. H., Balasubramanian, S., Padmanaban, S., Bhaskar, M. S., Fedak, V., & Arunkumar, G. (2019). *Reduction of Main-Grid Dependence in Future DC Micro-Grids Using Electric Springs*. 397–402. DOI: 10.1109/edpe.2019.8883923

Charles, C., & Bagavathy, S. (2016a). DC Electric Spring for Microgrids. *International Journal of Recent Trends In Engineering And Research*, *2*(April), 0–7.

Charles, C., & Bagavathy, S. (2016b). *DC Electric Spring for Microgrids*. *April*, 0–7.

Chen, X., Shi, M., Sun, H., Li, Y., & He, H. (2018). Distributed Cooperative Control and Stability Analysis of Multiple DC Electric Springs in a DC Microgrid. *IEEE Transactions on Industrial Electronics*, *65*(7), 5611–5622. DOI: 10.1109/TIE.2017.2779414

Chen, Z., Zhou, J., Ren, C., & Wang, Y. (2020). Distributed cooperative control of multiple dc electric springs for voltage regulation in DC microgrid. *Proceedings - 2020 5th Asia Conference on Power and Electrical Engineering, ACPEE 2020*, 538–542. DOI: 10.1109/ACPEE48638.2020.9136532

Chidurala, A., Saha, T. K., Mithulananthan, N., & Bansal, R. C. (2014). Harmonic emissions in grid connected PV systems: A case study on a large scale rooftop PV site. *IEEE Power and Energy Society General Meeting*, *2014-Octob*(October). DOI: 10.1109/PESGM.2014.6939147

Faisal, M., Hannan, M. A., Ker, P. J., Hussain, A., Mansor, M. Bin, & Blaabjerg, F. (2018). Review of energy storage system technologies in microgrid applications: Issues and challenges. In *IEEE Access* (Vol. 6, pp. 35143–35164). Institute of Electrical and Electronics Engineers Inc. DOI: 10.1109/ACCESS.2018.2841407

Farrokhabadi, M., Lagos, D., Wies, R. W., Paolone, M., Liserre, M., Meegahapola, L., Kabalan, M., Hajimiragha, A. H., Peralta, D., Elizondo, M. A., Schneider, K. P., Canizares, C. A., Tuffner, F. K., Reilly, J., Simpson-Porco, J. W., Nasr, E., Fan, L., Mendoza-Araya, P. A., Tonkoski, R., … Hatziargyriou, N. (2020). Microgrid Stability Definitions, Analysis, and Examples. *IEEE Transactions on Power Systems*, *35*(1), 13–29. DOI: 10.1109/TPWRS.2019.2925703

Gawande, S. P., Nagpure, A. R., Dhawad, K., & Chaturvedi, P. (2020). Characteristics Behavior of Shunt DC Electric Spring for Mitigating DC Microgrid Issues. *Proceedings of 2020 IEEE 1st International Conference on Smart Technologies for Power, Energy and Control, STPEC 2020*, 2–7. DOI: 10.1109/STPEC49749.2020.9297772

Gerber, D. L., Vossos, V., Feng, W., Marnay, C., Nordman, B., & Brown, R. (2018). A simulation-based efficiency comparison of AC and DC power distribution networks in commercial buildings. *Applied Energy*, *210*, 1167–1187. DOI: 10.1016/j.apenergy.2017.05.179

Ghanbari, N., Bhattacharya, S., & Mobarrez, M. (2018). Modeling and Stability Analysis of a DC Microgrid Employing Distributed Control Algorithm. *2018 9th IEEE International Symposium on Power Electronics for Distributed Generation Systems, PEDG 2018*. DOI: 10.1109/PEDG.2018.8447707

Gimenes, T. K., Silva, M. P. C. da, Ledesma, J. J. G., & Ando, O. H. (2022). Impact of distributed energy resources on power quality: Brazilian scenario analysis. *Electric Power Systems Research*, *211*(August 2021). DOI: 10.1016/j.epsr.2022.108249

Guerrero, J. M., Vasquez, J. C., Matas, J., De Vicuña, L. G., & Castilla, M. (2011). Hierarchical control of droop-controlled AC and DC microgrids - A general approach toward standardization. *IEEE Transactions on Industrial Electronics*, *58*(1), 158–172. DOI: 10.1109/TIE.2010.2066534

Hashem, R. A., Soliman, Y., Al-Sharm, S., & Massoud, A. (2018). Design of an electric spring for power quality improvement in PV-based DC grid. *ISCAIE 2018 - 2018 IEEE Symposium on Computer Applications and Industrial Electronics*, 156–161. DOI: 10.1109/ISCAIE.2018.8405462

Hosseinipour, A., & Hojabri, H. (2020). Small-Signal Stability Analysis and Active Damping Control of DC Microgrids Integrated with Distributed Electric Springs. *IEEE Transactions on Smart Grid*, *11*(5), 3737–3747. DOI: 10.1109/TSG.2020.2981132

House of Commons of Canada. (2020). *Bill C-12: An Act respecting transparency and accountability in Canada's efforts to acheive net-zero greenhouse gas emissions by the year 2050*. 16.

Huang, W., & Abu Qahouq, J. A. (2015). Energy Sharing Control Scheme for State-of-Charge Balancing of Distributed Battery Energy Storage System. *IEEE Transactions on Industrial Electronics*, *62*(5), 2764–2776. DOI: 10.1109/TIE.2014.2363817

Hui, S. Y., Lee, C. K., & Wu, F. F. (2012). Electric springs - A new smart grid technology. *IEEE Transactions on Smart Grid*, *3*(3), 1552–1561. DOI: 10.1109/TSG.2012.2200701

IEA. (2021). Net Zero by 2050: A Roadmap for the Global Energy Sector. *International Energy Agency*, 224. Retrieved from https://www.iea.org/reports/net-zero-by-2050

IRENA. (2021). World energy transitions outlook: 1.5 degrees pathway. In *International Renewable Energy Agency*. Retrieved from https://irena.org/publications/2021/March/World-Energy-Transitions-Outlook

Jena, S., & Padhy, N. P. (2019). A Distributed Cooperative Droop Control Framework for Unified Operation of Shunt DC Electric Springs. *2019 National Power Electronics Conference, NPEC 2019*, 1–6. DOI: 10.1109/NPEC47332.2019.9034715

Kakigano, H., Miura, Y., & Ise, T. (2013). Distribution voltage control for DC microgrids using fuzzy control and gain-scheduling technique. *IEEE Transactions on Power Electronics*, *28*(5), 2246–2258. DOI: 10.1109/TPEL.2012.2217353

Kikstra, J. S., Vinca, A., Lovat, F., Boza-Kiss, B., van Ruijven, B., Wilson, C., Rogelj, J., Zakeri, B., Fricko, O., & Riahi, K. (2021). Climate mitigation scenarios with persistent COVID-19-related energy demand changes. *Nature Energy*, *6*(12), 1114–1123. DOI:

10.1038/s41560-021-00904-8

Leu, C. S., & Nha, Q. T. (2013). A half-bridge converter with input current ripple reduction for DC distribution systems. *IEEE Transactions on Power Electronics*, *28*(4), 1756–1763. DOI: 10.1109/TPEL.2012.2213269

Liang, X., & Andalib-Bin-Karim, C. (2018). Harmonics and Mitigation Techniques Through Advanced Control in Grid-Connected Renewable Energy Sources: A Review. *IEEE Transactions on Industry Applications*, *54*(4), 3100–3111. DOI: 10.1109/TIA.2018.2823680

Liao, J., Zhou, N., Huang, Y., & Wang, Q. (2020). Unbalanced Voltage Suppression in a Bipolar DC Distribution Network Based on DC Electric Springs. *IEEE Transactions on Smart Grid*, *11*(2), 1667–1678. DOI: 10.1109/TSG.2019.2941874

Liao, J., Zhou, N., Huang, Y., & Wang, Q. (2021). Decoupling Control for DC Electric Spring-Based Unbalanced Voltage Suppression in a Bipolar DC Distribution System. *IEEE Transactions on Industrial Electronics*, *68*(4), 3239–3250. DOI: 10.1109/TIE.2020.2978714

Loh, P. C., Li, D., Chai, Y. K., & Blaabjerg, F. (2013). Autonomous operation of hybrid microgrid with ac and dc subgrids. *IEEE Transactions on Power Electronics*, *28*(5), 2214–2223. DOI: 10.1109/TPEL.2012.2214792

Mahmoud, M. S. (2016). Microgrid: Advanced Control Methods and Renewable Energy System Integration. In *Microgrid: Advanced Control Methods and Renewable Energy System Integration*.

McKinsey. (2022a). Global Energy Perspective 2022 McKinsey ' s Global Energy Perspective is a collaboration between Energy Insights and adjacent practices. *Executive Summary*, *April*. En ligne. <https://www.mckinsey.com/~/media/McKinsey/Industries/Oil and Gas/Our Insights/Global Energy Perspective 2022/Global-Energy-Perspective-2022-Executive-Summary.pdf>

McKinsey. (2022b). The net-zero transition. *McKinsey & Company*, *January*, 1–64.

Mok, K. T., Wang, M. H., Tan, S. C., & Hui, S. Y. (2015). DC electric springs - An emerging technology for DC grids. *Conference Proceedings - IEEE Applied Power Electronics Conference and Exposition - APEC*, *2015-May*(May), 684–690. DOI: 10.1109/APEC.2015.7104424

Mok, K. T., Wang, M. H., Tan, S. C., & Hui, S. Y. R. (2017). DC electric springs - A technology for stabilizing DC power distribution systems. *IEEE Transactions on Power Electronics*, *32*(2), 1088–1105. DOI: 10.1109/TPEL.2016.2542278

Olivares, D. E., Mehrizi-Sani, A., Etemadi, A. H., Cañizares, C. A., Iravani, R., Kazerani, M., Hajimiragha, A. H., Gomis-Bellmunt, O., Saeedifard, M., Palma-Behnke, R., Jiménez-Estévez, G. A., & Hatziargyriou, N. D. (2014). Trends in microgrid control. *IEEE Transactions on Smart Grid*, *5*(4), 1905–1919. DOI: 10.1109/TSG.2013.2295514

Position, E., & Planet, A. C. (2018). *A strategic long-term vision for a prosperous , modern , competitive & climate-neutral economy EU vision for 2050 – " A Clean Planet for All ." 19853116579*, 1–12.

Riccobono, A., & Santi, E. (2014). Comprehensive review of stability criteria for DC power distribution systems. *IEEE Transactions on Industry Applications*, *50*(5), 3525–3535. DOI: 10.1109/TIA.2014.2309800

Stoyanov, I., Iliev, T., Evstatiev, B., & Mihaylov, G. (2019). Harmonic Distortion by Single-Phase Photovoltaic Inverter. *2019 11th International Symposium on Advanced Topics in Electrical Engineering, ATEE 2019*, 19–22. DOI: 10.1109/ATEE.2019.8725009

Tiwari, S., Sabzehgar, R., & Rasouli, M. (2017, July). Load balancing in a microgrid with uncertain renewable resources and loads. *2017 IEEE 8th International Symposium on Power Electronics for Distributed Generation Systems, PEDG 2017*. DOI: 10.1109/PEDG.2017.7972505

Ton, D., & Smith, M. (2012). Doi:10.1016/J.Tej.2012.09.013. *The Electricity Journal*.

Toro, V., Mojica-Nava, E., & Rakoto-Ravalontsalama, N. (2021). Stability Analysis of DC Microgrids With Switched Events. *IFAC-PapersOnLine*, *54*(14), 221–226. DOI: 10.1016/J.IFACOL.2021.10.356

Van den Broeck, G., Stuyts, J., & Driesen, J. (2018). A critical review of power quality standards and definitions applied to DC microgrids. *Applied Energy*, *229*, 281–288. DOI: 10.1016/j.apenergy.2018.07.058

van der Blij, N. H., Ramirez-Elizondo, L. M., Spaan, M. T. J., & Bauer, P. (2018). A state-space approach to modelling DC distribution systems. *IEEE Transactions on Power Systems*, *33*(1), 949–950. DOI: 10.1109/TPWRS.2017.2691547

Wang, J., Chang, X., Li, S., -, al, Guo, Y., Deng, F., Shi, Z., & Huang, L. (2020). Stability analysis of DC microgrid considering the action characteristics of relay protection. *IOP Conference Series: Earth and Environmental Science*, *431*(1), 012011. DOI: 10.1088/1755-1315/431/1/012011

Wang, M. H., Mok, K. T., Tan, S. C., & Hui, S. Y. (2018). Multifunctional DC Electric Springs for Improving Voltage Quality of DC Grids. *IEEE Transactions on Smart Grid*, *9*(3), 2248–2258. DOI: 10.1109/TSG.2016.2609658

Wang, M. H., Mok, K. T., Tan, S. C., & Hui, S. Y. R. (2015). Series and shunt DC electric springs. *2015 IEEE Energy Conversion Congress and Exposition, ECCE 2015*, 6683–6690. DOI: 10.1109/ECCE.2015.7310595

Wang, M. H., Yan, S., Tan, S. C., & Hui, S. Y. R. (2018). Hybrid-DC Electric Springs for DC Voltage Regulation and Harmonic Cancellation in DC Microgrids. *IEEE Transactions on Power Electronics*, *33*(2), 1167–1177. DOI: 10.1109/TPEL.2017.2681120

Wang, M. H., Yan, S., Tan, S. C., Xu, Z., & Hui, S. Y. (2020). Decentralized Control of DC Electric Springs for Storage Reduction in DC Microgrids. *IEEE Transactions on Power Electronics*, *35*(5), 4634–4646. DOI: 10.1109/TPEL.2019.2942604

Wang, M., He, Y., Xu, X., Dong, Z., & Lei, Y. (2021). A Review of AC and DC Electric Springs. *IEEE Access*, *9*(iii), 14398–14408. DOI: 10.1109/ACCESS.2021.3051340

Wang, Q., Cheng, M., Chen, Z., & Wang, Z. (2015). Steady-State Analysis of Electric Springs with a Novel δ Control. *IEEE Transactions on Power Electronics*, *30*(12), 7159–7169. DOI: 10.1109/TPEL.2015.2391278

Wang, Q., Cheng, M., Jiang, Y., Chen, Z., Deng, F., & Wang, Z. (2016). DC electric springs with DC/DC converters. *2016 IEEE 8th International Power Electronics and Motion Control Conference, IPEMC-ECCE Asia 2016*, 3268–3273. DOI: 10.1109/IPEMC.2016.7512818

Wang, Q., Zha, D., Cheng, M., Deng, F., & Buja, G. (2020). Energy Management System for DC Electric Spring with Parallel Topology. *IEEE Transactions on Industry Applications*, *56*(5), 5385–5395. DOI: 10.1109/TIA.2020.3010498

Xu, Q., Zhang, C., Wen, C., & Wang, P. (2019). A Novel Composite Nonlinear Controller for Stabilization of Constant Power Load in DC Microgrid. *IEEE Transactions on Smart Grid*, *10*(1), 752–761. DOI: 10.1109/TSG.2017.2751755

Yang, Y., Tan, S. C., & Hui, S. Y. R. (2018). Mitigating distribution power loss of dc microgrids with DC electric springs. *IEEE Transactions on Smart Grid*, *9*(6), 5897–5906. DOI: 10.1109/TSG.2017.2698578

Zha, D., Wang, Q., Cheng, M., & Deng, F. (2019). Energy Management System Applied in DC Electric Springs. *ICPE 2019 - ECCE Asia - 10th International Conference on*

Power Electronics - ECCE Asia, *3*, 1435–1439.